CO_2 Photoreduction by 4-Ferrocenyl Appended Bipyridine Coordinated Re(I) Complexes

Shriya Saha[a], Dolores G. Gil-Gavilán[b], Matthias J. Gutmann[c], Debasish Manna[d], Souvik Roy[*b], Raja Mitra[*a,e]

[a]School of Chemical and Materials Sciences, Indian Institute of Technology Goa, Farmagudi, Goa 403401, India. Email: rajamitra@iitgoa.ac.in

[b]School of Natural Sciences, University of Lincoln, Green Lane, Lincoln, Lincolnshire, LN6 7DL, UK.

[c]Rutherford Appleton Laboratory, ISIS Facility, Chilton Didcot, Oxfordshire OX11 0QX, UK.

[d]Department of Chemistry, Indian Institute of Science Education and Research Bhopal, Bhopal, MP 462066, India

[e]Center of Excellence in Sustainable Energy, Indian Institute of Technology Goa, Ponda, Goa – 403401, India

Table of Contents:

Methods and Materials

Ethanol (99%) was received from LabChem; toluene and diethyl ether were received from SRL Chemicals. Ethanol and diethyl ether were used as received, and toluene was dried over sodium prior to use. Ferrocene carboxaldehyde and 1-acetonylpyridiniumchloride were purchased from BLD Pharma India Pvt. Ltd. Ammonium acetate (NH_4OAc) and potassium hydroxide (KOH) were purchased from SRL Chemicals. Rheniumpentacarbonyl bromide [$Re(CO)_5Br$] was purchased from Sigma-Aldrich. All reagents were used as received. The synthesis of all metal complexes was carried out using the Schlenk technique[1]. Filtration and other manipulations were performed in open air. For the cyclic voltammetric measurements, acetonitrile was dried over phosphorus pentoxide.

Instrumentation

The melting points of the ligands were recorded using a DBK-programmable melting point apparatus (max = 320 °C). ^1H and $^{13}C\{^1H\}$ NMR spectra were acquired on a Bruker ASCEND™ spectrometer using 400 MHz (^1H NMR) in $CDCl_3$ (δ = 7.26 ppm); DMSO-d_6 (δ = 2.50 ppm) or 101 MHz ($^{13}C\{^1H\}$ NMR) in $CDCl_3$ (δ = 77.1 ppm); and DMSO-d_6 (δ = 39.5 ppm) at 298 K. Multiplicities of the signals are reported using the following abbreviations: s, singlet; d, doublet; dd, doublet of doublet; t, triplet; dt, doublet of triplet; m, multiplet; br, broad. Structural assignments were made using additional information from ^1H–^1H COSY, ^1H–^{13}C HSQC, and ^1H–^{13}C HMBC correlation experiments. The UV–vis absorption spectral measurements of ligands and complexes in spectroscopic grade acetonitrile solution were performed with a JASCO–V-770 UV–visible/NIR double-beam spectrophotometer. In the ATR mode, the infrared (IR) spectra were recorded using a Shimadzu IRAffinity-1S spectrophotometer (40 scans, scanned in 4000–400 cm^{-1}, resolution 4 cm^{-1}). Reverse-phase HPLC was performed on a C18 column (100 mm × 2.1 mm i.d., 3 μm), maintained at 40 °C, using aqueous methanol/acetonitrile gradients containing 1% ammonium formate as the mobile phase with a flow rate of 0.2 mL min^{-1}. Unless otherwise stated, a photodiode array (PDA) detector set at 254 nm was used. Mass spectra were recorded using a JOEL Japan-AccuTOF GCV mass spectrometer (IIT Bombay), Bruker MicroTOF QII LC-HRMS (IISER Bhopal), and Water's XEVO G2 QToF (IISER Berhampur). Elemental analysis was done using a varioMICRO CHNS analyzer (IISER Bhopal). Thermogravimetry of the complexes was carried out using a NETZSCH TG 209F1 Libra thermoanalyzer, in the temperature range of 25–600 °C, with a heating rate of 10 $Kmin^{-1}$, under a nitrogen environment. Electrochemical analysis was performed using a CHI1200C

potentiostat. Cyclic voltammetry measurements were performed in a one-compartment, three-electrode setup using a glassy carbon working electrode (3 mm diameter), a platinum wire as the counter electrode, and a non-aqueous $Ag|Ag^+$ pseudo-reference electrode, $Ag|AgNO_3$ (10 mM) in 0.1 M *n*-Bu_4NBF_4 in acetonitrile. The voltammograms were referenced by adding ferrocene as an internal standard after the final experiment, and all potentials given in this work are reported against the $Fc^{+/0}$ couple. The potential of the $Fc^{+/0}$ couple was found to be in the range of 0.07 to 0.09 V *vs.* the non-aqueous $Ag|Ag^+$ pseudo-reference. The supporting electrolyte was *n*-Bu_4NBF_4 (0.1 M), purified by recrystallization from 1 : 2 ethanol/water followed by drying at 80 °C in a hot air oven. Single crystal analysis: By the vapor diffusion technique, single crystals of $C_{22}H_{22}FeN_2$ (**2c**) were obtained from a mixture of chloroform and *n*-hexane. A suitable crystal was selected and diffracted on a Bruker APEX-II CCD diffractometer. The crystal was kept at 140.0 K during data collection. Using Olex2[2–4], the structure was solved with the Olex2.solve structure solution program using Charge Flipping and refined with the olex2.refine refinement package using Gauss-Newton minimisation and the ORTEP[5,6] diagram was drawn using the MERCURY[7] software provided by CSD.

R_f value calculation from TLC

Silica-coated alumina plates are used to monitor the reactions and calculate the R_f values of **1a**–**d** and **2a**–**d**. A TLC with spotting of ferrocene carboxaldehyde (1), chalcone intermediate (2; **1d**), and the corresponding bipyridine derivative (3; **2d**) is done as an example to show the calculation of R_f values of each compound. The mobile phase used for TLC was ethyl acetate: pet ether (10% *v/v*).

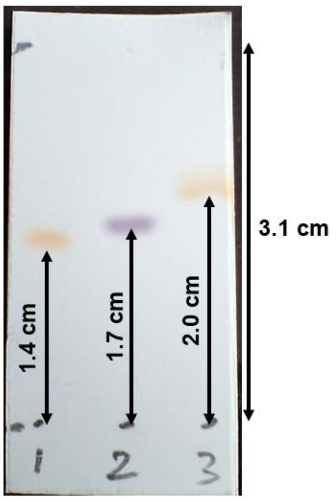

R_f of (1): $\frac{1.4\ cm}{3.1\ cm} = 0.45$

R_f of (2): $\frac{1.7\ cm}{3.1\ cm} = 0.55$

R_f of (3): $\frac{2.0\ cm}{3.1\ cm} = 0.64$

Synthesis and Characterisation

Synthesis of **1a**–**d**:

In a round-bottom flask with a stirbar, 2–acetylpyridine (1.00 equiv.) was dissolved in 2.0 mL of ethanol (EtOH), followed by the addition of KOH (3.33 equiv.). The solution was stirred until the color changed from colorless to slightly orange. Ferrocene carboxaldehyde (1.00 equiv.) was added and stirred at 40 °C for 2 hours. For **1a** & **1d**, the crude product was obtained as a precipitate, filtered, washed with water, and dried under the air. The crude product was then loaded on a silica column (by dissolving in a minimum amount of DCM and then adsorbing on dry silica) and eluted with 2% ethyl acetate to remove the trace impurities. For **1b** and **1c**, no precipitate formation was observed. EtOH was removed under vacuum (complete removal is necessary for a better yield), and the crude mixture was directly loaded onto the silica column. The pure product was obtained using 2% ethyl acetate: pet ether as the eluent.

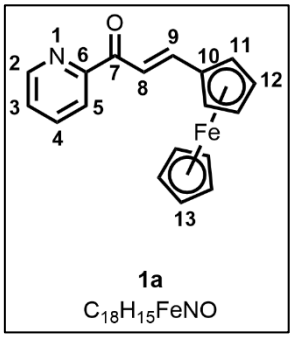

1a
$C_{18}H_{15}FeNO$

Yield: 92% (650 mg, 2.04 mmol). R_f 0.53 (mobile phase: ethyl acetate: pet ether, 10% *v/v*). M.P.: 157 °C (Lit. value[8]: 160–161 °C). ^{1}H NMR (400 MHz, $CDCl_3$) δ (ppm): 8.73 (dt, *J* = 4.0 & 1.0 Hz, 1H, H_2), 8.18 (dt, *J* = 7.6 & 1.0 Hz, 1H, H_5), 7.93–7.82 (merged, 3H, H_3, H_8 & H_9), 7.45 (ddd, *J* = 7.5, 4.9 & 1.0 Hz, 1H, H_4), 4.67 (s, 2H, H_{11}), 4.49 (s, 2H, H_{12}), 4.18 (s, 5H, H_{13}). ^{13}C{^{1}H} NMR (101 MHz, $CDCl_3$) δ (ppm): 188.5 (C_7), 154.7 (C_6), 148.7 (C_9), 147.2 (C_2), 136.9 (C_4), 126.5 (C_3), 122.9 (C_5), 117.8 (C_8), 79.4 (C_{10}), 71.5 (C_{12}), 69.8 (C_{13}), 69.4 (C_{11}). The ^{1}H and ^{13}C{^{1}H} values match those in previous reports[9]. ATR–IR (ν cm^{-1}): 3102, 1696, 1662, 1590, 1569, 1318, 1010, 749. UV–vis (λ nm / ε x 10^6 $M^{-1}cm^{-1}$): 273 (0.38), 329 (0.56), 400 (0.10), 515 (0.12). RP–HPLC: 2.186 min (methanol and 1% ammonium formate in water) 95 : 5 (*v/v*). HRMS (*m/z*): calcd for [M+H$^+$] 318.0622, found for [M+H$^+$] 318.0569. ·

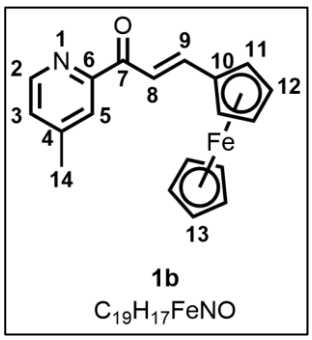

1b
$C_{19}H_{17}FeNO$

Yield: 65% (480 mg, 1.45 mmol). R_f 0.55 (mobile phase: ethyl acetate: pet ether, 10% *v/v*). ^{1}H NMR (400 MHz, $CDCl_3$) δ (ppm): 8.58 (d, *J* = 4.3 Hz, 1H, H_2), 8.00 (s, 1H, H_5), 7.86 (dd, *J* = 15.5 Hz, 2H, H_8 & H_9), 7.28 (d, *J* = 4.2 Hz, 1H, H_3), 4.67 (s, 2H, H_{11}), 4.48 (s, 2H, H_{12}), 4.17 (s, 5H, H_{13}), 2.44 (s, 3H, H_{14}). ^{13}C{^{1}H} NMR (101 MHz, $CDCl_3$) δ (ppm): 188.9 (C_7), 157.8 (C_6), 154.2 (C_2), 146.7 (C_4), 137.0 (C_9), 126.2 (C_3), 120.0 (C_5), 118.2 (C_8), 79.7 (C_{10}), 71.4 (C_{12}), 69.8 (C_{13}), 69.4 (C_{11}), 24.6 (C_{14}).

ATR–IR (ν cm^{-1}): 3085, 1692, 1654, 1577, 1297, 1109, 817. UV–vis (λ nm / ε x 10^6 $M^{-1}cm^{-1}$): 271 (0.75), 327 (0.82), 395 (0.17), 507 (0.16). RP–HPLC: 6.536 min (methanol and 1% ammonium formate in water) 95 : 5 (*v/v*). HRMS (*m/z*): calcd for [M+H^+] 332.0779; found for [M+H^+] 332.0726.

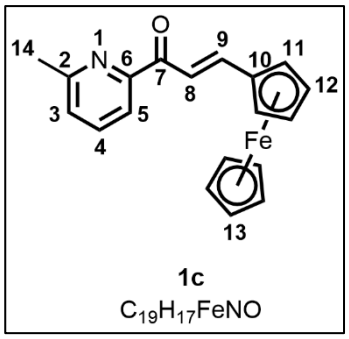

1c
$C_{19}H_{17}FeNO$

Yield: 68% (500 mg, 1.51 mmol). R_f 0.55 (mobile phase: ethyl acetate: pet ether, 10% *v/v*). M.P.: 143 °C. ^{1}H NMR (400 MHz, $CDCl_3$) δ (ppm): 7.98 (d, *J* = 7.8 Hz, 1H, H_5), 7.87 (br, 2H, H_8 & H_9), 7.73 (t, *J* = 7.9 Hz, 1H, H_4), 7.32 (d, *J* = 7.9 Hz, 1H, H_3), 4.67 (s, 2H, H_{11}), 4.49 (s, 2H, H_{12}), 4.19 (s, 5H, H_{13}), 2.67 (s, 3H, H_{14}). ^{13}C{^{1}H} NMR (101 MHz, $CDCl_3$) δ (ppm): 188.9 (C_7), 157.8 (C_2), 154.2 (C_6), 146.7 (C_9), 137.0 (C_4), 126.2 (C_3), 120.0 (C_5), 118.2 (C_8), 79.7 (C_{10}), 71.4 (C_{12}), 69.8 (C_{13}), 69.4 (C_{11}), 24.6 (C_{14}). ATR–IR (ν cm^{-1}): 3098, 1678, 1654, 1573, 1445, 1103, 808. UV–vis (λ nm / ε x 10^6 $M^{-1}cm^{-1}$): 282 (0.56), 328 (0.82), 396 (0.13), 512 (0.15). RP–HPLC: 7.115 min (methanol and 1% ammonium formate in water) 95 : 5 (*v/v*). HRMS (*m/z*): calcd for [M+H^+] 332.0779, found for [M+H^+] 332.0735.

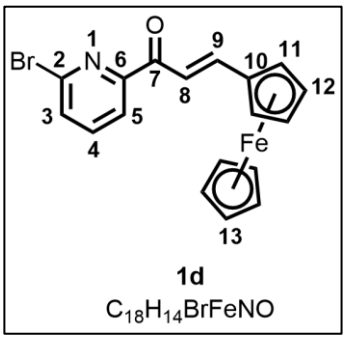

1d
$C_{18}H_{14}BrFeNO$

Yield: 90% (795 mg, 2.04 mmol). R_f 0.55 (mobile phase: ethyl acetate: pet ether, 10% *v/v*). M.P.: 187 °C. ^{1}H NMR (400 MHz, $CDCl_3$) δ (ppm): 8.13 (d, *J* = 7.2 Hz, 1H, H_5), 7.91 (d, *J* = 15.6 Hz, 1H, H_9), 7.70 (merged, 3H, H_3, H_4 & H_8), 4.69 (s, 2H, H_{11}), 4.53 (s, 2H, H_{12}), 4.20 (s, 5H, H_{13}). ^{1}H NMR spectrum matched the reported values[10]. ^{13}C{^{1}H} NMR (101 MHz, $CDCl_3$) δ (ppm): 186.8 (C_7), 155.6 (C_6), 148.2 (C_2), 141.2 (C_9), 139.2 (C_4), 131.1 (C_3), 121.7 (C_5), 117.2 (C_8), 79.2 (C_{10}), 71.8 (C_{12}), 69.9 (C_{13}), 69.6 (C_{11}). ATR–IR (ν cm^{-1}): 3101, 1683, 1650, 1573, 1314, 1038, 800. UV–vis (λ nm / ε x 10^6 $M^{-1}cm^{-1}$): 287 (0.48), 334 (0.80), 409 (0.12), 530 (0.19). RP–HPLC: 2.649 min (methanol and 1% ammonium formate in water) 95 : 5 (*v/v*). HRMS (*m/z*): calcd for [M+H^+] 395.9728, found for [M+H^+] 395.9676, and calcd for [M+Na^+] 417.9552, found for [M+Na^+] 417.9498.

Synthesis of **2a**–**d**:

To a round bottom flask with a stirbar, **1a**–**d** (1.00 equiv.) was added and stirred with 4.0 mL of EtOH for 15 min. 1–acetonylpyridiniumchloride (1.00 equiv.) was added to the chalcone by

dissolving it in 4.0 mL of EtOH. Solid NH_4OAc (50.0 equiv.) and further 5.0 mL of EtOH were added to the reaction mixture properly (vigorous stirring is required to ensure better yield). The contents were refluxed (an air condenser was attached to the flask for refluxing) for 20 h and monitored using thin-layer chromatography (TLC). If the chalcone was unreacted, the reaction was continued for another 16 h. After cooling the reaction, EtOH was removed under high vacuum (0.120 mbar at rt for 2 h; a necessary step for better yield), and the obtained solid was directly loaded onto a silica column for purification. The pure product was eluted with 5% ethyl acetate: pet ether. The orange-colored solid obtained was washed thrice (3 × 10 mL) with chloroform (to remove any eluent impurities) before applying vacuum (0.120 mbar at rt for 1 h) to remove any trace amount of eluting solvent.

One-pot synthesis of **2a**–**d** from 2-acetylpyridine: To a round bottom flask with a stirbar, 2-acetylpyridine (1.00 equiv.) with 2.0 mL of EtOH is added, followed by KOH (3.33 equiv.). The solution was stirred for 10 min, and ferrocene carboxaldehyde (1.00 equiv.) was added, and the reaction mixture was stirred at 40 °C for 2 h. 1-acetonylpyridiumchloride (1.00 equiv.) was added to the same flask by dissolving it in 5.0 mL of EtOH. Solid NH_4OAc (50.0 equiv.) was added along with an additional 8.0 mL of EtOH to ensure proper stirring, and the reaction mixture was stirred for 20 h under refluxing conditions. The reaction was monitored by TLC, and purification was performed as mentioned.

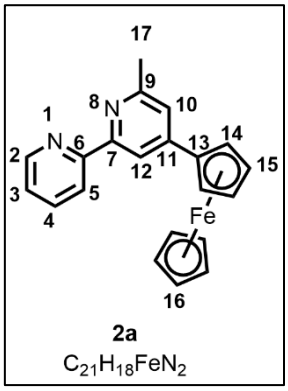

2a
$C_{21}H_{18}FeN_2$

Yield: 46% (257 mg, 0.73 mmol). R_f 0.62 (mobile phase: ethyl acetate: pet ether, 10% *v/v*). M.P.: 112 °C. ^{1}H NMR (400 MHz, $CDCl_3$) δ (ppm): 8.71 (d, J = 4.2 Hz, 1H, H_5), 8.43 (d, J = 8.0 Hz, 1H, H_2), 8.24 (s, 1H, H_{12}), 7.82 (t, J = 7.8 Hz, 1H, H_4), 7.31 (t, J = 5.9 Hz, 1H, H_3), 7.22 (s, 1H, H_{10}), 4.84 (s, 2H, H_{14}), 4.42 (s, 2H, H_{15}), 4.07 (s, 5H, H_{16}), 2.64 (s, 3H, H_{17}). ^{13}C{^{1}H} NMR (101 MHz, $CDCl_3$) δ (ppm): 157.8 (C_9), 156.7 (C_7), 155.6 (C_6), 149.7 (C_{11}), 149.1 (C_5), 136.8 (C_4), 123.4 (C_3), 121.4 (C_2), 120.0 (C_{12}), 115.2 (C_{10}), 81.5 (C_{13}), 70.0 (C_{15}), 69.9 (C_{16}), 67.2 (C_{14}), 24.7 (C_{17}). ATR–IR (ν cm^{-1}): 2919, 1607, 1577, 1471, 1412, 1029, 787. UV–vis (λ nm / ε x 10^6 M^{-1}cm^{-1}): 237 (1.12), 285 (0.92), 363 (0.07), 455 (0.03). RP–HPLC: 2.696 min (methanol and 1% ammonium formate in water) 95 : 5 (*v/v*). HRMS (*m/z*): calcd for [M+H$^+$] 355.0939, found for [M+H$^+$] 355.0952.

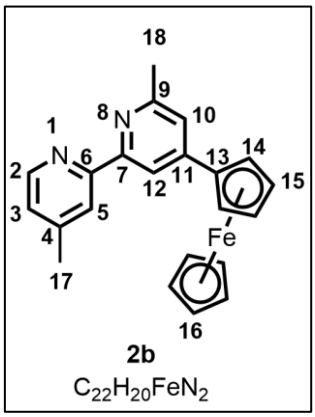

2b

$C_{22}H_{20}FeN_2$

Yield: 23% (130 mg, 0.35 mmol). R_f 0.63 (mobile phase: ethyl acetate: pet ether, 10% *v/v*). M.P.: 137 °C. ^{1}H NMR (400 MHz, $CDCl_3$) δ (ppm): 8.57 (d, *J* = 5.1 Hz, 1H, *H*$_2$), 8.25 (s, 1H, *H*$_5$), 8.23 (s, 1H, *H*$_{12}$), 7.22 (s, 1H, *H*$_{10}$), 7.13 (d, *J* = 5.2 Hz, 1H, *H*$_3$) 4.84 (s, 2H, *H*$_{14}$), 4.41 (s, 2H, *H*$_{15}$), 4.06 (s, 5H, *H*$_{16}$), 2.64 (s, 3H, *H*$_{18}$), 2.45 (s, 3H, *H*$_{17}$). ^{13}C{^{1}H} NMR (101 MHz, $CDCl_3$) δ (ppm): 157.6 (*C*$_9$), 156.4 (*C*$_7$), 155.7 (*C*$_6$), 149.6 (*C*$_{11}$), 148.9 (*C*$_4$), 148.0 (*C*$_5$), 124.4 (*C*$_{12}$), 122.1 (*C*$_2$), 119.9 (*C*$_3$), 115.3 (*C*$_{10}$), 81.5 (*C*$_{13}$), 70.0 (*C*$_{15}$), 69.9 (*C*$_{16}$), 67.0 (*C*$_{14}$), 24.7 (*C*$_{18}$), 21.2 (*C*$_{17}$). ATR–IR (ν cm^{-1}): 2924, 1619, 1577, 1454, 1102. UV–vis (λ nm / ε x 10^6 M^{-1}cm^{-1}): 207 (1.26), 238 (1.08), 285 (0.79), 348 (0.16), 447 (0.03). RP–HPLC: 1.606 min (methanol and 1% ammonium formate in water) 95 : 5 (*v/v*). HRMS (*m/z*): calcd for [M+H$^+$] 369.1095, found for [M+H$^+$] 369.1066.

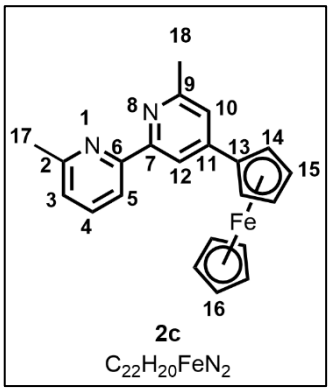

2c

$C_{22}H_{20}FeN_2$

Yield: 69% (346 mg, 0.94 mmol). R_f 0.63 (mobile phase: ethyl acetate: pet ether, 10% *v/v*). M.P.: 143 °C. ^{1}H NMR (400 MHz, $CDCl_3$) δ (ppm): 8.22 (s, 1H, *H*$_{12}$), 8.18 (d, *J* = 8.0 Hz, 1H, *H*$_3$), 7.69 (t, *J* = 7.8 Hz, 1H, *H*$_4$), 7.21 (s, 1H, *H*$_{10}$), 7.17 (d, *J* = 7.8 Hz, 1H, *H*$_5$), 4.83 (s, 2H, *H*$_{14}$), 4.42 (s, 2H, *H*$_{15}$), 4.07 (s, 5H, *H*$_{16}$), 2.67 (s, 3H, *H*$_{18}$), 2.63 (s, 3H, *H*$_{17}$). ^{13}C{^{1}H} NMR (101 MHz, $CDCl_3$) δ (ppm): 157.9 (*C*$_9$), 157.7 (*C*$_6$), 156.1 (*C*$_7$), 156.0 (*C*$_2$), 149.5 (*C*$_{11}$), 137.0 (*C*$_3$), 123.0 (*C*$_4$), 119.9 (*C*$_5$), 118.4 (*C*$_{10}$), 115.5 (*C*$_{12}$), 81.8 (*C*$_{14}$), 69.9 (*C*$_{15}$ & *C*$_{16}$), 67.1 (*C*$_{14}$), 24.7 (*C*$_{18}$ & *C*$_{17}$). ATR–IR) (ν cm^{-1}): 2919, 1611, 1577, 1547, 1407, 1025. 800. UV–vis (λ nm / ε x 10^6 M^{-1}cm^{-1}): 239 (1.45), 288 (1.35), 361 (0.10), 453 (0.04). RP–HPLC: 3.624 min (methanol and 1% ammonium formate in water) 95 : 5 (v/v). HRMS (*m/z*): calcd for [M+H$^+$] 369.1095, found for [M+H$^+$] 369.1109.

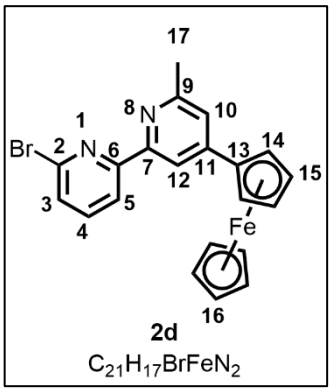

2d

$C_{21}H_{17}BrFeN_2$

Yield: 44% (241 mg, 0.05 mmol). R_f 0.64 (mobile phase: ethyl acetate: pet ether, 10% *v/v*). M.P.: 134 °C. ^{1}H NMR (400 MHz, $CDCl_3$) δ (ppm): 8.41 (d, *J* = 7.2 Hz, 1H, *H*$_3$), 8.21 (s, 1H, *H*$_{12}$), 7.66 (t, *J* = 7.8 Hz, 1H, *H*$_4$), 7.48 (d, *J* = 7.8 Hz, 1H, *H*$_5$), 7.23 (s, 1H, *H*$_{10}$), 4.84 (s, 2H, *H*$_{14}$), 4.43 (s, 2H, *H*$_{15}$), 4.07 (s, 5H, *H*$_{16}$), 2.62 (s, 3H, *H*$_{17}$). ^{13}C{^{1}H} NMR (101 MHz, $CDCl_3$) δ (ppm): 157.9 (*C*$_9$), 157.8 (*C*$_6$), 153.9 (*C*$_7$), 149.9 (*C*$_2$), 141.5 (*C*$_{11}$), 139.1 (*C*$_3$), 127.7 (*C*$_4$),

120.5 (C_5), 120.0 (C_{10}), 115.5 (C_{12}), 81.3 (C_{13}), 70.1 (C_{15}), 69.9 (C_{16}), 67.1 (C_{14}), 24.6 (C_{17}). ATR–IR (ν cm^{-1}): 2969, 1611, 1569, 1543, 1403, 1097, 808. UV–vis (λ nm / ε x 10^6 $M^{-1}cm^{-1}$): 240 (0.63), 292 (0.54), 359 (0.03), 456 (0.02). RP–HPLC: 8.228 min (methanol and 20% methanol in water) 95 : 5 (*v/v*). HRMS (*m/z*): calcd for [M+H^+] 433.0044, found for [M+H^+] 433.0015.

Synthesis of by-product **2d′**:

In a 15 mL Schlenk flask with a stirbar, 2-acetyl-6-bromopyridine (3.00 equiv.) was dissolved in 6 mL of EtOH, followed by the addition of KOH (6.00 equiv.). After 10 mins of stirring, ferrocenecarboxaldehyde (1.00 equiv.) was added, and the solution was stirred at 40 °C for 2 h. After 2 h, TLC of the reaction mixture showed the product and a faint spot for ferrocene carboxaldehyde (5% *v/v* ethyl acetate: pet ether as the mobile phase). The solvent was removed under vacuum, and the resulting solid was loaded onto a silica column. The unreacted ferrocenecarboxyaldehyde was eluted with a 2% *v/v* ethyl acetate: pet ether mixture, and the expected product was also collected in the same eluent. The TLC of this spot showed two closely spaced spots with a 5% *v/v* ethyl acetate: pet ether mobile phase, which were inseparable. The ^1H and ^{13}C NMR spectra showed the presence of diastereoisomers.

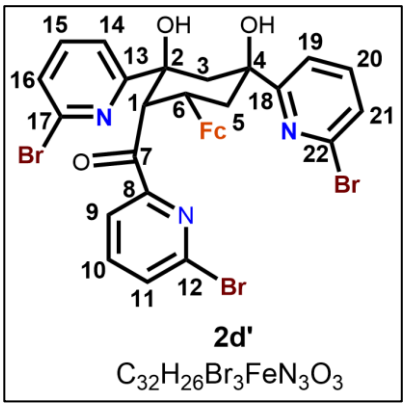

2d'

$C_{32}H_{26}Br_3FeN_3O_3$

Yield: 43% (153 mg, 0.19 mmol). ^1H NMR (400 MHz, $CDCl_3$) δ 7.90 (d, *J* = 7.6 Hz, 1H), 7.64 (d, *J* = 1.3 Hz, 3H), 7.53 (d, *J* = 7.7 Hz, 1H), 7.43 (d, *J* = 6.2 Hz, 4H), 7.13 (d, *J* = 7.7 Hz, 1H), 5.97 (s, 1H), 5.92 (d, *J* = 1.6 Hz, 1H), 5.04 (d, *J* = 11.7 Hz, 1H), 4.25 (s, 1H), 4.22 (s, 1H), 4.16 (s, 2H), 4.05 (s, 5H), 2.61 (t, *J* = 8.3 Hz, 2H), 2.42 (d, *J* = 13.5 Hz, 1H), 2.08 (q, *J* = 5.4 Hz, 1H). $^{13}C\{^1H\}$ NMR (101 MHz, $CDCl_3$) δ 197.3, 196.6, 142.2, 141.7, 140.4, 139.6, 138.8, 136.0, 132.2, 131.9, 131.4, 131.1, 130.6, 130.3, 130.2, 129.9, 129.6, 128.6, 127.8, 126.8, 125.8, 123.2, 123.0, 122.6, 122.3, 96.9, 84.9, 69.9, 69.8, 69.0, 26.6. ATR–IR (ν cm^{-1}): 3406, 1677, 1547, 1399. UV–vis (λ nm / ε x 10^3 $M^{-1}cm^{-1}$): 240 (6.1), 333 (5.3), 460 (0.97). RP–HPLC (purity): 8.218 min (80%) (mobile phase: methanol and 1% ammonium formate in water) 95:5 (*v/v*)). HRMS (*m/z*): calcd for [M–Br+Na^+] 740.9635, found for [M–Br+Na^+] 740.9421; calcd for [M–Br^+] 717.9737, found for [M–Br^+] 717.9544.

Synthesis of **2e**[11,12]:

In a 50 mL round bottom flask with a stirbar, acetophenone (1.00 equiv.) was dissolved in 4 mL of EtOH with stirring, followed by adding KOH (3.33 equiv.). When the color changed from colorless to slight orange, ferrocenecarboxyaldehyde (1.00 equiv.) was added and stirred at 45 °C for two hours, with a precipitate formation. After two hours of stirring, the reaction mixture was cooled down, and 10 mL of water was added; the precipitate was filtered and washed with water (3 × 10 mL). The red precipitate was then air-dried for 24 hours and then vacuum-dried (0.096 mbar at rt) for two hours to remove the remaining water. TLC showed a single spot. In another 50 mL round-bottom flask with a stirbar, the red precipitate obtained (1.00 equiv.) was added, followed by 4 mL of EtOH. Under stirring, 2–acetylpyridine (1.00 equiv.) and KOH (3.33 equiv.) were added and stirred for two hours at 45 °C. After two hours, the reaction mixture was cooled down, and the precipitate obtained was filtered and washed with water (3 × 10 mL). The solid obtained was then air-dried for 24 hours. The orange solid obtained was then kept in the oven at 85 °C for 4 hours to remove the water completely. The solid obtained was further used without purification. The orange precipitate was added to a 100 mL round-bottom flask with a stirbar, followed by 4 mL of EtOH. Ammonia solution (60% in water) (50 equiv.) was added and refluxed for 12 hours. After 12 hours, the solution was cooled and kept at –4 °C overnight for precipitation. After 16 hours, the solution showed no precipitation. TLC showed a new spot, along with unreacted orange precipitate. The ethanol was removed by high vacuum (0.120 mbar at 30 °C) and then purified by silica column chromatography, with 0–10% *v/v* ethyl acetate and pet ether mixture as eluent.

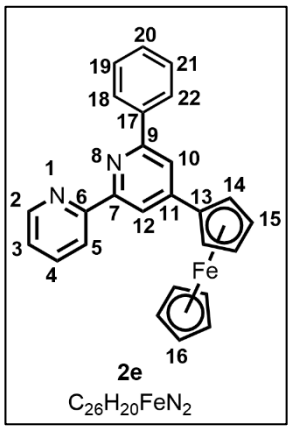

2e
$C_{26}H_{20}FeN_2$

Yield: 34% (340 mg, 0.84 mmol). ^{1}H NMR (400 MHz, $CDCl_3$) δ (ppm): 8.74 (d, J = 4.3 Hz, 1H), 8.67 (d, J = 7.9 Hz, 1H), 8.45 (s, 1H), 8.19 (d, J = 7.6 Hz, 2H), 7.86 (t, J = 7.6 Hz, 1H), 7.82 (s, 1H), 7.54 (t, J = 7.4 Hz, 2H), 7.46 (t, J = 7.0 Hz, 1H), 7.34 (t, J = 6.0 Hz, 1H), 4.93 (s, 2H), 4.46 (s, 2H), 4.10 (s, 5H). ^{13}C{^{1}H} NMR (101 MHz, $CDCl_3$) δ (ppm): 156.6, 155.8, 150.5, 149.1, 139.8, 136.9, 129.0, 128.8, 127.1, 123.8, 121.6, 117.3, 116.3), 81.8, 70.2, 70.1, 67.3. ATR–IR (ν cm^{-1}): 3098, 2922, 1602, 1550. UV–vis (λ nm / ε x 10^3 $M^{-1}cm^{-1}$): 248 (15.1), 284 (10.7), 366 (0.97), 454 (0.47). RP−HPLC (purity): 8.062 min (98%) (mobile phase: acetonitrile and 1% ammonium formate in water) 95:5 (*v/v*)). HRMS (*m/z*): calcd for $[M+H]^+$ 417.1054, found for $[M+H^+]$ 417.1069.

Synthesis of **3a**–**e**:

The Re(I) complexes were synthesized using a modified procedure for the [Re(I)(bpy)(CO)$_3$Cl] complex[13]. A Schlenk flask with a magnetic stirbar was charged with the ligand (1.00 equiv.) in 3 mL of dry toluene under Ar atmosphere. Re(CO)$_5$Br (1.00 equiv.) was added to this solution, and the reaction mixture was refluxed at 110 °C, where the color changed from brown to red. After the color change was observed, the mixture was stirred for another four hours and then cooled to room temperature, leading to a dark-colored precipitate. The solution was kept at –4 °C overnight to obtain more precipitate. The dark red solution was decanted, and the precipitate was washed with toluene (2 × 5 mL) and cold diethyl ether (2 × 5 mL). The compound was dried under vacuum at 0.30 mbar for 20 min.

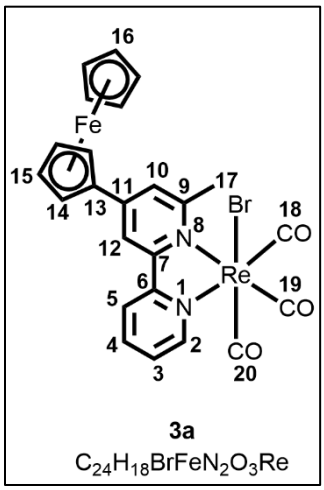

3a

$C_{24}H_{18}BrFeN_2O_3Re$

Yield: 69% (59.0 mg, 0.084 mmol). ^{1}H NMR (400 MHz, $CDCl_3$) δ (ppm): 9.12 (d, *J* = 5.4 Hz, 1H), 8.19 (d, *J* = 8.2 Hz, 1H), 8.02 (t, *J* = 7.9 Hz, 1H), 7.90 (s, 1H), 7.48 (t, *J* = 6.4 Hz, 1H), 7.42 (s, 1H), 4.81 (d, *J* = 9.4 Hz, 2H), 4.59 (s, 2H), 4.12 (s, 5H), 3.02 (s, 3H). ^{1}H NMR (400 MHz, DMSO-D_6) δ 9.06 (d, *J* = 5.4 Hz, 1H, H_5), 8.95 (d, *J* = 8.5 Hz, 1H, H_2), 8.51 (s, 1H, H_{12}), 8.33 (t, *J* = 8.3 Hz, 1H, H_3), 7.90 (s, 1H, H_{10}), 7.75 (t, *J* = 6.5 Hz, 1H, H_4), 5.31 (s, 2H, H_{14}), 4.67 (s, 2H, H_{15}), 4.12 (s, 5H, H_{16}), 2.91 (s, 3H, H_{17}). ^{13}C{^{1}H} NMR (101 MHz, DMSO-D_6) δ 197.8 (CO), 197.2 (CO), 189.3 (CO), 160.6 (C_9), 156.6 (C_6), 155.9 (C_7), 153.8 (C_{11}), 152.6 (C_5), 140.1 (C_8), 127.4 (C_3), 124.7 (C_4), 122.9 (C_{10}), 117.9 (C_{12}), 78.0 (C_{13}), 71.7 (C_{15}), 70.2 (C_{16}), 68.2 (C_{14}), 30.1 (C_{17}). ATR–IR (ν cm^{-1}): 2009, 1896, 1874 (CO peaks). UV–vis (λ nm / ε x 10^6 M^{-1}cm^{-1}): 248 (0.49), 309 (0.44), 363 (0.11), 505 (0.05). RP–HPLC: 3.168 min (methanol and 1% ammonium formate in water) 95 : 5 (*v*/*v*). HRMS (*m*/*z*): calcd for [M]$^+$ 703.9408, found [M]$^+$ 703.9379. Anal calcd (in %) for $C_{24}H_{18}BrFeN_2O_3Re$: C, 40.91; H, 2.58; N, 3.98. Found: C, 41.70; H, 2.66; N, 4.11.

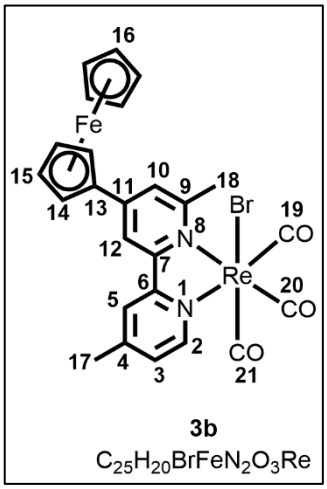

3b

$C_{25}H_{20}BrFeN_2O_3Re$

Yield: 75% (65 mg, 0.091 mmol). ^{1}H NMR (400 MHz, DMSO-D$_6$) δ (ppm): 8.88 (d, *J* = 5.5 Hz, 1H, *H*$_2$), 8.81 (s, 1H, *H*$_5$), 8.48 (s, 1H, *H*$_{12}$), 7.90 (s, 1H, *H*$_{10}$), 7.58 (d, *J* = 5.9 Hz, 1H, *H*$_3$), 5.31 (s, 2H, *H*$_{14}$), 4.68 (s, 2H, *H*$_{15}$), 4.13 (s, 5H, *H*$_{16}$), 2.90 (s, 3H, *H*$_{18}$), 2.60 (s, 3H, *H*$_{17}$). ^{13}C{^{1}H} NMR (101 MHz, DMSO-D$_6$) δ (ppm): 197.7 (CO), 197.4 (CO), 189.3 (CO), 160.5 (*C*$_9$), 156.1 (*C*$_6$), 156.0 (*C*$_7$), 153.6 (*C*$_4$), 152.1 (*C*$_{11}$), 151.9 (*C*$_2$), 128.0 (*C*$_3$), 125.1 (*C*$_5$), 122.7 (*C*$_{10}$), 117.6(*C*$_{12}$), 78.0 (*C*$_{13}$), 71.6 (*C*$_{15}$), 70.1 (*C*$_{16}$), 68.0 (*C*$_{14}$), 30.5 (*C*$_{18}$), 20.9 (*C*$_{17}$). ATR–IR (ν cm^{-1}): 2008, 1884 (CO peaks). UV–vis (λ nm / ε x 10^6 M^{-1}cm^{-1}): 206 (1.24), 249 (0.61), 306 (0.44), 324 (0.34), 505 (0.05). RP–HPLC: 2.092 min (methanol and 1% ammonium formate in water) 95 : 5 (*v*/*v*). HRMS (*m*/*z*): calcd for [M]$^+$ 717.9564, found [M]$^+$ 717.9556. Anal calcd (in %) for $C_{25}H_{20}BrFeN_2O_3Re$: C, 41.78; H, 2.81; N, 3.90. Found: C, 40.46; H, 2.79; N, 3.79.

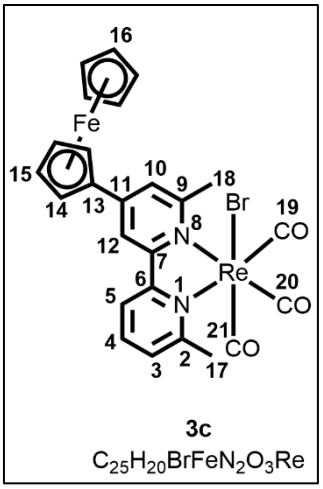

3c

$C_{25}H_{20}BrFeN_2O_3Re$

Yield: 50% (43 mg, 0.061 mmol). ^{1}H NMR (400 MHz, DMSO-D$_6$) δ (ppm): 8.77 (d, *J* = 7.8 Hz, 1H, *H*$_3$), 8.45 (s, 1H, *H*$_{12}$), 8.20 (t, *J* = 7.9 Hz, 1H, *H*$_4$), 7.84 (s, 1H, *H*$_{10}$), 7.75 (d, *J* = 7.8 Hz, 1H, *H*$_5$), 5.31 (s, 2H, *H*$_{14}$), 4.66 (s, 2H, *H*$_{15}$), 4.11 (s, 5H, *H*$_{16}$), 3.00 (s, 3H, *H*$_{17}$), 2.95 (s, 3H, *H*$_{18}$). ^{13}C{^{1}H} NMR (101 MHz, DMSO-D$_6$) δ (ppm): 197.1 (CO), 197.1 (CO), 189.0 (CO), 161.3 (*C*$_9$), 160.5 (*C*$_2$), 157.8 (*C*$_6$), 157.2 (*C*$_7$), 153.6 (*C*$_{11}$), 139.9 (*C*$_4$), 126.8 (*C*$_5$), 122.3 (*C*$_{10}$), 122.0 (*C*$_3$), 117.9 (*C*$_{12}$), 78.0 (*C*$_{13}$), 71.5 (*C*$_{15}$), 70.0 (*C*$_{16}$), 68.0 (*C*$_{14}$), 29.6 (*C*$_{17}$), 29.3 (*C*$_{18}$). ATR–IR (ν cm^{-1}): 2007, 1872 (CO peaks). UV–vis (λ nm / ε x 10^6 M^{-1}cm^{-1}): 252 (0.86), 305 (0.73), 332 (0.54), 369 (0.16), 503 (0.08). RP–HPLC: 2.040 min (methanol and 1% ammonium formate in water) 95 : 5 (*v*/*v*). HRMS (*m*/*z*): calcd for [M]$^+$ 717.9564, found [M]$^+$ 717.9532. Anal calcd (in %) $C_{25}H_{20}BrFeN_2O_3Re$: C, 41.78; H, 2.81; N, 3.90. Found: C, 40.73; H, 3.13; N, 4.04.

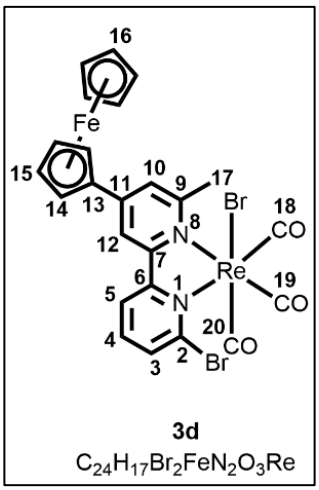

3d

$C_{24}H_{17}Br_2FeN_2O_3Re$

Yield: 72% (68 mg, 0.087 mmol).^{1}H NMR (400 MHz, DMSO-D_6) δ (ppm): 8.96 (d, *J* = 7.8 Hz, 1H, *H*$_3$), 8.46 (s, 1H, *H*$_{12}$), 8.21 (t, *J* = 8.0 Hz, 1H, *H*$_4$), 8.14 (d, *J* = 7.5 Hz, 1H, *H*$_5$), 7.85 (s, 1H, *H*$_{10}$), 7.25 (t, *J* = 7.5 Hz, 1H) (Toluene), 7.16 (d, *J* = 7.4 Hz, 1H) (Toluene), 5.32 (s, 2H, *H*$_{14}$), 4.67 (s, 2H, *H*$_{15}$), 4.12 (s, 5H, *H*$_{16}$), 2.94 (s, 3H, *H*$_{17}$), 2.30 (s, 1.5H) (Toluene). ^{13}C{^{1}H} NMR (101 MHz, DMSO-D_6) δ (ppm): 197.4 (CO), 197.3 (CO), 189.8 (CO), 160.7 (*C*$_9$), 159.8 (*C*$_6$), 157.0 (*C*$_5$), 153.7 (*C*$_2$), 145.7 (*C*$_7$), 141.8 (*C*$_5$), 137.3 (Toluene), 131.0 (Toluene), 128.9 (Toluene), 128.2 (Toluene), 125.3 (*C*$_4$), 123.5 (*C*$_3$), 122.4 (*C*$_{10}$), 118.8 (*C*$_{12}$), 77.9 (*C*$_{13}$), 71.7 (*C*$_{15}$), 70.1 (*C*$_{16}$), 68.1 (*C*$_{14}$), 29.3 (*C*$_{17}$), 21.0 (Toluene). ATR–IR (ν cm^{-1}): 2006, 1883 (CO peaks). UV–vis (λ nm / ε x 10^6 M^{-1}cm^{-1}): 247 (0.44), 317 (0.39), 339 (0.30), 371 (0.96), 513 (0.05). RP–HPLC: 2.137 min (methanol and 1% ammonium formate in water) 95 : 5 (*v*/*v*). HRMS (*m*/*z*): calcd for [M]$^+$ 781.8513, found [M]$^+$ 781.8480. Anal calcd (in %) for $C_{24}H_{17}Br_2FeN_2O_3Re\cdot(0.5)CH_3C_6H_5$: C, 39.86; H, 2.56; N, 3.38. Found: C, 40.25; H, 2.69; N, 3.31.

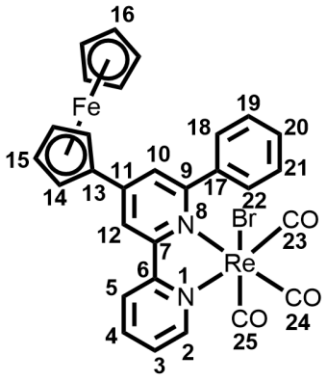

3e

$C_{29}H_{20}BrFeN_2O_3Re$

Yield: 78% (37.0 mg, 0.050 mmol). ^{1}H NMR (400 MHz, $CDCl_3$) δ (ppm): 9.11 (d, *J* = 5.0 Hz, 1H), 8.29 (d, *J* = 8.2 Hz, 1H), 8.07 (s, 1H), 8.03 (t, *J* = 4.6 Hz, 1H), 7.66 (s, 2H), 7.59 (s, 3H), 7.52 (d, *J* = 1.6 Hz, 1H), 7.48 (t, *J* = 6.5 Hz, 1H), 4.85 (d, *J* = 24.7 Hz, 2H), 4.61 (s, 2H), 4.13 (s, 5H). ^{1}H NMR (400 MHz, DMSO–D_6) δ 9.04 (d, *J* = 5.3 Hz, 1H, *H*$_1$), 8.97 (d, *J* = 8.2 Hz, 1H, *H*$_4$), 8.65 (s, 1H, *H*$_7$), 8.35 (t, *J* = 7.9 Hz, 1H, *H*$_3$), 7.80 (s, 1H, *H*$_9$), 7.74 (t, *J* = 6.5 Hz, 1H, *H*$_2$), 7.62 (bs, 2H, *H*$_{18}$ & *H*$_{22}$), 7.58 (bs, 3H, *H*$_{19,}$ *H*$_{20}$ & *H*$_{21}$), 5.40 (d, *J* = 14.6 Hz, 2H, *H*$_{14}$), 4.67 (s, 2H, *H*$_{15}$), 4.13 (s, 5H, *H*$_{16}$). ^{13}C{^{1}H} NMR (101 MHz, DMSO–D_6) δ 197.6 (CO), 193.5 (CO), 191.1 (CO), 162.6 (*C*$_6$), 157.2 (*C*$_5$), 156.4 (*C*$_{10}$), 154.3 (*C*$_1$), 152.9 (*C*$_4$), 142.0 (*C*$_3$), 139.9 (*C*$_2$), 129.9 (*C*$_7$), 129.3 (*C*$_8$ & *C*$_{11}$), 127.3 (*C*$_9$), 125.3 (*C*$_{12}$ & *C*$_{16}$), 122.9 (*C*$_{13}$ & *C*$_{15}$), 118.9 (*C*$_{14}$), 77.8 (*C*$_{17}$), 72.1 (*C*$_{19}$), 70.5 (*C*$_{20}$), 68.6 (*C*$_{18}$), 68.2 (*C*$_{18}$). ATR–IR (ν cm^{-1}): 2020, 1919, 1892 (CO peaks). UV-vis (λ nm / ε x 10^3 M^{-1}cm^{-1}): 254 (4.89), 312 (4.49), 366 (1.11), 512 (0.57). RP−HPLC (purity): 4.183 min (97%) (mobile phase: acetonitrile and 1% ammonium formate in water) 95:5 (*v*/*v*)). HRMS (*m*/*z*): calcd for [M+Na]$^+$ 788.9480, found [M+Na]$^+$ 788.8940; calcd for [M–Br]$^+$

687.0400, found $[M–Br]^+$ 686.9947. Anal calcd (in %) for $C_{29}H_{20}BrFeN_2O_3Re$: C, 45.43; H, 2.61; N, 3.65. Found: C, 45.47; H, 2.68; N, 3.86.

Characterisation of chalcones:

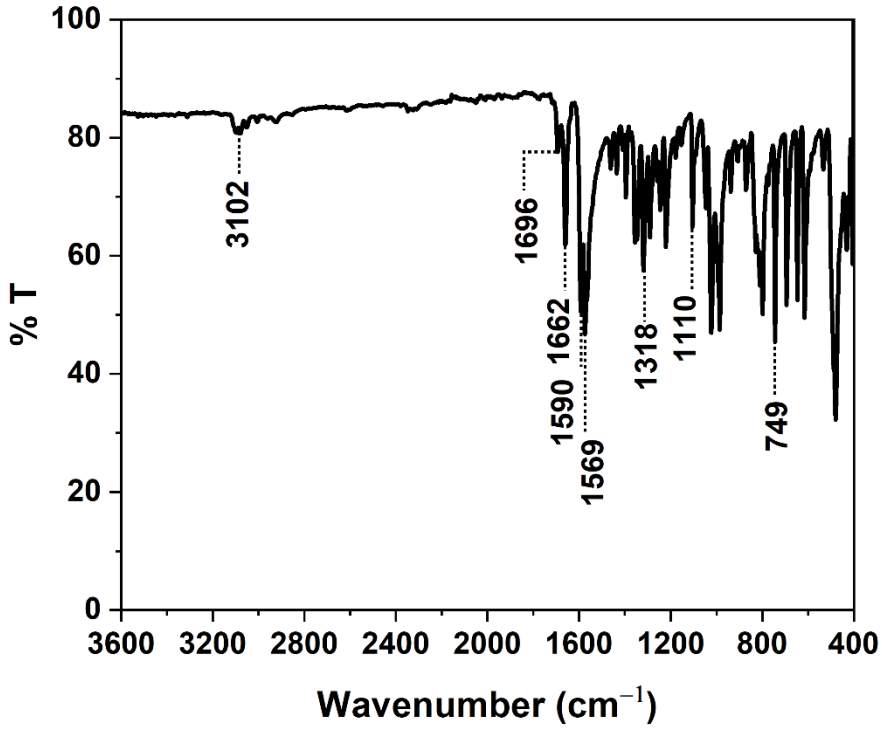

Figure S1a: ATR–IR spectrum of **1a**.

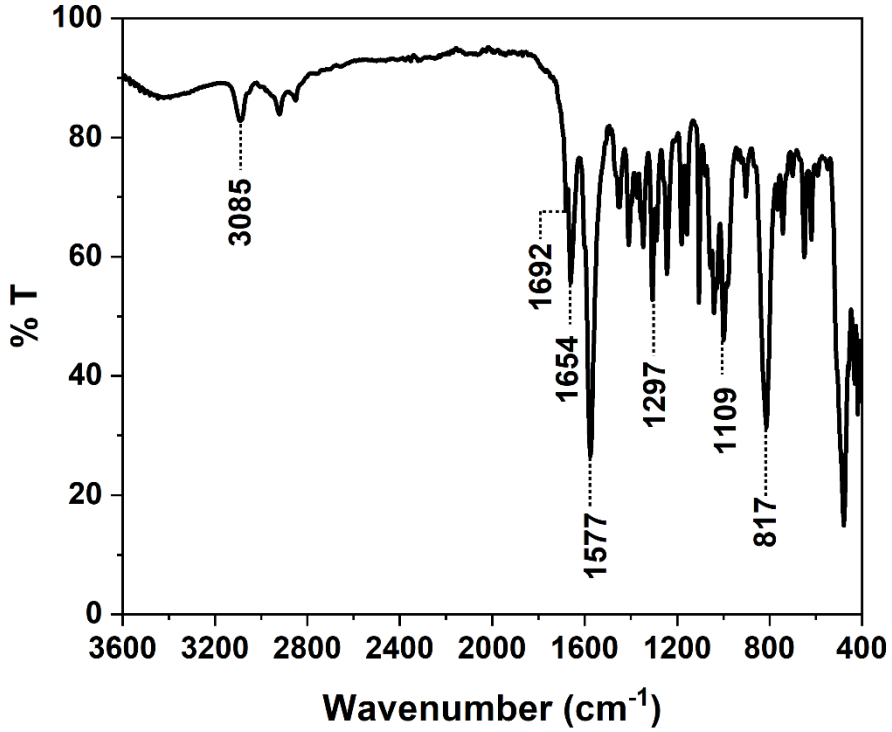

Figure S1b: ATR–IR spectrum of **1b**.

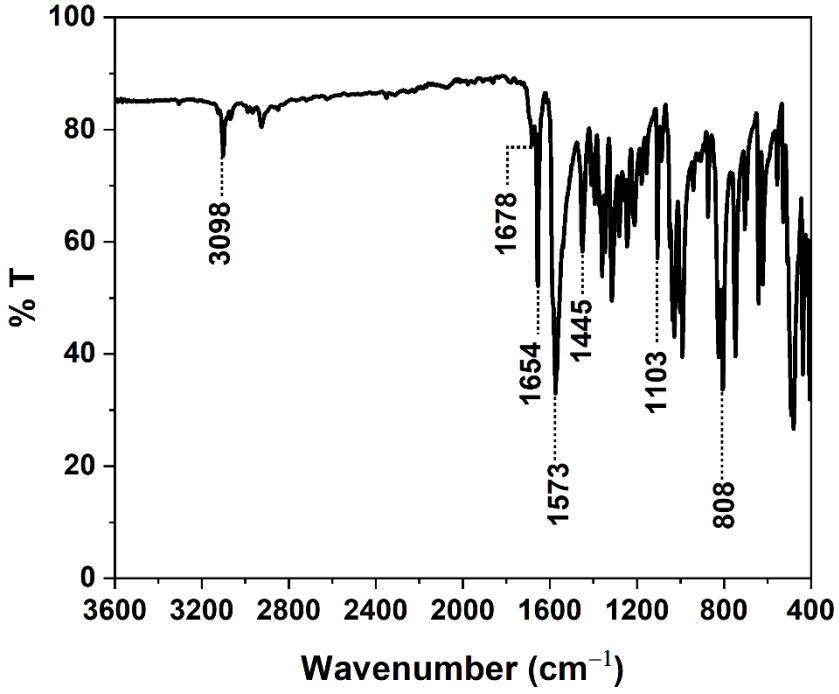

Figure S1c: ATR–IR spectrum of **1c**.

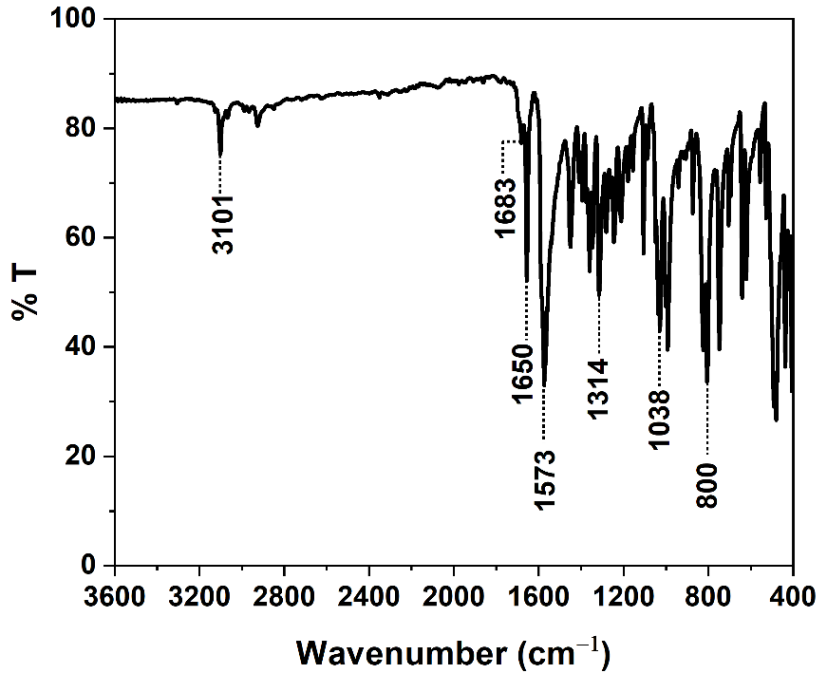

Figure S1d: ATR–IR spectrum of **1d**.

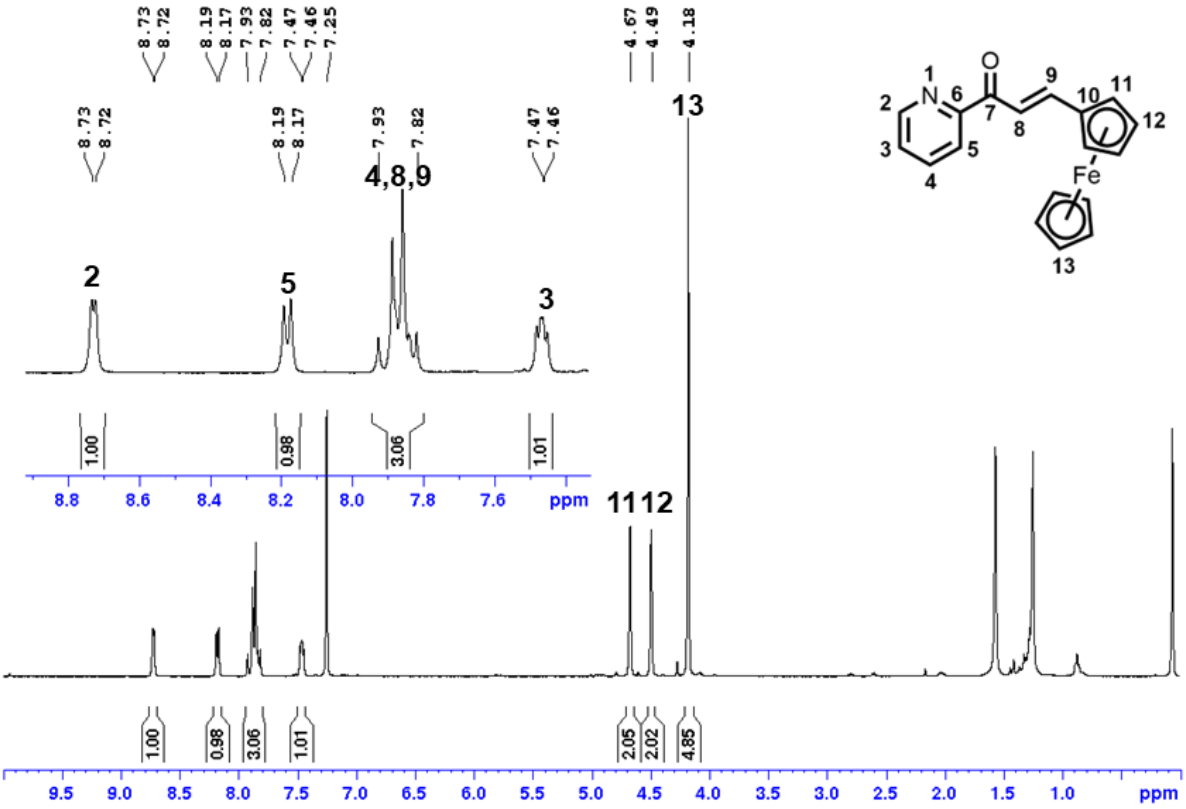

Figure S1e: ^{1}H NMR spectrum (400 MHz, $CDCl_3$) of **1a**.

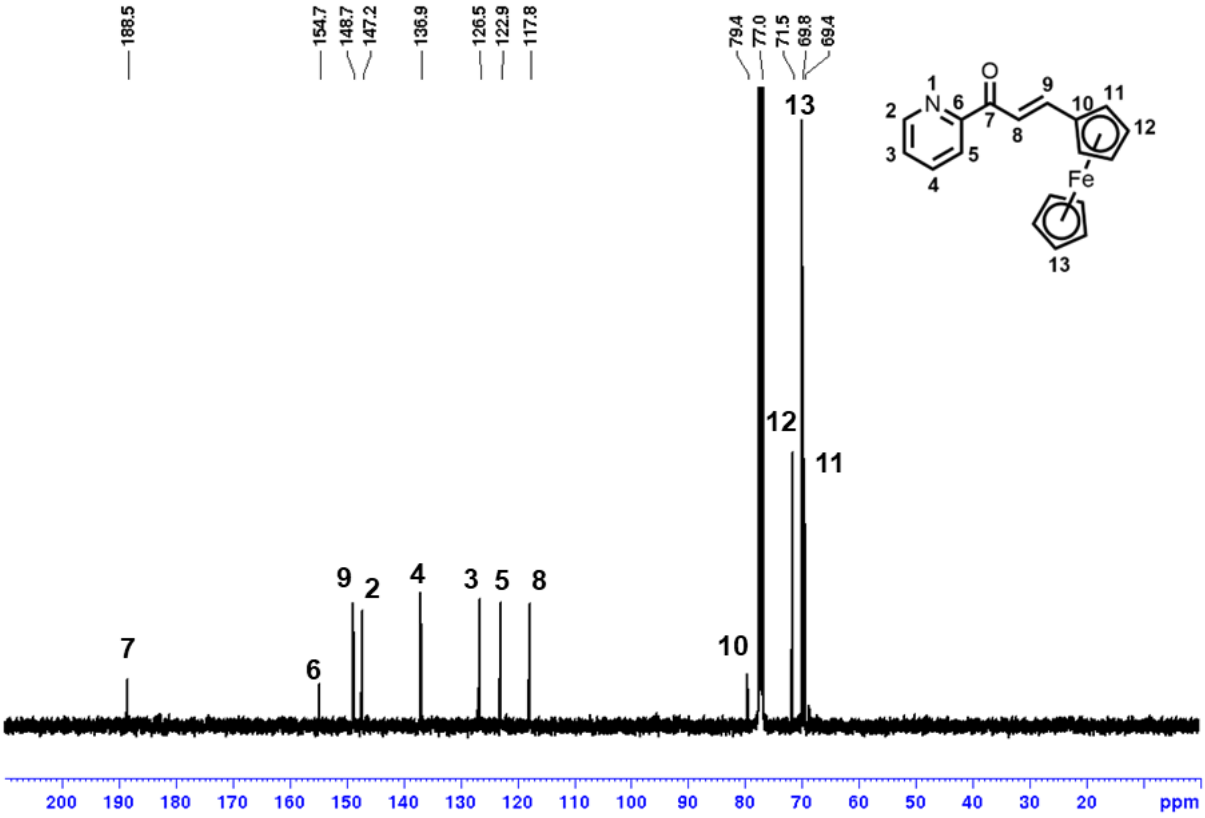

Figure S1f: $^{13}C\{^{1}H\}$ NMR spectrum (101 MHz, $CDCl_3$) of **1a**.

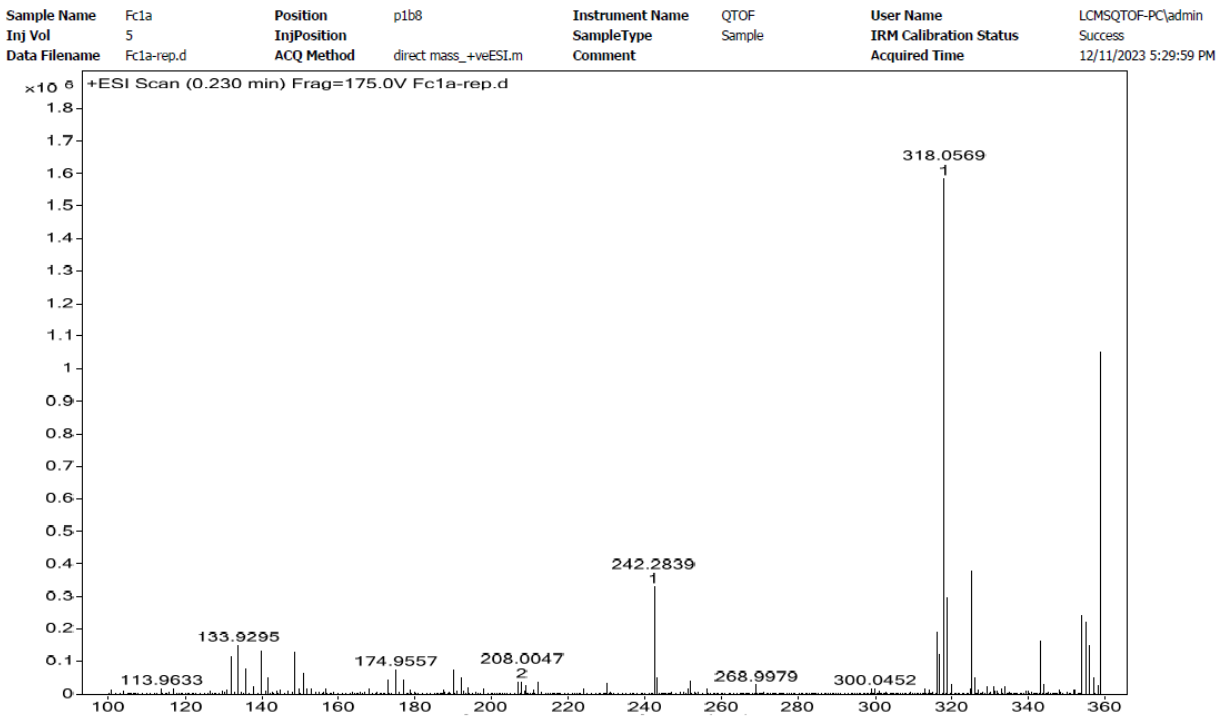

Figure S1g: HRMS spectrum of **1a** (M: $C_{18}H_{15}FeNO$); *m/z* calcd. for [M+H$^+$] 318.0622, *m/z* found for [M+H$^+$] 318.0569.

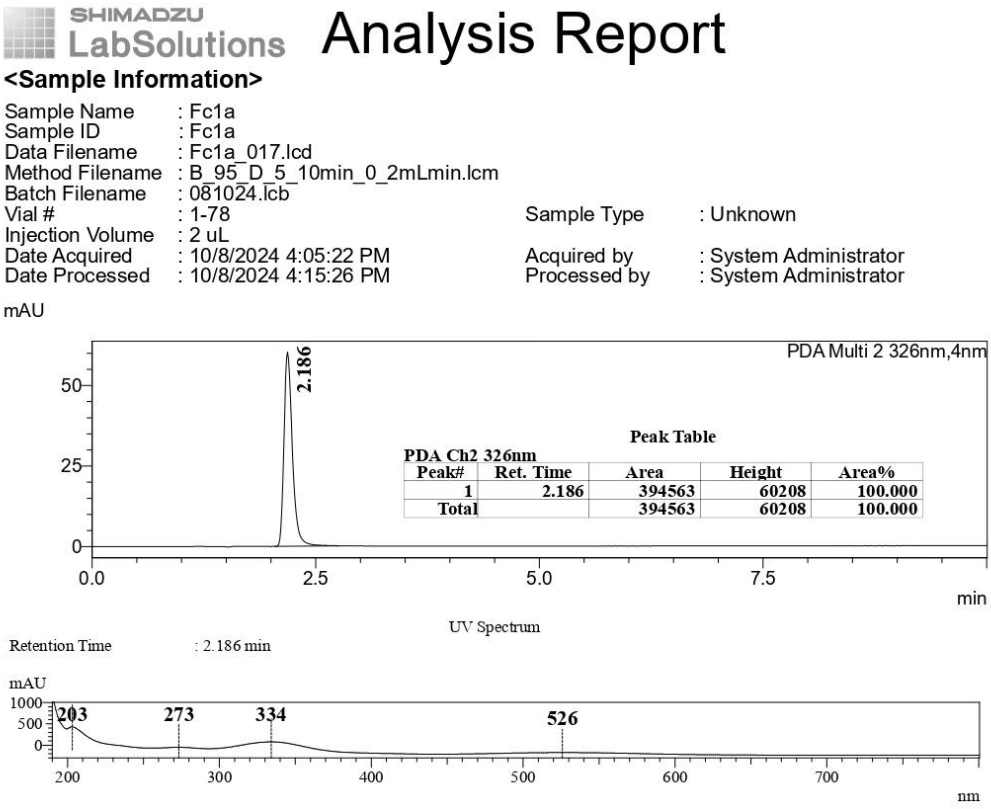

Figure S1h: RP–HPLC–MS **1a**; HPLC purity 100%; UV–vis spectrum shown at Rt = 2.186 min.

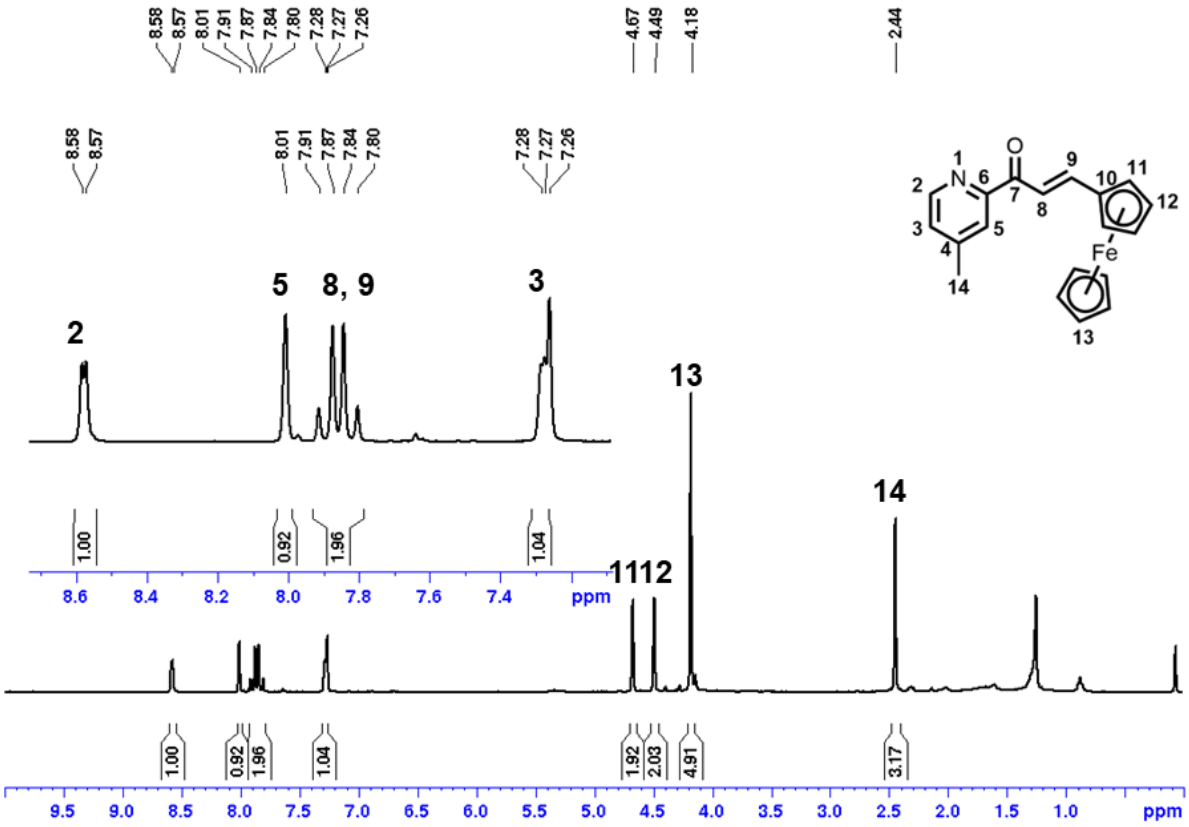

Figure S1i: ^{1}H NMR spectrum (400 MHz, $CDCl_3$) of **1b**.

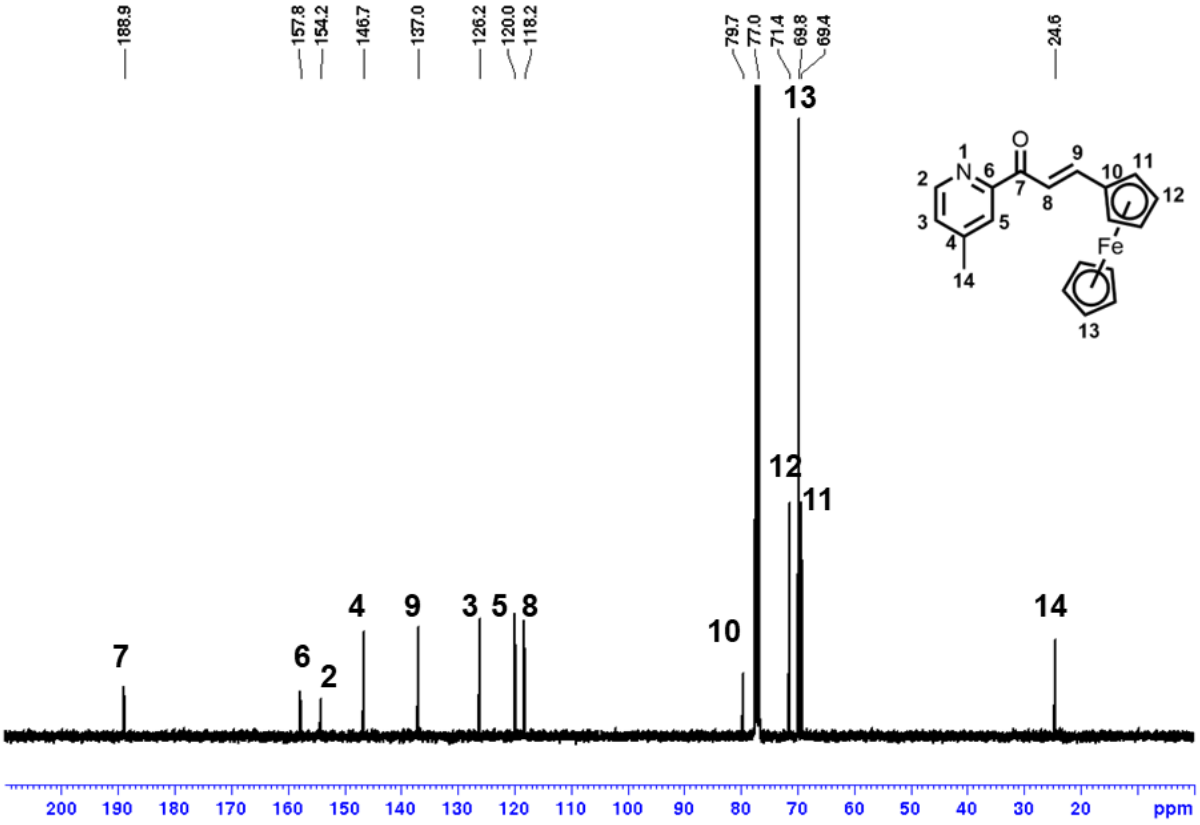

Figure S1j: $^{13}C\{^{1}H\}$ NMR spectrum (101 MHz, $CDCl_3$) of **1b**.

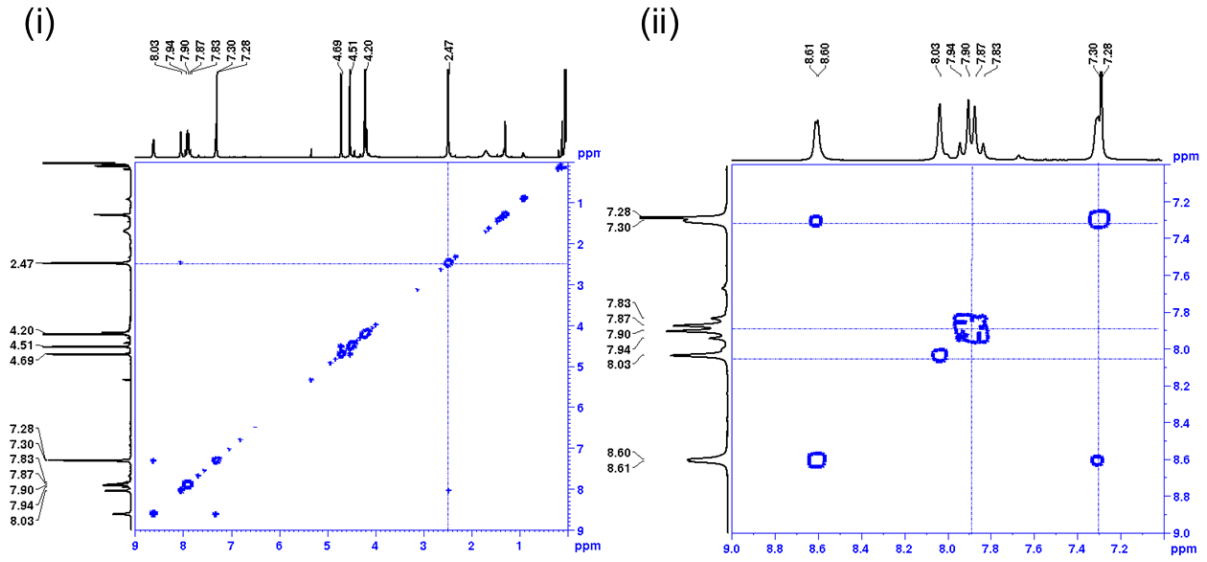

Figure S1k: (i) $^{1}H–^{1}H$ correlation spectrum of **1b** (0–9 ppm) shows the correlation between methyl and aromatic protons; (ii) Section of $^{1}H–^{1}H$ correlation spectrum (7–9 ppm) shows the correlations amongst the aromatic protons.

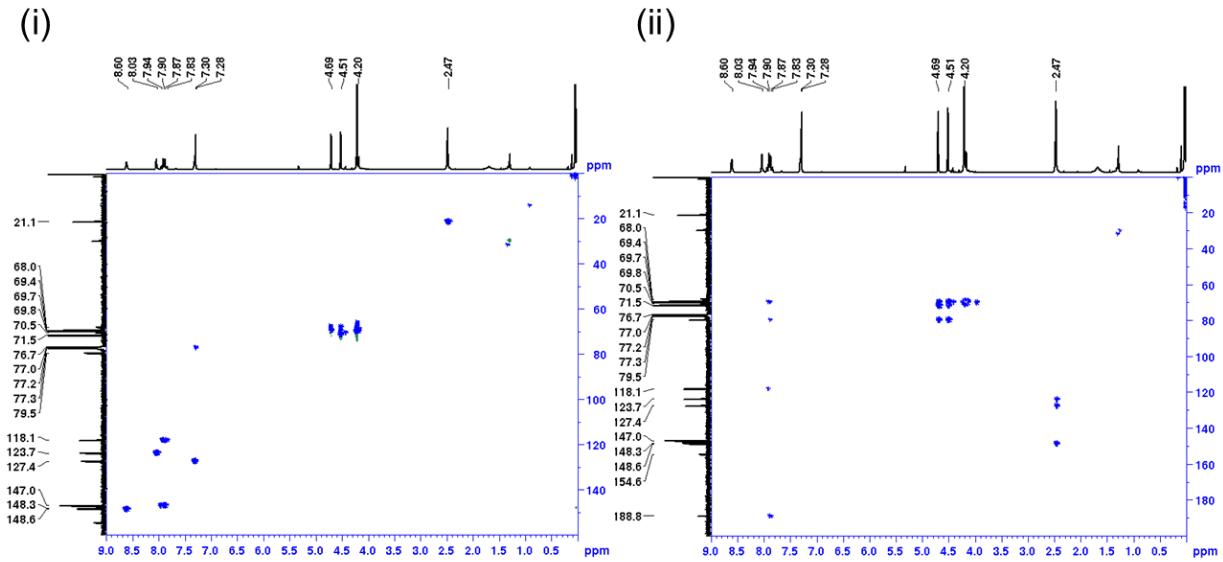

Figure S1l: (i) HSQC and (ii) HMBC spectra of **1b**.

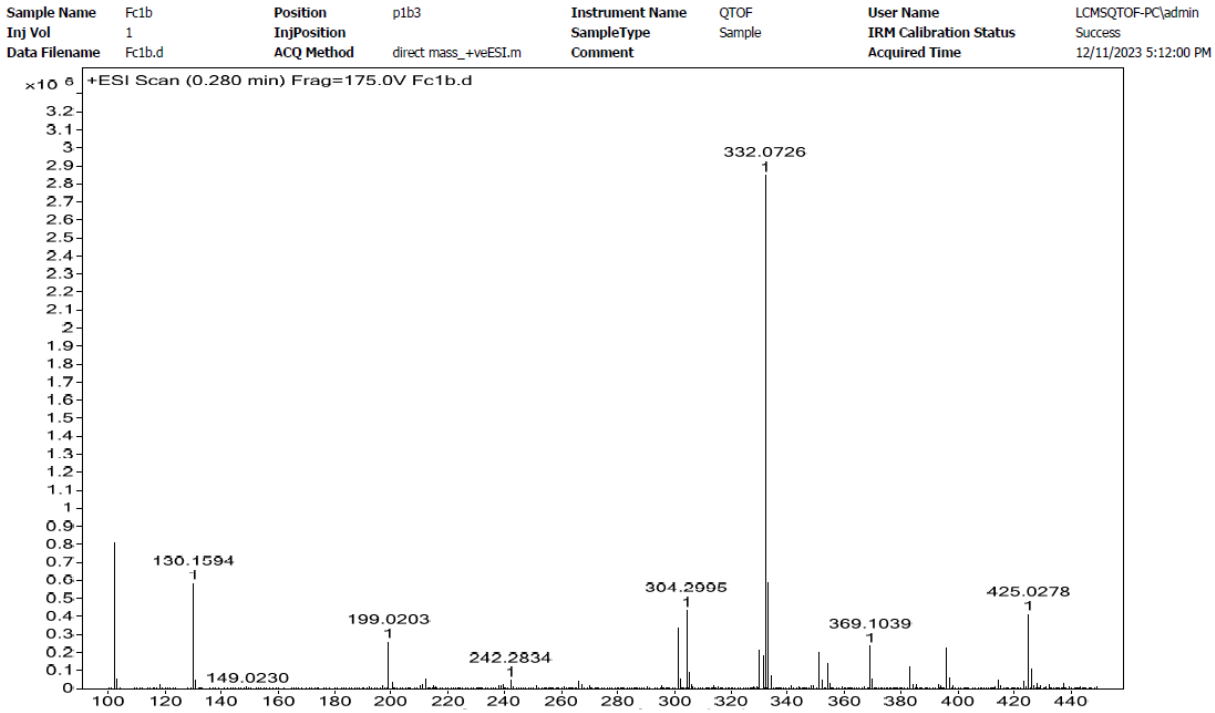

Figure S1m: HRMS spectrum of **1b** (M: $C_{19}H_{17}FeNO$); *m/z* calcd. for [M+H$^+$] 332.0779, *m/z* found for [M+H$^+$] 332.0726.

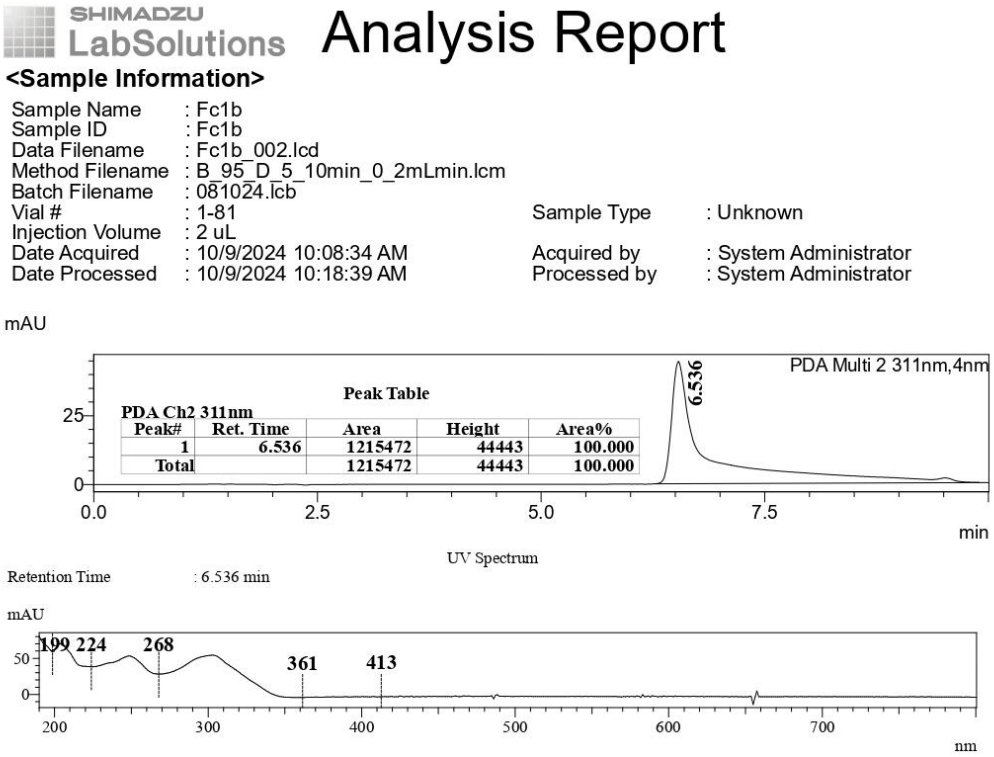

Figure S1n: RP–HPLC–MS **1b**; HPLC purity 100%; UV–vis spectrum shown at Rt = 6.536 min.

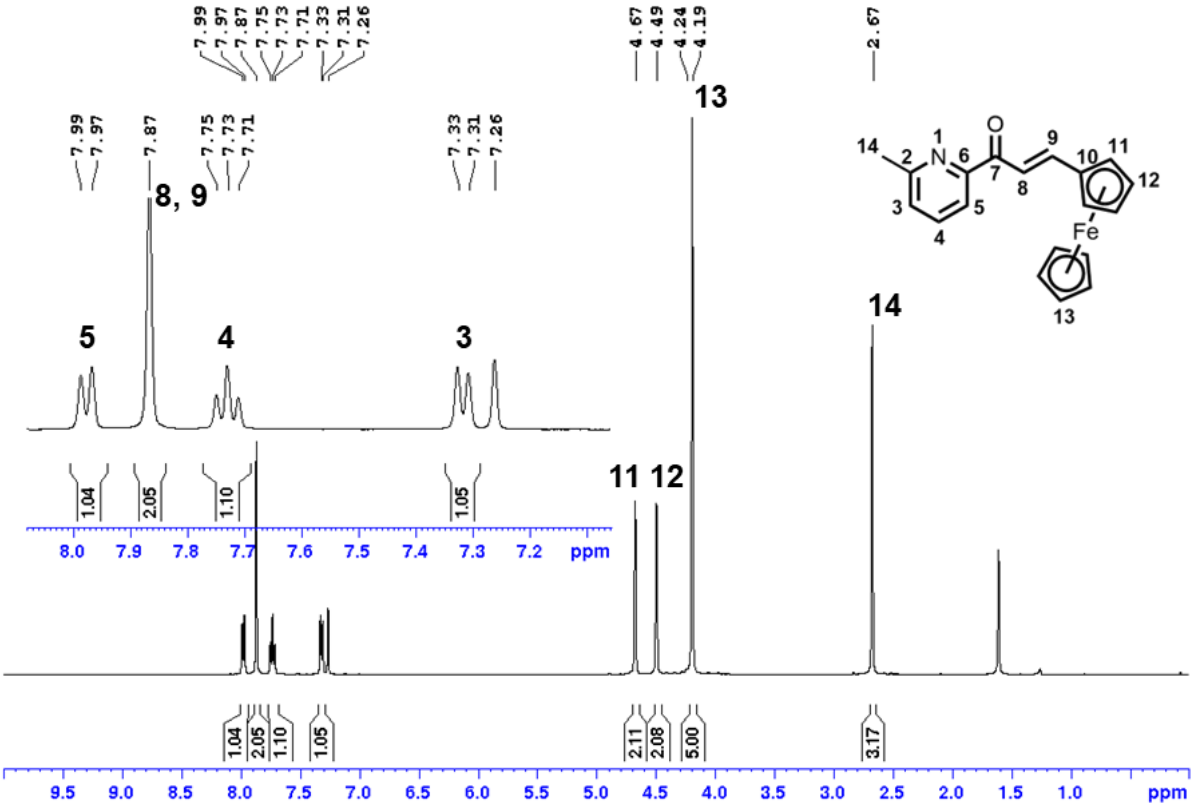

Figure S1o: ^{1}H NMR spectrum (400 MHz, $CDCl_3$) of **1c**.

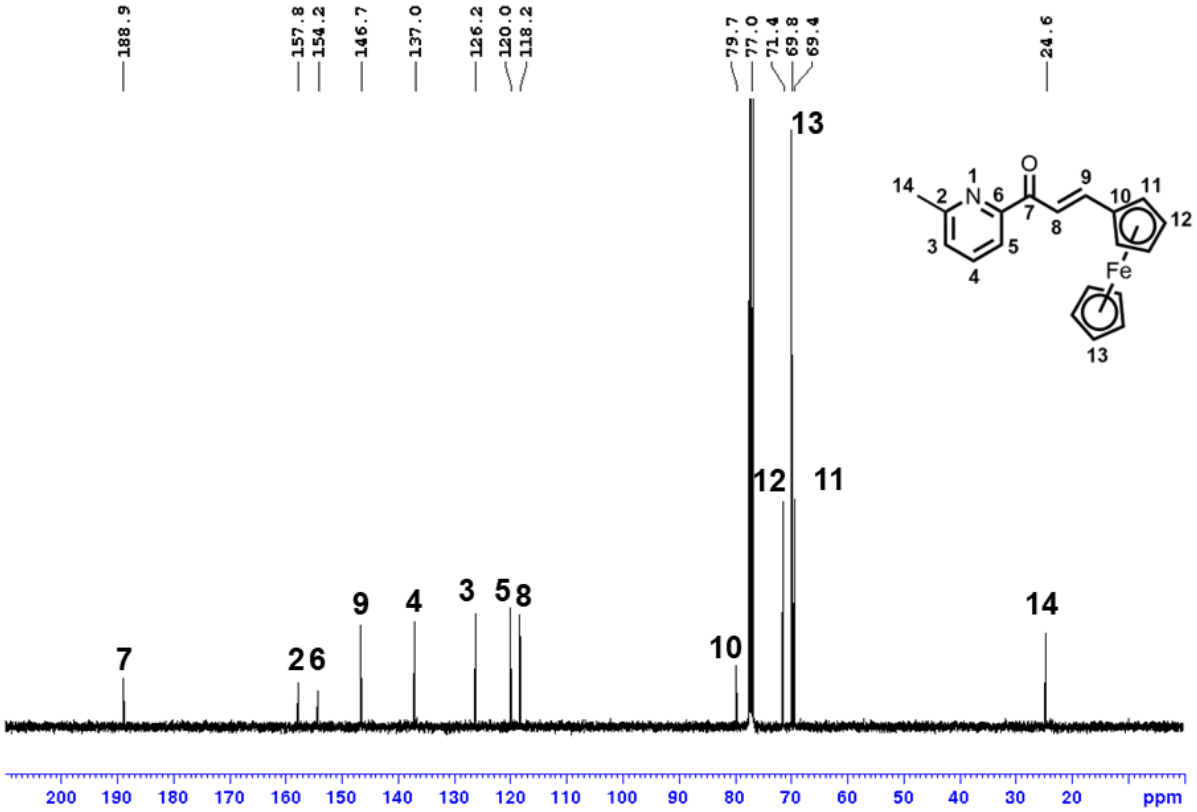

Figure S1p: $^{13}C\{^{1}H\}$ NMR spectrum (101 MHz, $CDCl_3$) of **1c**.

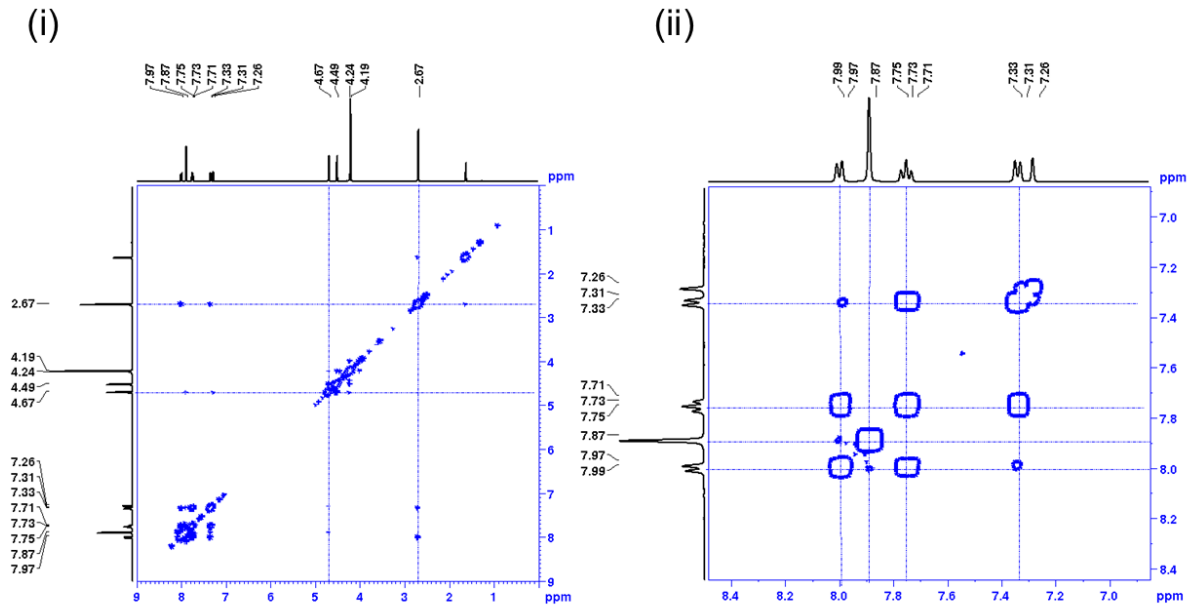

Figure S1q: (i) ^{1}H–^{1}H correlation spectrum of **1c** (0–9 ppm) shows the correlation between methyl-aromatic protons, and ferrocene protons with aromatic protons; (ii) Section of ^{1}H–^{1}H correlation spectrum (7–9 ppm) shows the correlations amongst the aromatic protons.

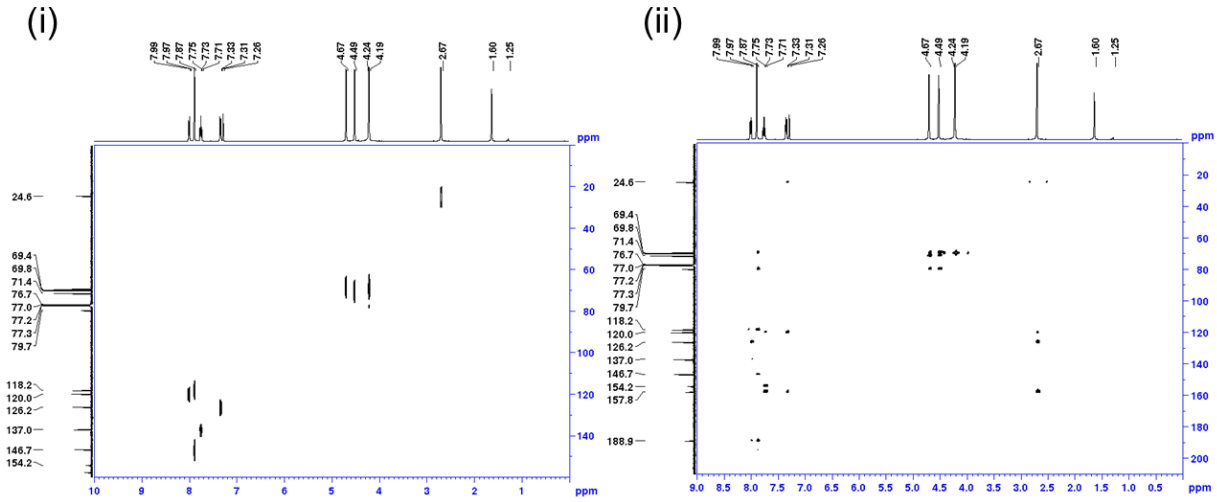

Figure S1r: (i) HSQC and (ii) HMBC spectra of **1c**.

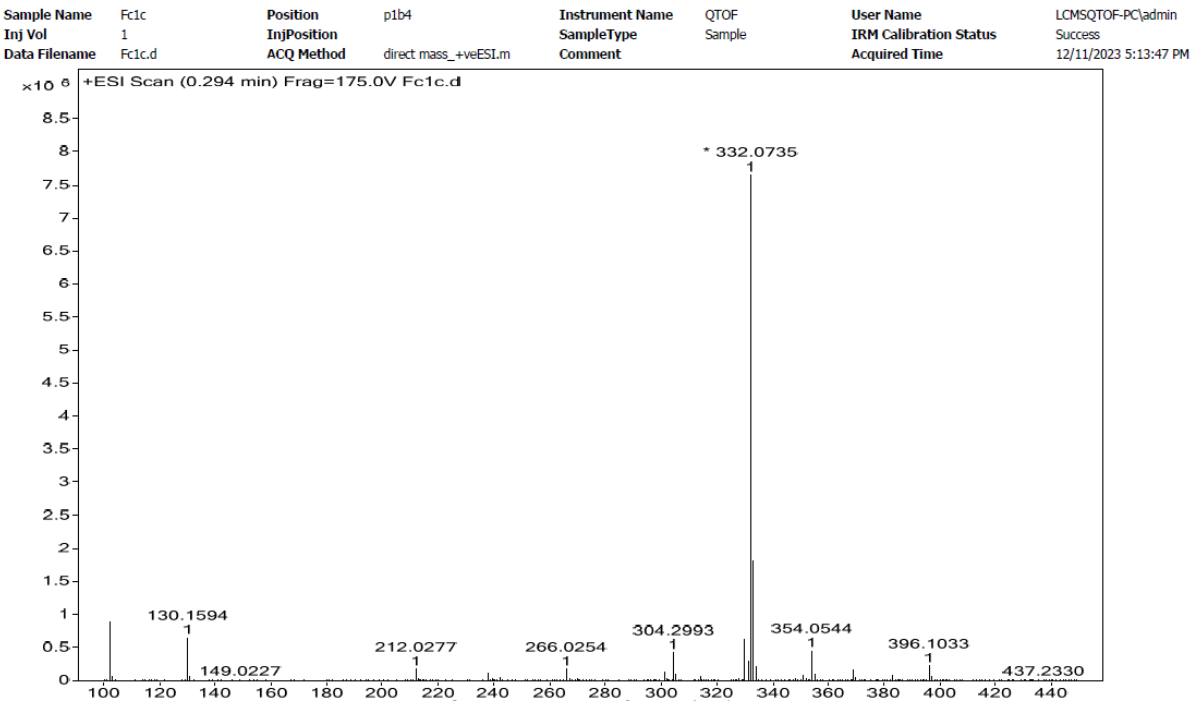

Figure S1s: HRMS spectrum of **1c** (M: $C_{19}H_{17}FeNO$); *m/z* calcd for $[M+H^+]$ 332.0779, *m/z* found for $[M+H^+]$ 332.0735.

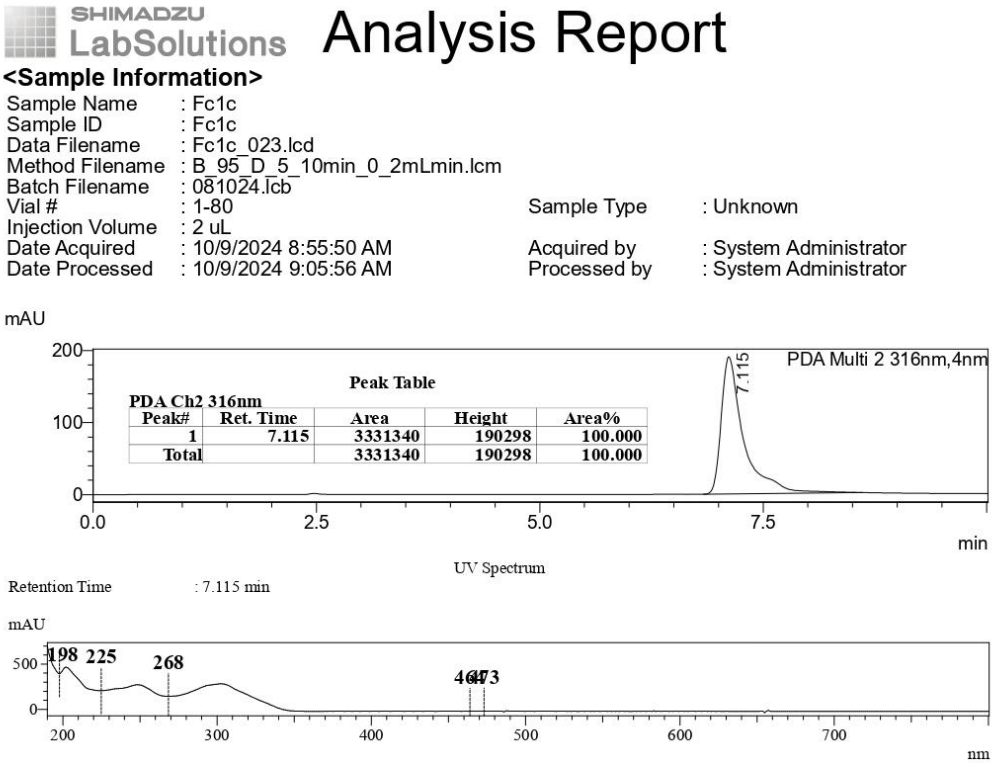

Figure S1t: RP–HPLC–MS **1c**; HPLC purity 100%; UV–vis spectrum shown at Rt = 7.115 min.

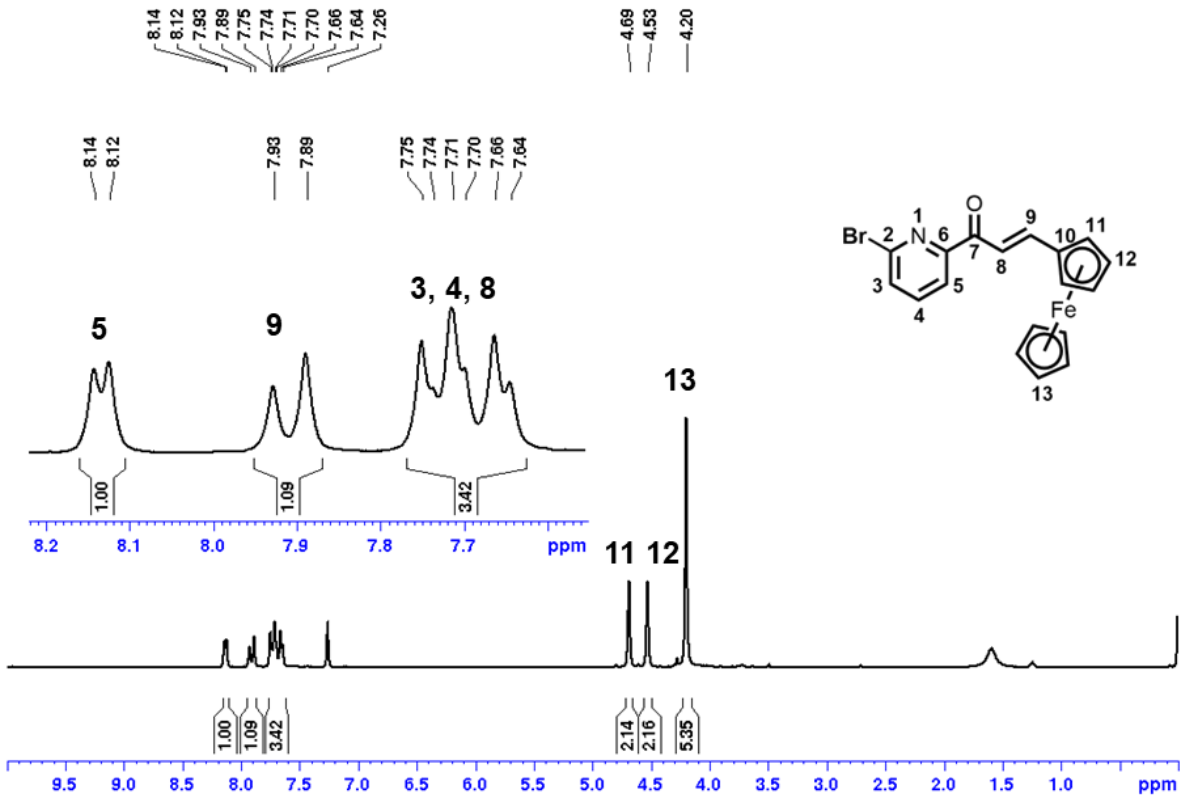

Figure S1u: ^{1}H NMR spectrum (400 MHz, $CDCl_3$) of **1d**.

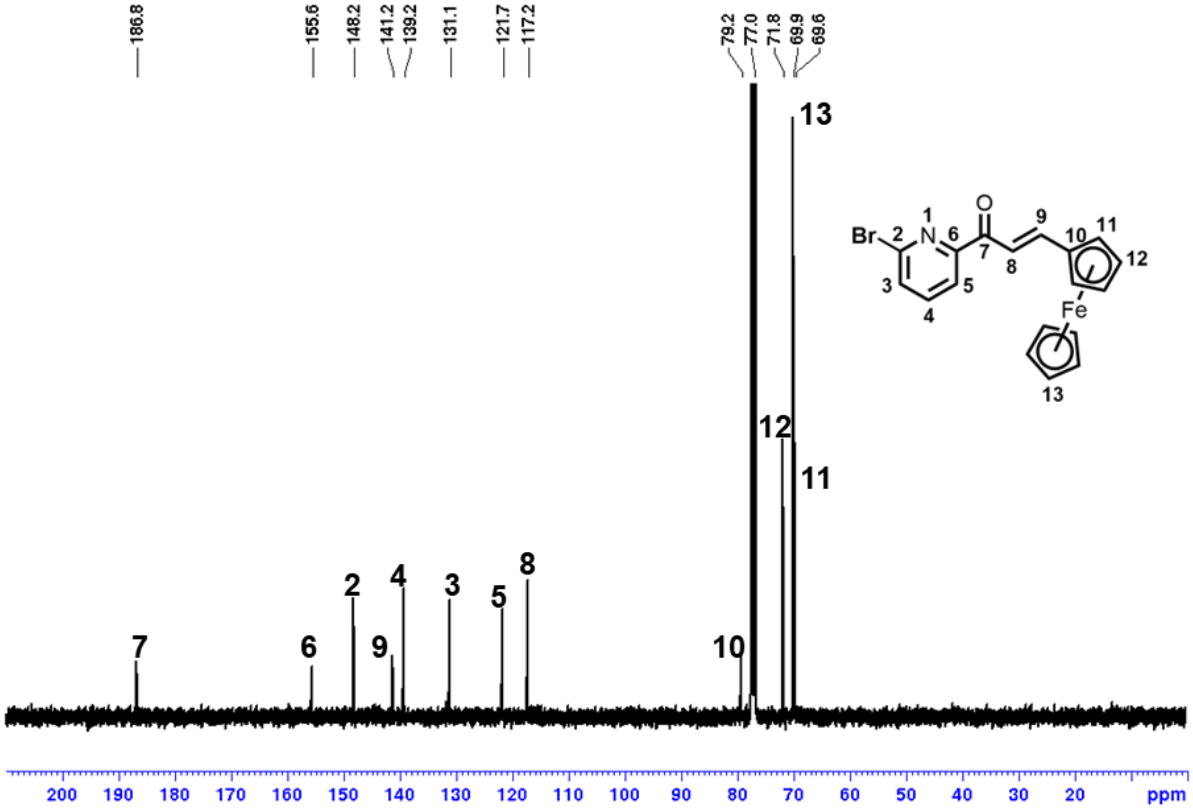

Figure S1v: $^{13}C\{^{1}H\}$ NMR spectrum (101 MHz, $CDCl_3$) of **1d**.

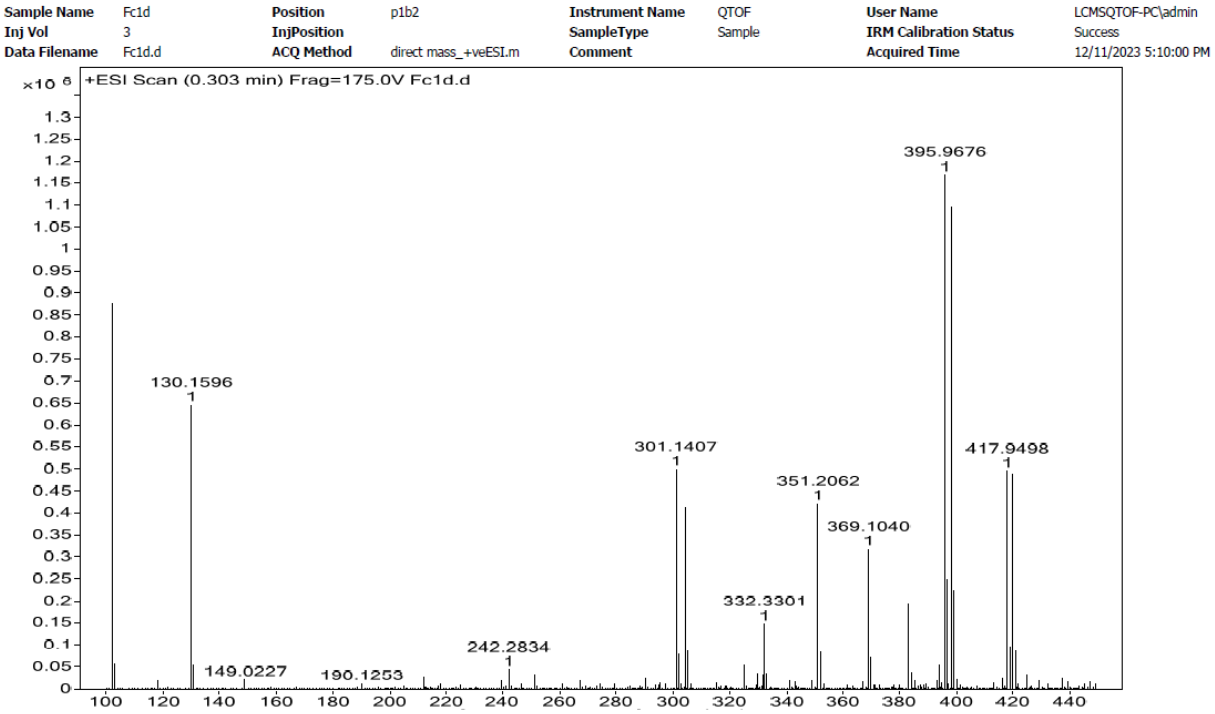

Figure S1w: HRMS spectrum of **1d** (M: $C_{18}H_{14}BrFeNO$); *m/z* calcd for [M+H$^+$] 395.9728, *m/z* found for [M+H$^+$] 395.9676, and *m/z* calcd for [M+Na$^+$] 417.9552, *m/z* found for [M+Na$^+$] 417.9498.

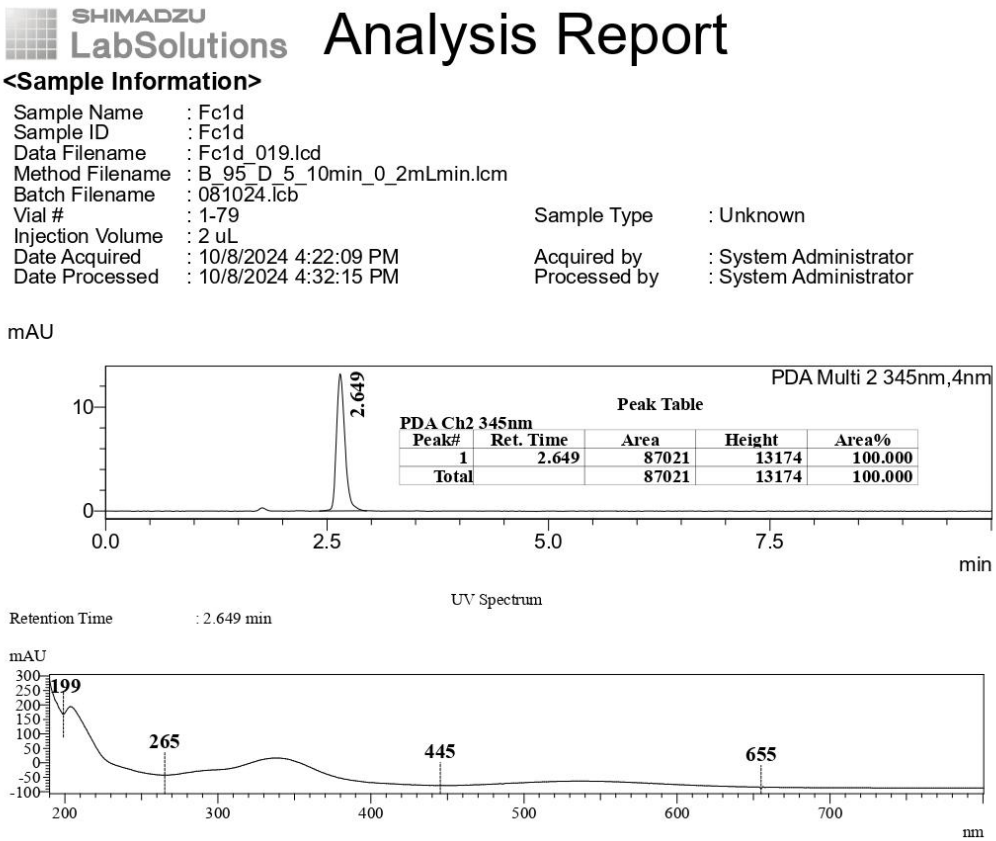

Figure S1x: RP–HPLC–MS **1d**; HPLC purity 100%; UV–vis spectrum shown at Rt = 2.649 min.

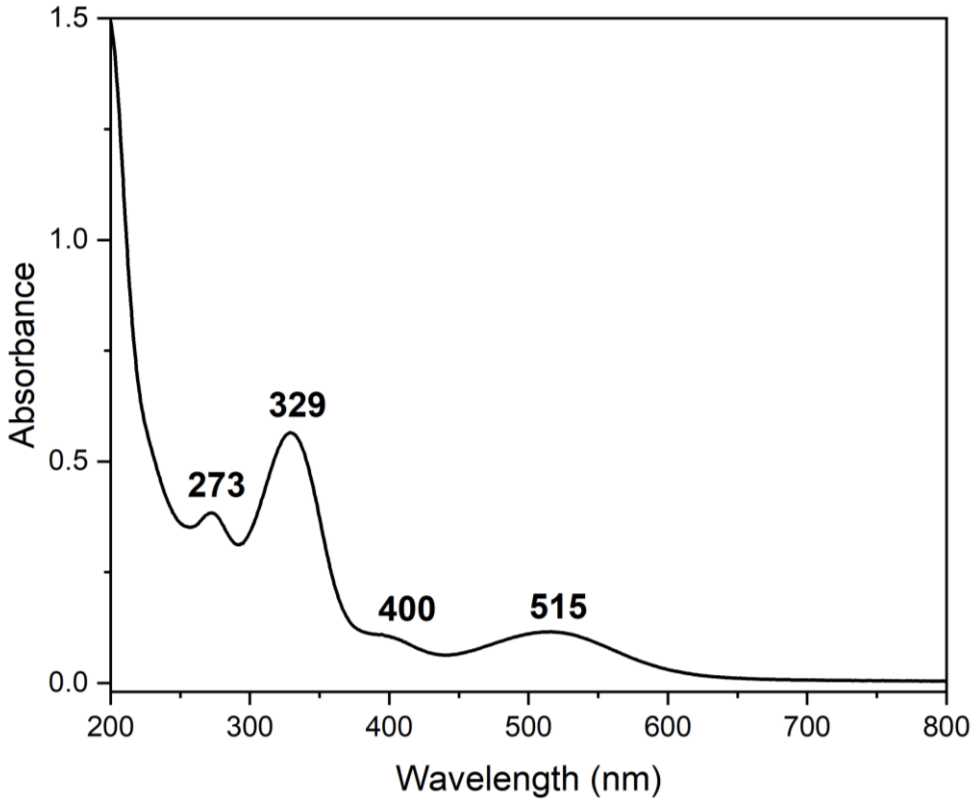

Figure S1y: Absorption spectra of **1a** (0.1 μM) in acetonitrile.

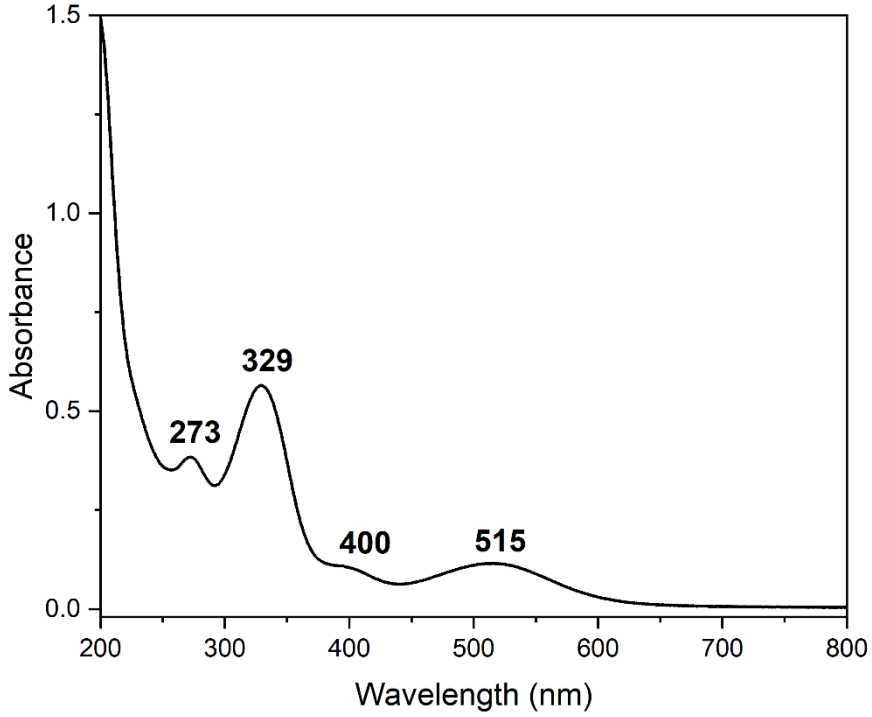

Figure S1z: Absorption spectrum of **1b** (0.1 μM) in acetonitrile.

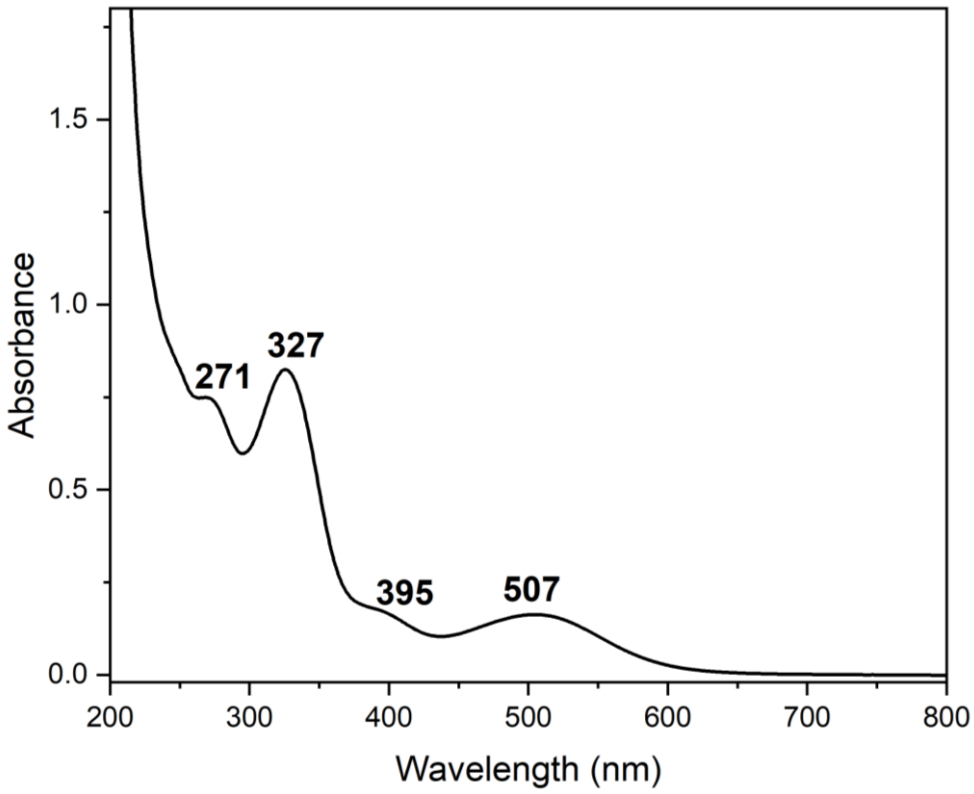

Figure S1aa: Absorption spectrum of **1c** (0.1 μM) in acetonitrile.

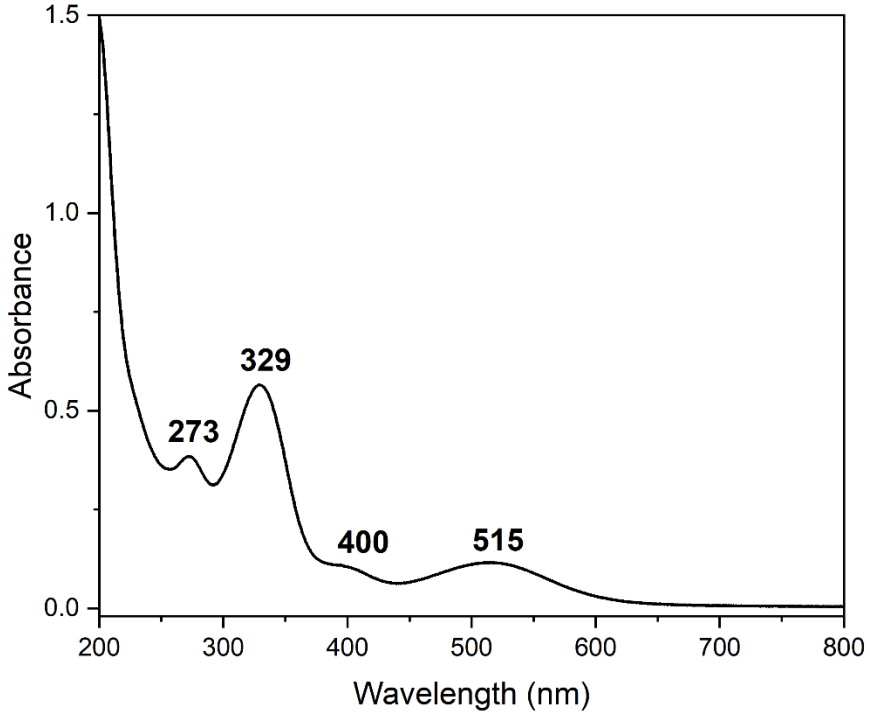

Figure S1ab: Absorption spectrum of **1d** (0.1 μM) in acetonitrile.

Characterisation of ligands and by-products

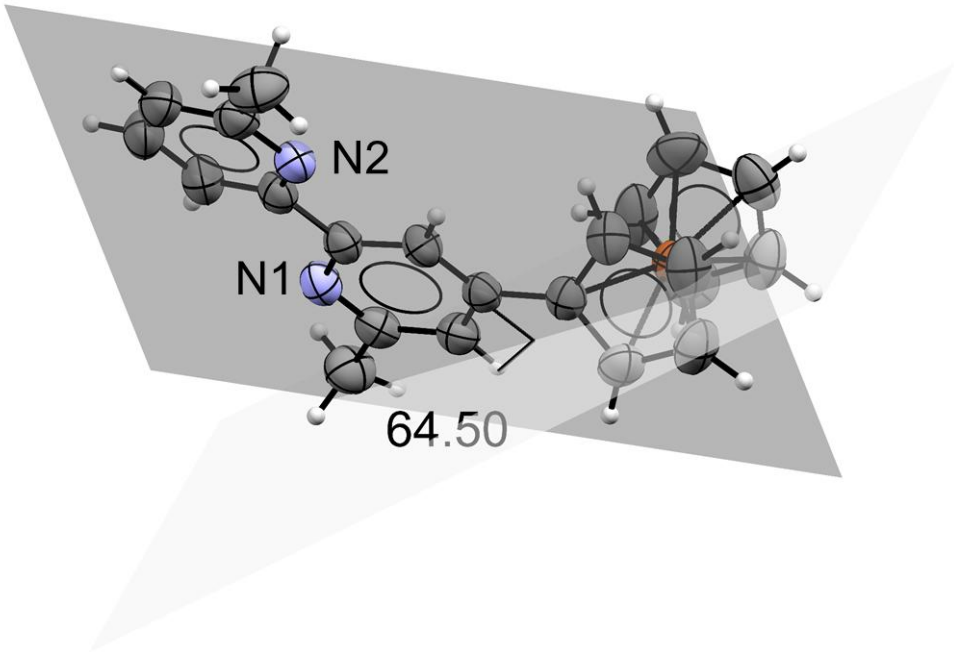

Figure 2a: The plane containing bpy rings (dark gray) and ferrocene unit (light gray) of ligand **2c**, present at an angle of 64.50° **2c** in a lattice unit cell.

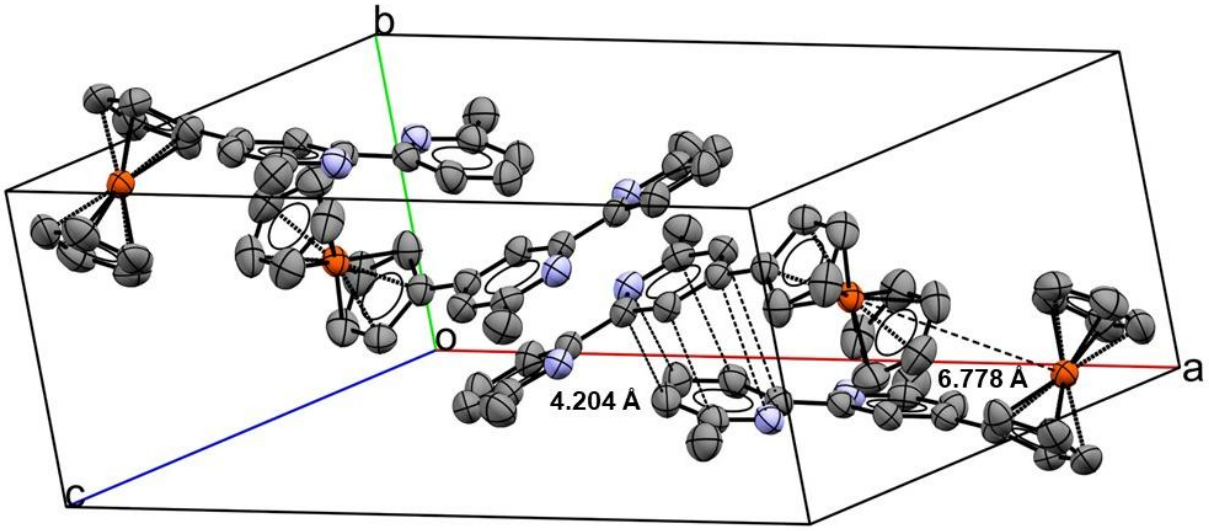

Figure 2b: 2c in a lattice unit cell, showing the weak interactions between two pyridine rings (Hydrogens omitted for better clarity).

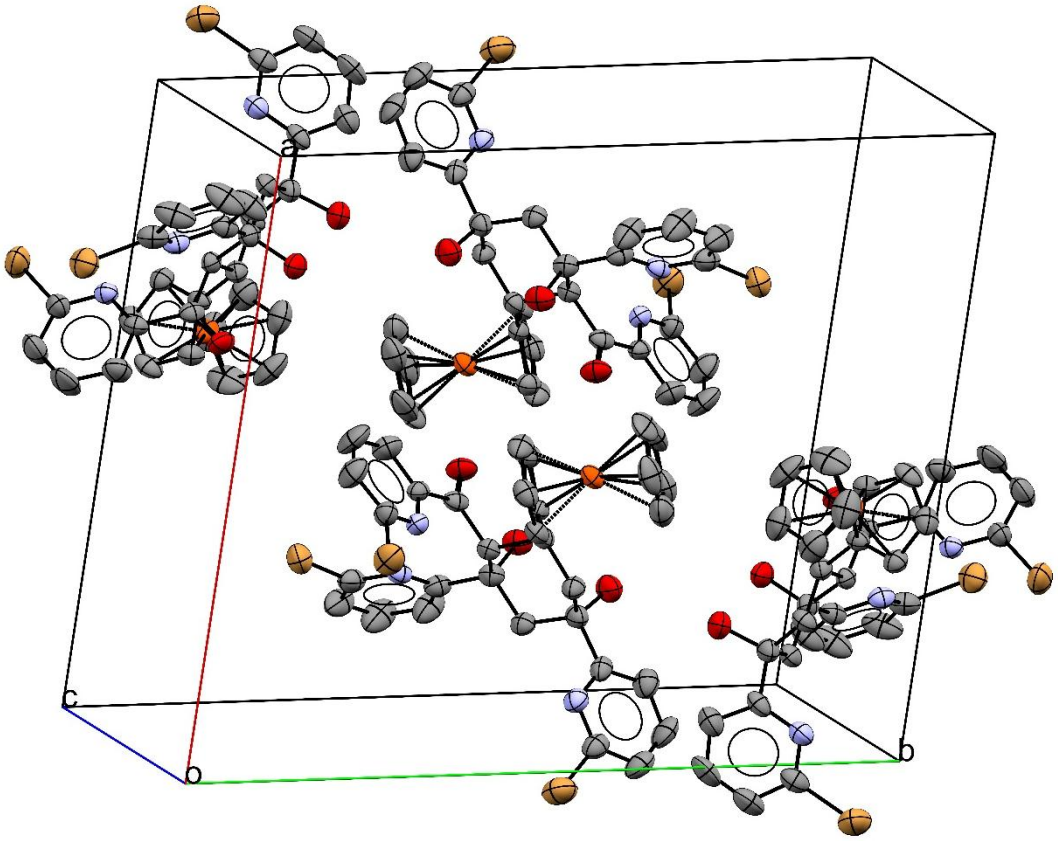

Figure 2c: 2d′ in a lattice unit cell (Hydrogens omitted for better clarity).

Table S1: Crystal data and structure refinement of **2c** and **2d′**.

Identification code	**2c**	**2d′**
CCDC deposition number	2443118	2532926
Empirical formula	$C_{22}H_{20}FeN_2$	$C_{32}H_{26}FeN_3O_3Br_3$
Formula weight	368.3	796.1
Temperature/K	294.4(4)	294.4
Crystal system	monoclinic	monoclinic
Space group	$P2_1/c$	$P2_1/c$
a/Å	21.0623(5)	18.0545(5)
b/Å	7.53961(18)	20.0248(4)
c/Å	11.3467(3)	8.56605(19)
α/°	90	90
β/°	102.639(2)	101.989(2)
γ/°	90	90
Volume/Å^3	1758.21(8)	3029.40(13)
Z	4	4
ρ_{calc} g/cm^3	1.3912	1.7456
μ/mm^{-1}	0.863	4.493
F(000)	768	1576
Crystal size/mm^3	0.299 × 0.222 × 0.011	0.469 × 0.049 × 0.026
Radiation	Mo Kα (λ = 0.71073)	Mo Kα (λ = 0.71073)
2Θ range for data collection/°	3.96 to 65.62	3.08 to 65.52
Index ranges	$-31 \le h \le 31$, $-11 \le k \le 10$, $-16 \le l \le 16$	$-27 \le h \le 27$, $-28 \le k \le 30$, $-12 \le l \le 12$
Reflections collected	56982	92048
Independent reflections	6156 [R_{int} = 0.0539]	10610 [R_{int} = 0.1078]
Data/restraints/parameters	6156/0/226	10610/4/387
Goodness-of-fit on F^2	1.105	1.125
Final R indexes [I>=2σ (I)]	R_1 = 0.0338, wR_2 = 0.1029	R_1 = 0.0583, wR_2 = 0.1553
Final R indexes [all data]	R_1 = 0.0667, wR_2 = 0.1191	R_1 = 0.1643, wR_2 = 0.2195
Largest diff. peak/hole / e Å^{-3}	0.13/–0.17	0.52/–0.28

Table S2: Selected bond lengths and bond angles for ligand **2c**.

Bond lengths of 2c					
atom	**atom**	**length/Å**	**atom**	**atom**	**length/Å**
N1	C13	1.337(2)	N2	C14	1.326(2)
N1	C7	1.342(2)	N2	C8	1.337(2)
C13	C8	1.491(2)	C13	C8	1.491(2)
C2	Fe1	2.037(1)	C5	Fe1	2.027(2)

Bond angles of 2c							
atom	**atom**	**atom**	**angle/°**	**atom**	**atom**	**atom**	**angle/°**
N2	C8	C13	116.23(12)	C8	N2	C14	118.27(12)
N1	C13	C8	116.86(12)	C21	C7	N1	115.81(14)
Fe1	C2	C1	125.91(9)	C20	C14	N2	116.20(12)

Table S3: Selected bond lengths and bond angles for ligand **2d′**.

Bond lengths of 2d′					
atom	**atom**	**length/Å**	**atom**	**atom**	**length/Å**
C8	C16	1.524(4)	C2	C5	1.494(4)
C16	C4	1.550(4)	C3	C7	1.523(4)
C4	C3	1.546(4)	C7	N2	1.334(4)
C3	C22	1.511(4)	C25	C17	1.521(4)
C22	C25	1.535(4)	C17	N3	1.346(4)
C25	O3	1.429(4)	C16	C1	1.501(4)
O2	C3	1.443(3)	C1	Fe1	2.047(3)
C4	C5	1.515(4)	Fe1	C12	2.038(4)
C5	O1	1.219(3)	C18	Br3	1.905(3)

Bond angles of 2d′							
atom	**atom**	**atom**	**angle/°**	**atom**	**atom**	**atom**	**angle/°**
C4	C3	C22	109.6(2)	C25	O3	H1O3	109.4(9)
C3	C22	C25	114.1(2)	C16	C1	Fe1	132.5(2)
C22	C25	C8	110.8(3)	C4	C5	O1	121.0(3)
C25	C8	C16	113.3(3)	C4	C5	C2	119.5(2)
C16	C4	C3	110.9(2)	C3	C7	N2	115.6(3)
C25	C17	N3	115.4(3)	C5	C2	N1	117.1(2)

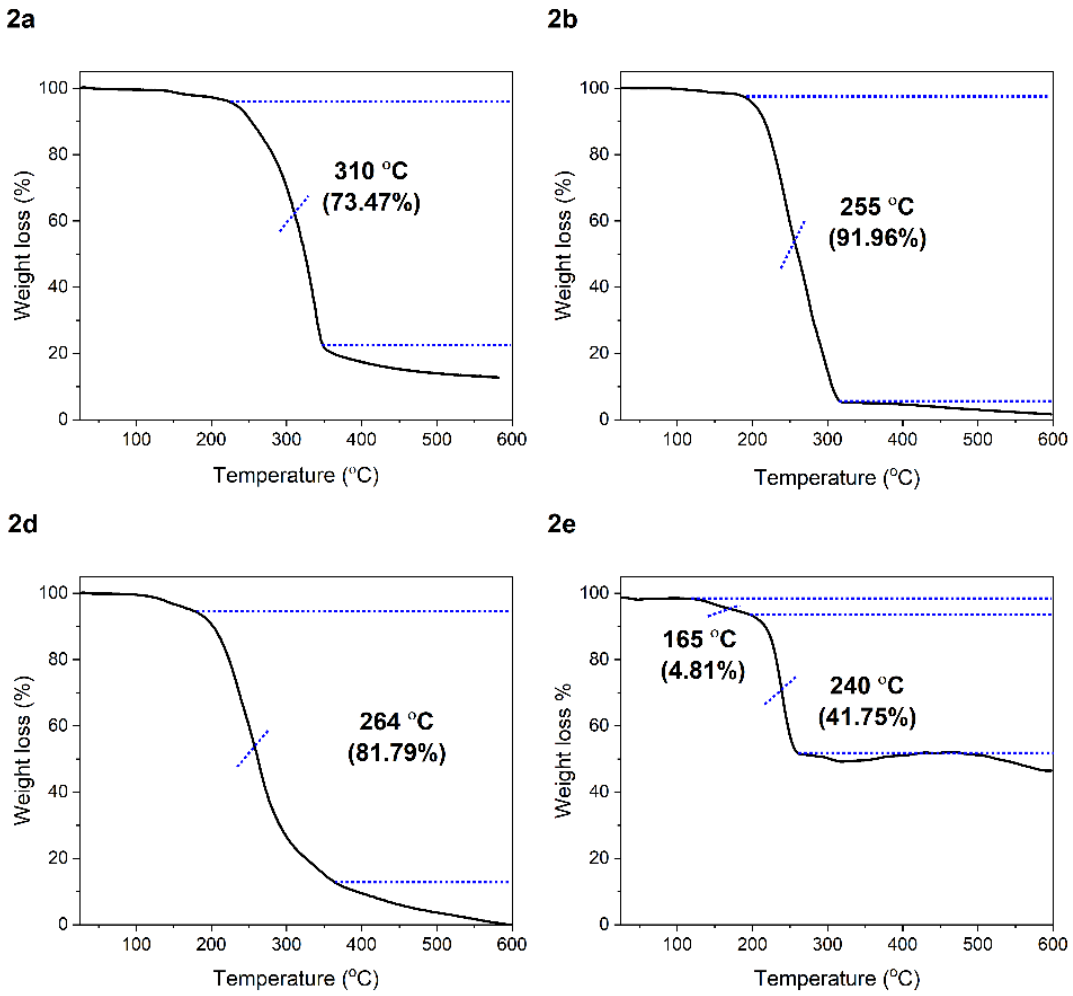

Figure S2d: Thermogravimetric profile of ligands **2a**, **2c, 2d,** and **2e** measured from 25–600 ˚C, with a heating rate of 10K/min under N_2 flow.

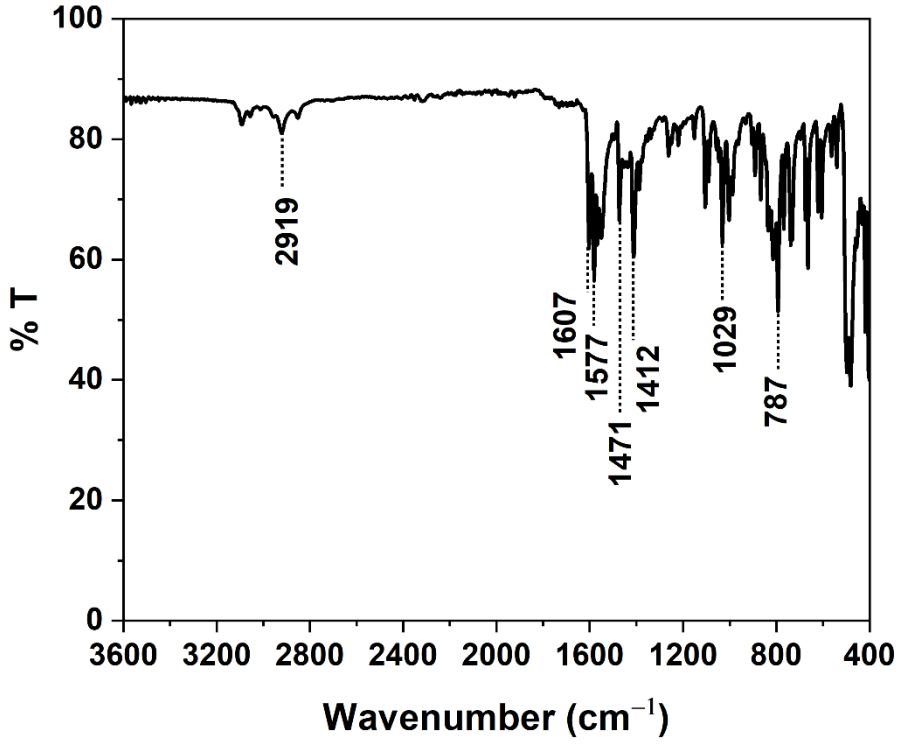

Figure S2e: ATR-IR spectrum of ligand **2a**.

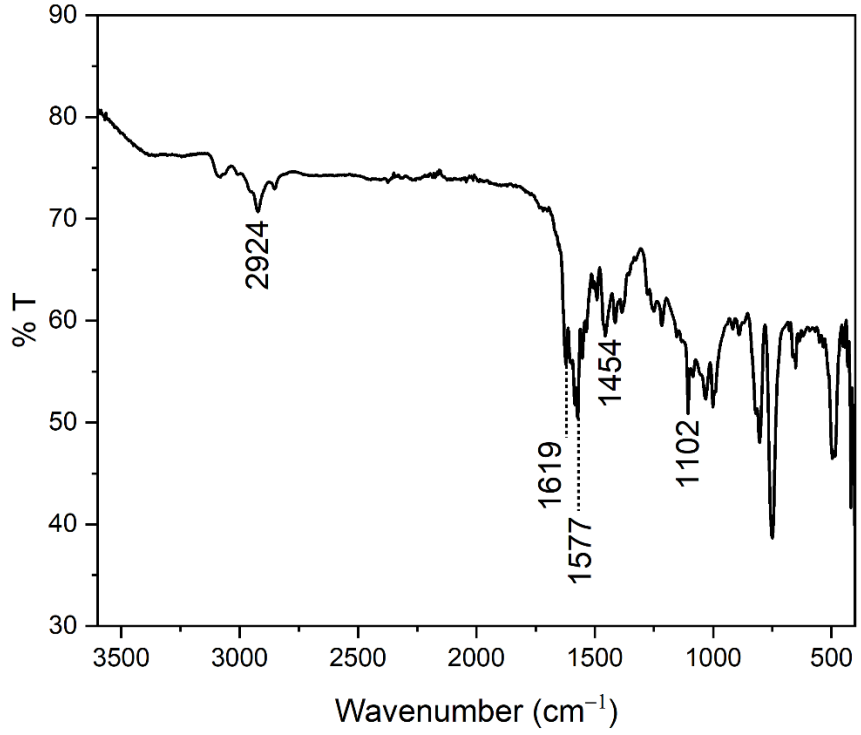

Figure S2f: ATR-IR spectrum of ligand **2b**.

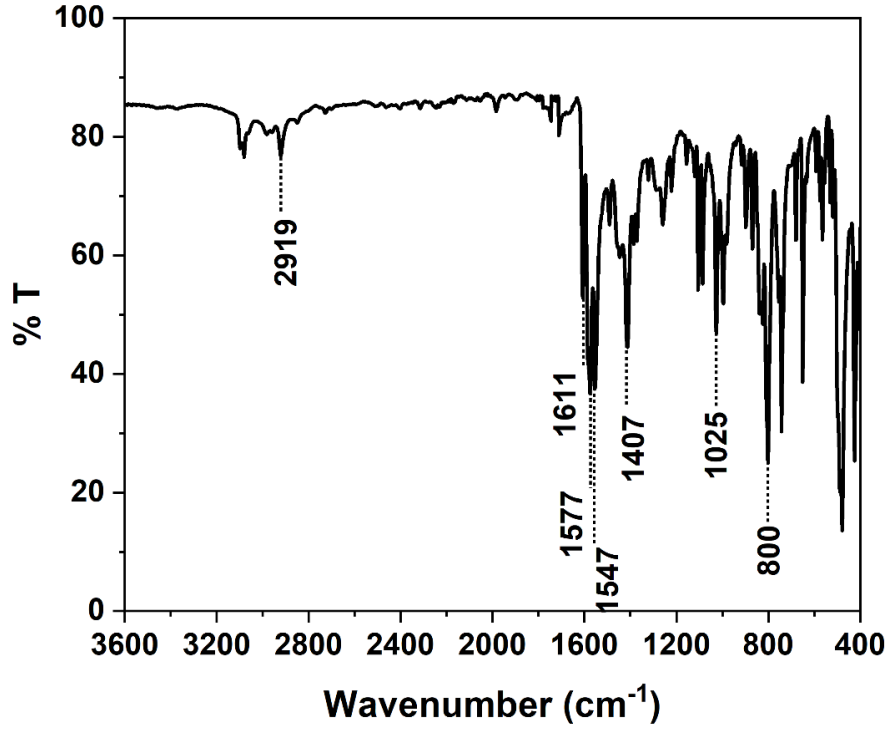

Figure S2g: ATR-IR spectrum of ligand **2c**.

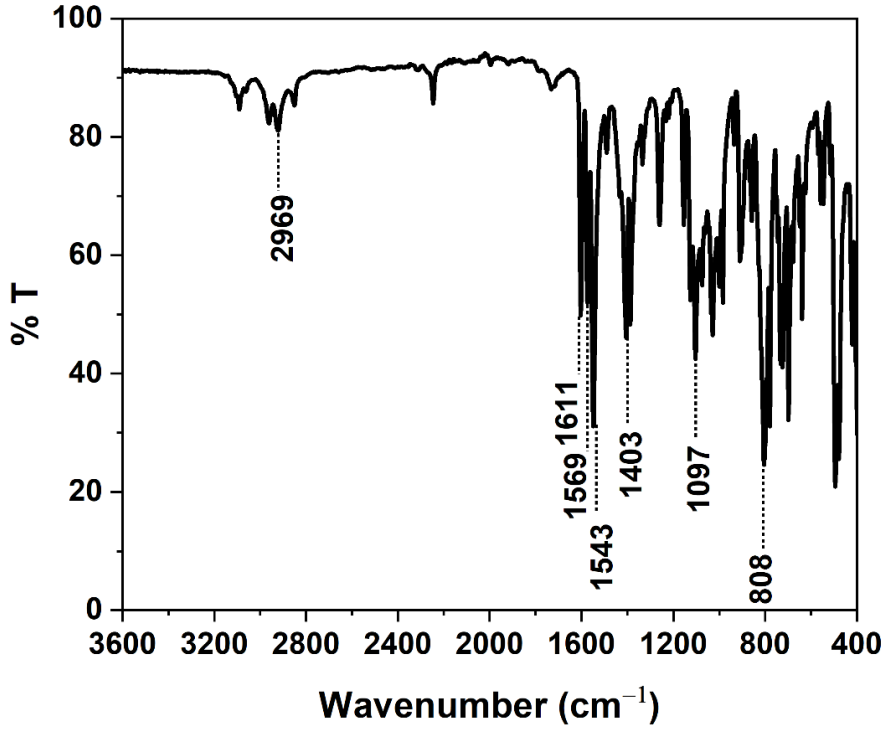

Figure S2h: ATR-IR spectrum of ligand **2d**.

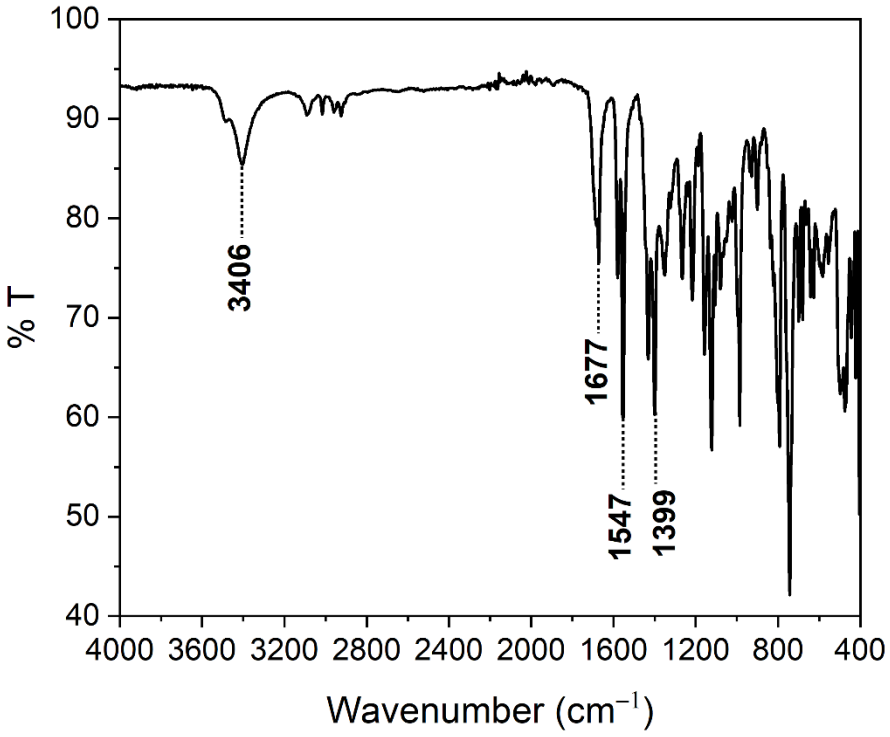

Figure S2i: ATR-IR spectrum of by-product **2d′**.

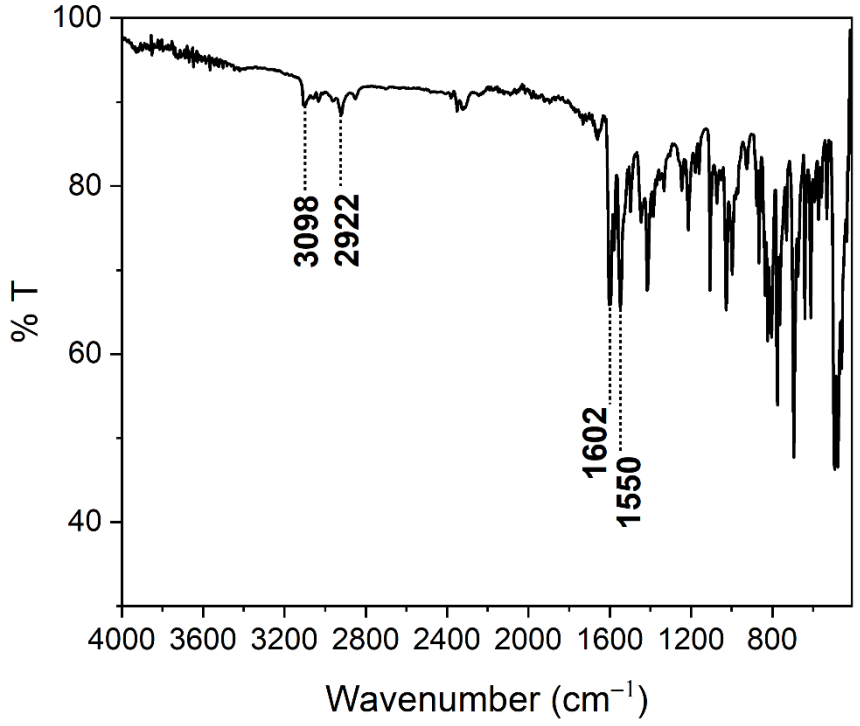

Figure S2j: ATR-IR spectrum of by-product **2e**.

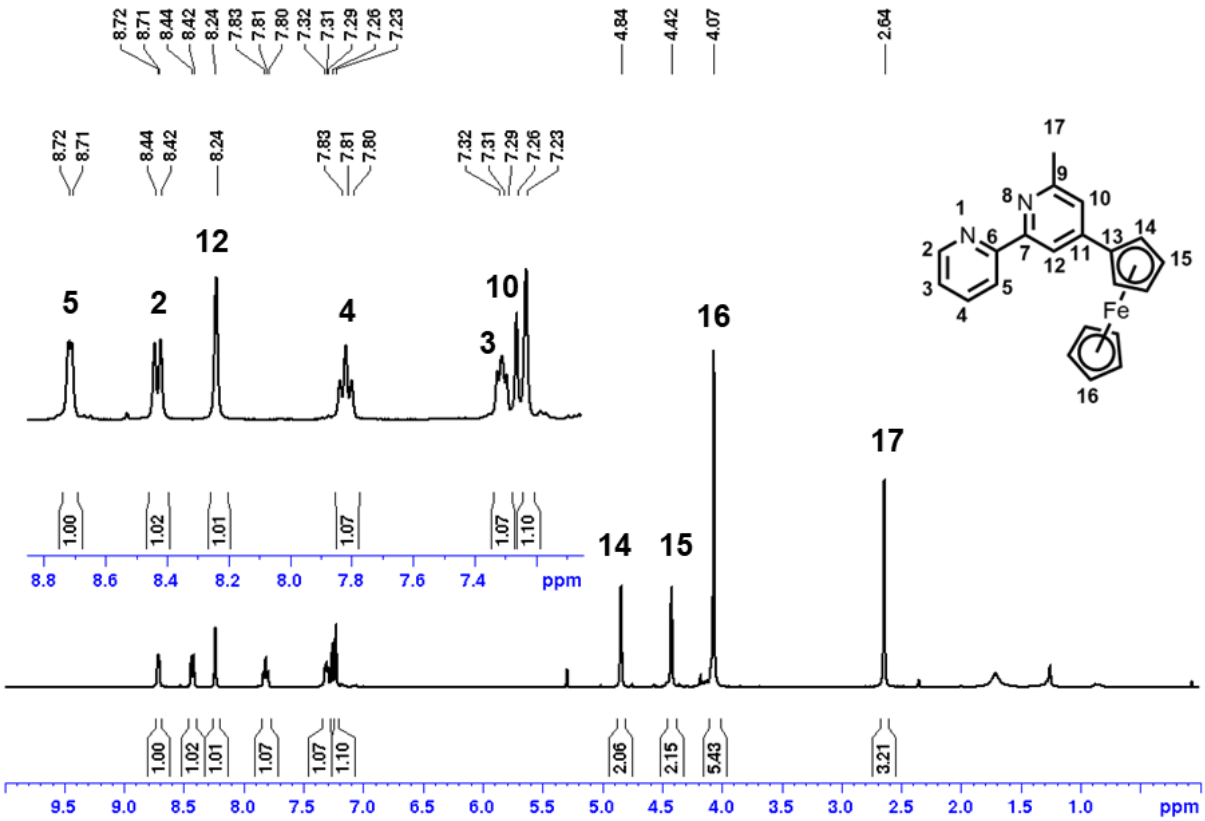

Figure S2k: ^{1}H NMR ($CDCl_3$, 400 MHz) spectrum of **2a**.

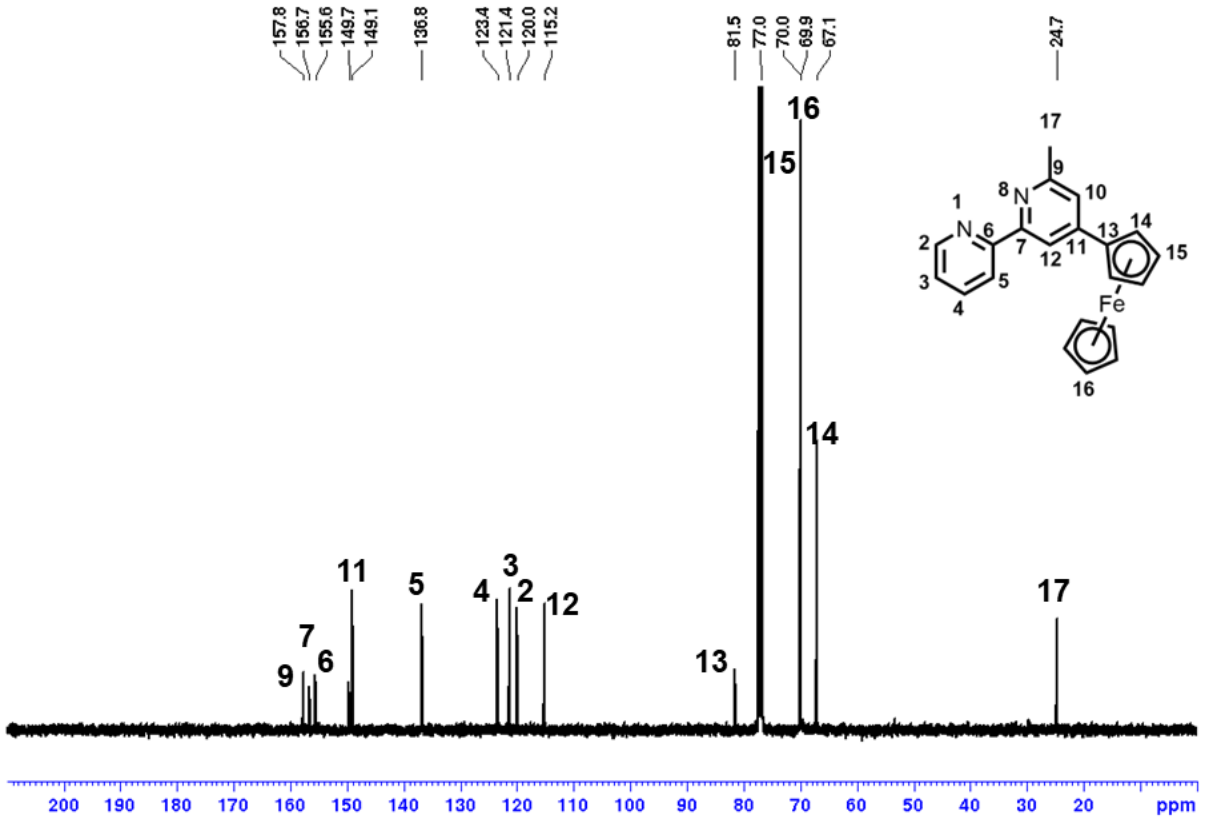

Figure S2l: $^{13}C\{^{1}H\}$ NMR (101 MHz, $CDCl_3$) spectrum of **2a**.

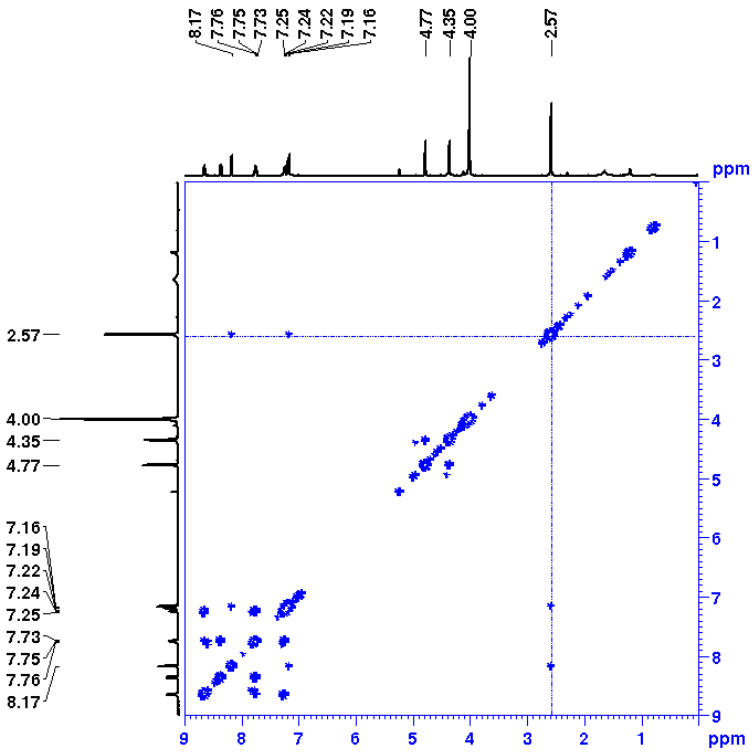

Figure S2m: $^{1}H–^{1}H$ correlation spectrum of **2a** (400 MHz, $CDCl_3$); shows the correlation between the methyl and aromatic protons.

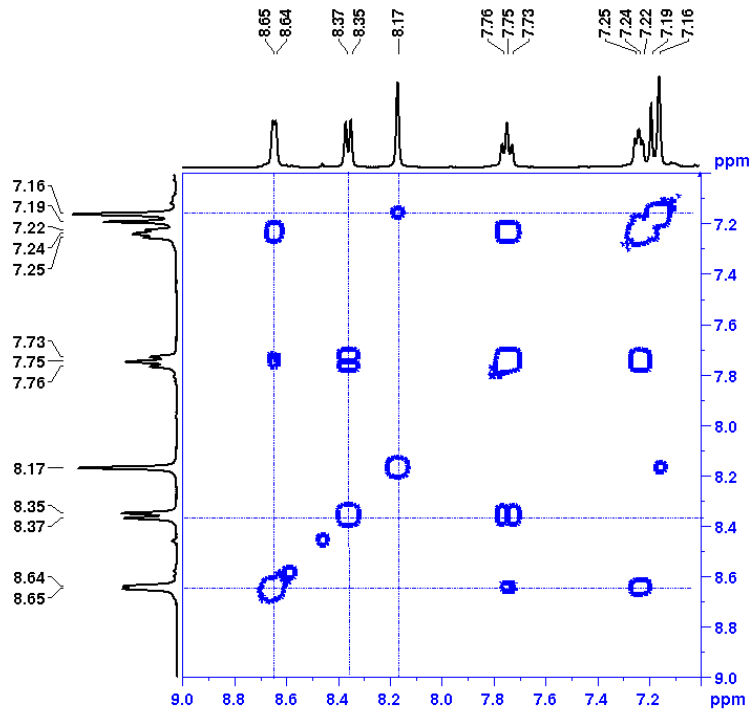

Figure S2n: $^{1}H–^{1}H$ correlation of **2a**, showing the correlations amongst the aromatic protons.

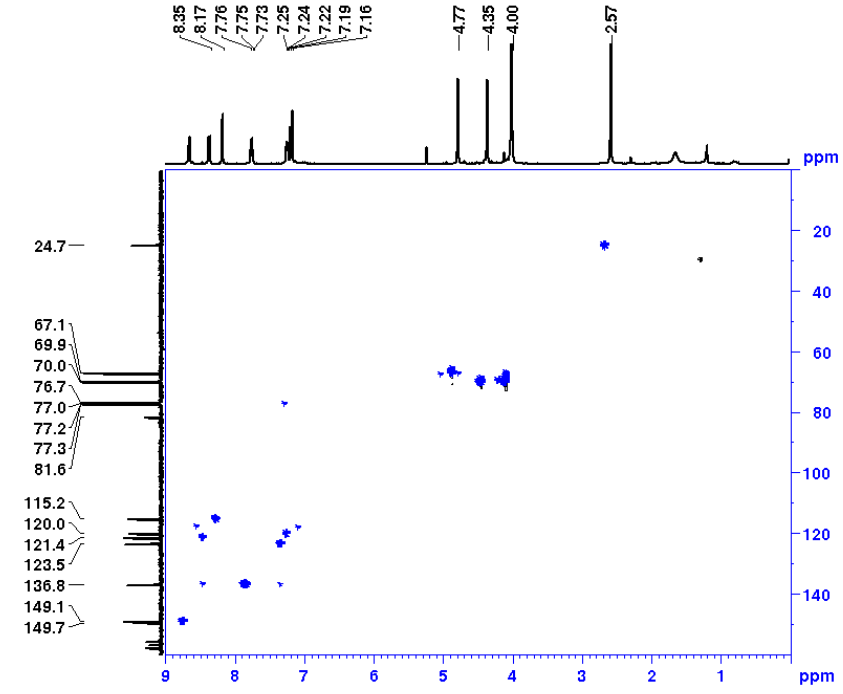

Figure S2o: HSQC spectrum of **2a** (400 MHz, $CDCl_3$).

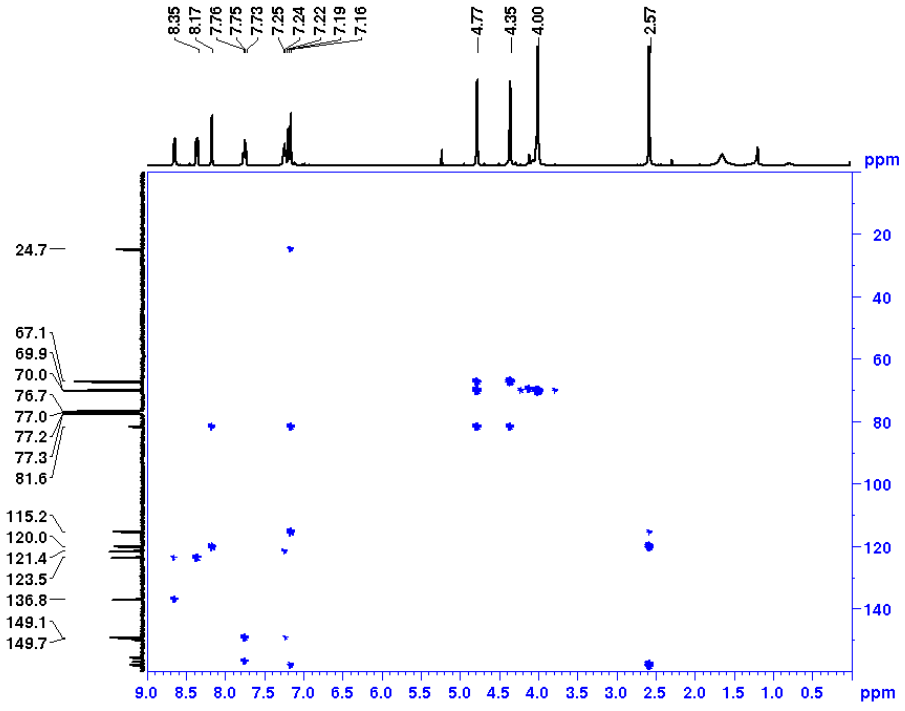

Figure S2p: HMBC spectrum of **2a** (400 MHz, $CDCl_3$).

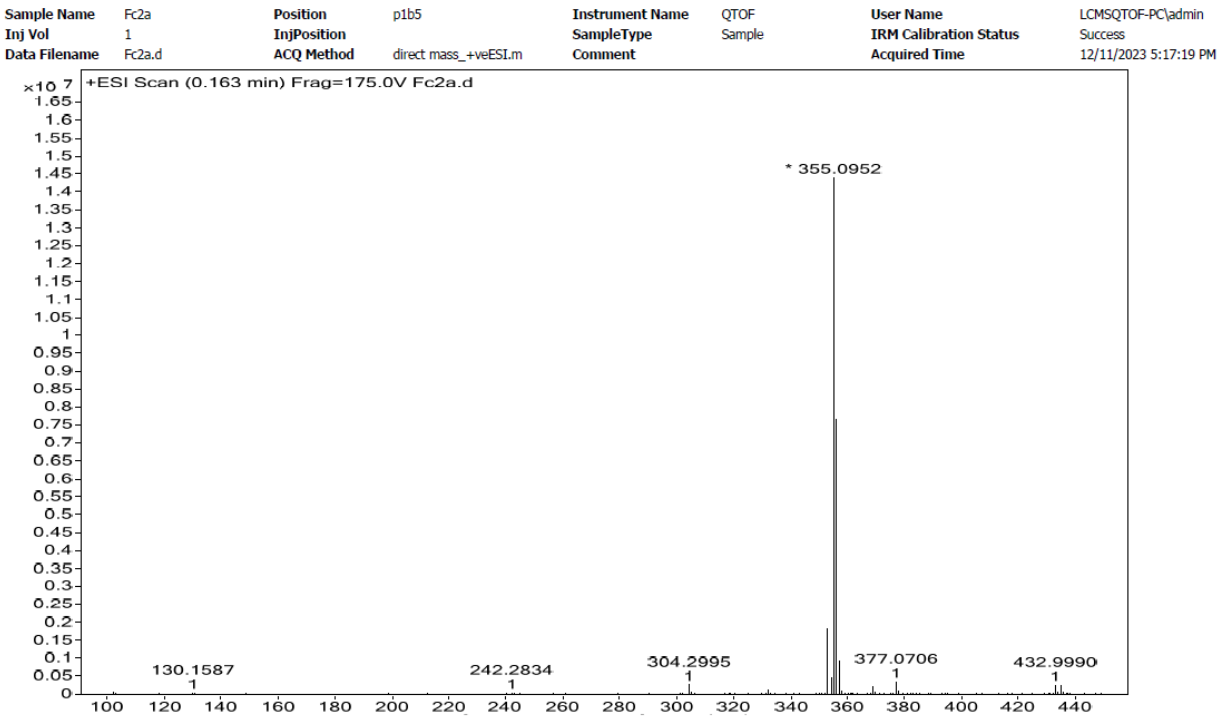

Figure S2q: HRMS spectrum of **2a** (M: $C_{21}H_{18}FeN_2$) *m/z* calcd for [M+H$^+$] 355.0939, *m/z* found for [M+H$^+$] 355.0952.

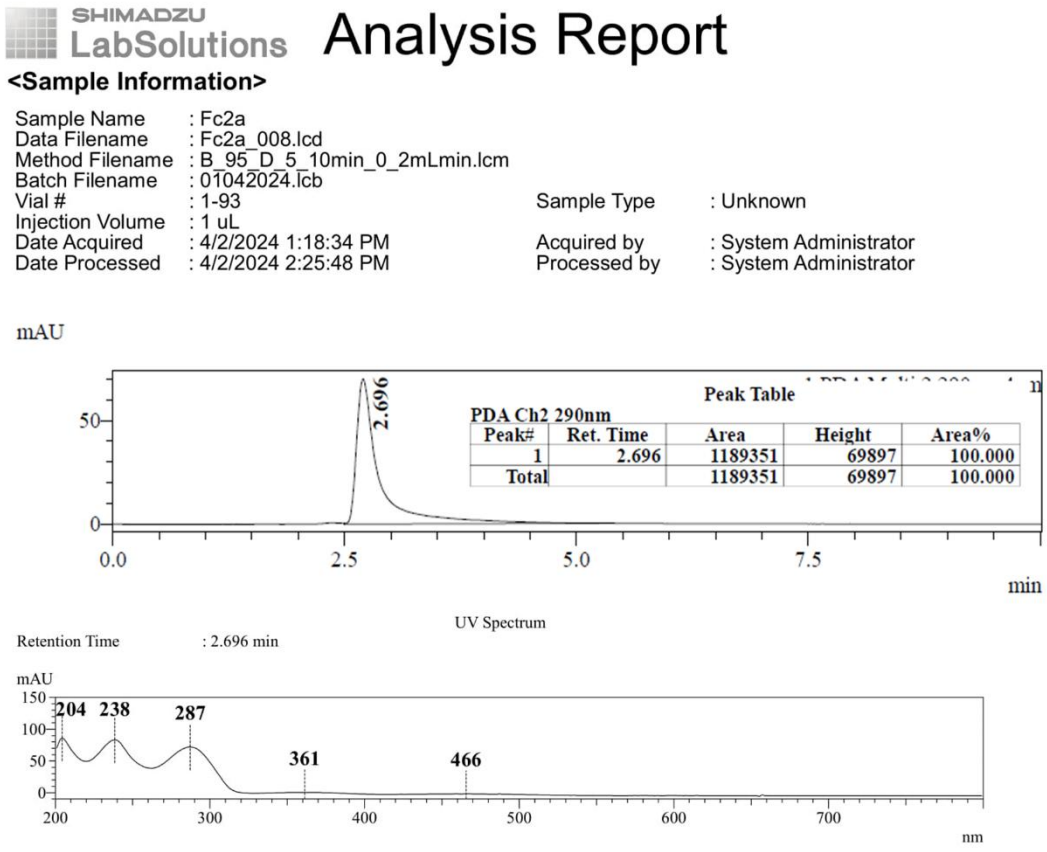

Figure S2r: RP–HPLC–MS of **2a**; HPLC purity 100%; UV–vis spectrum shown at Rt = 2.696 min.

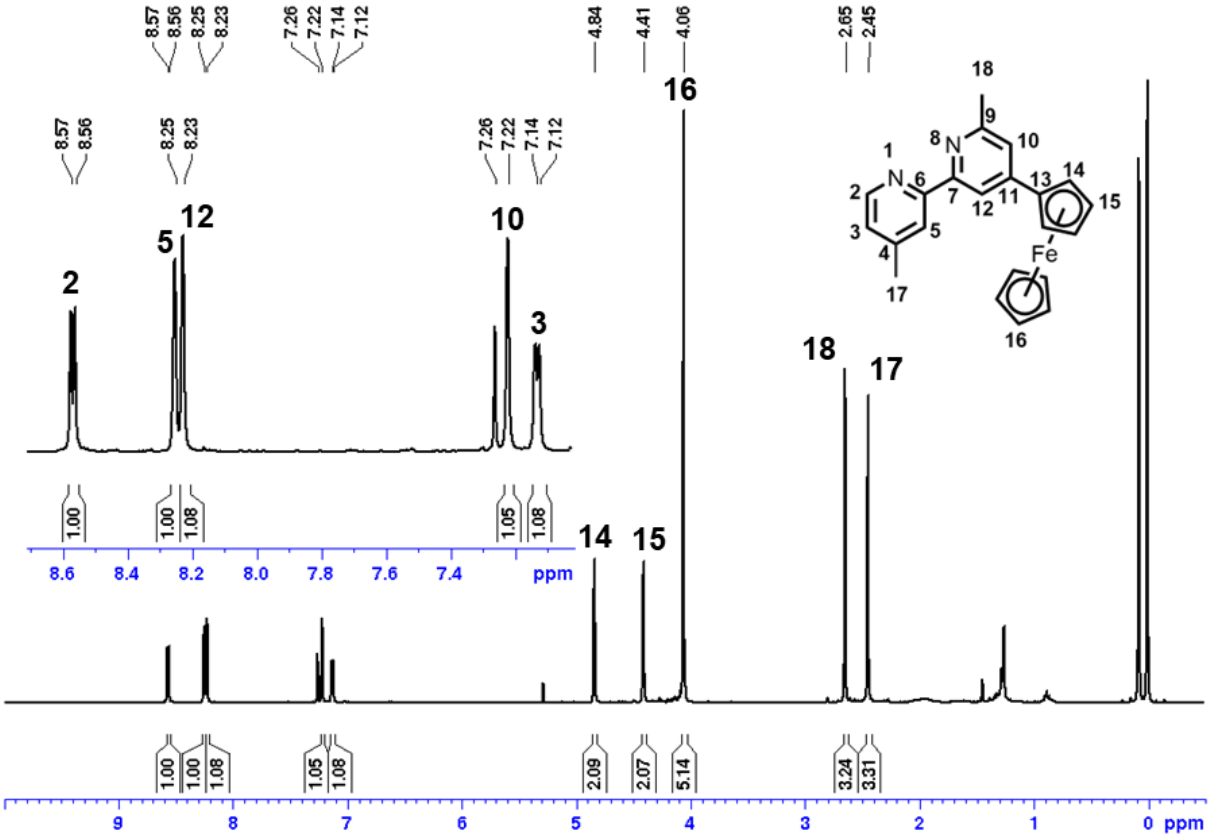

Figure S2s: ^{1}H NMR ($CDCl_3$, 400 MHz) spectrum of **2b**.

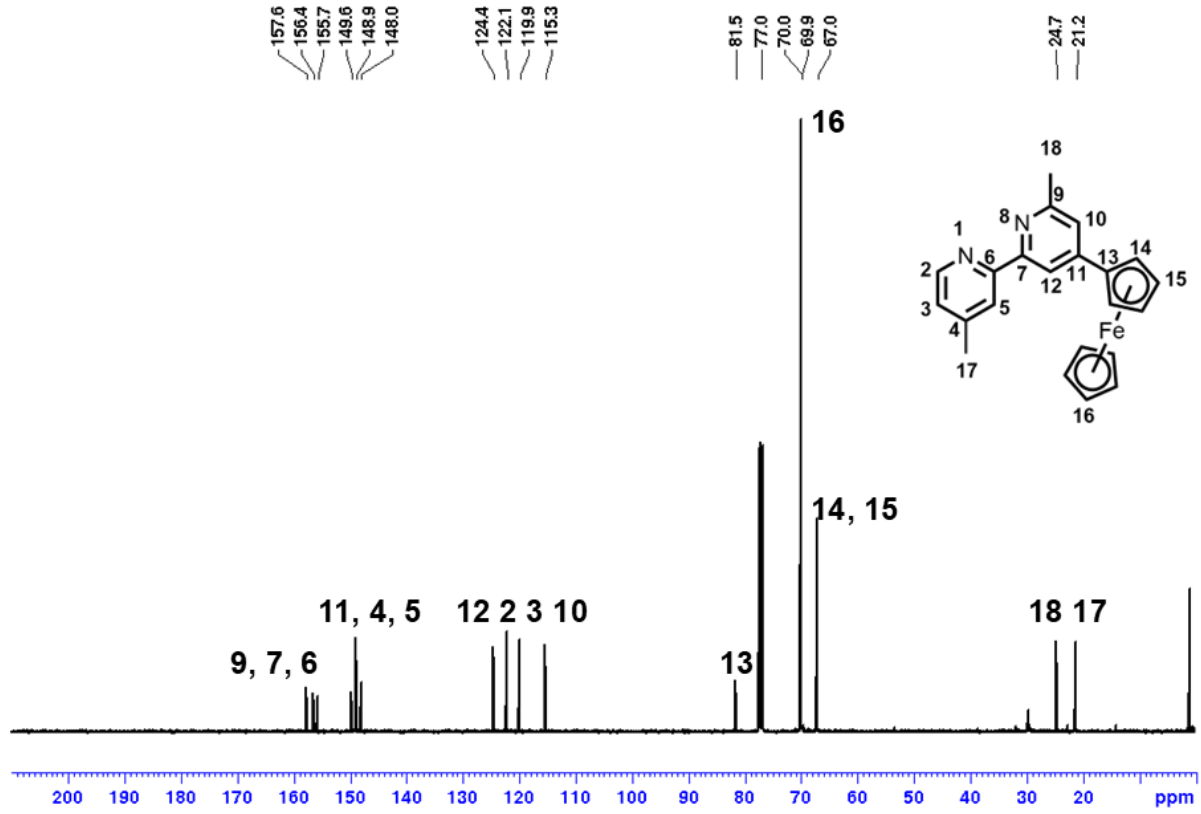

Figure S2t: $^{13}C\{^{1}H\}$ NMR (101 MHz, $CDCl_3$) spectrum of **2b**.

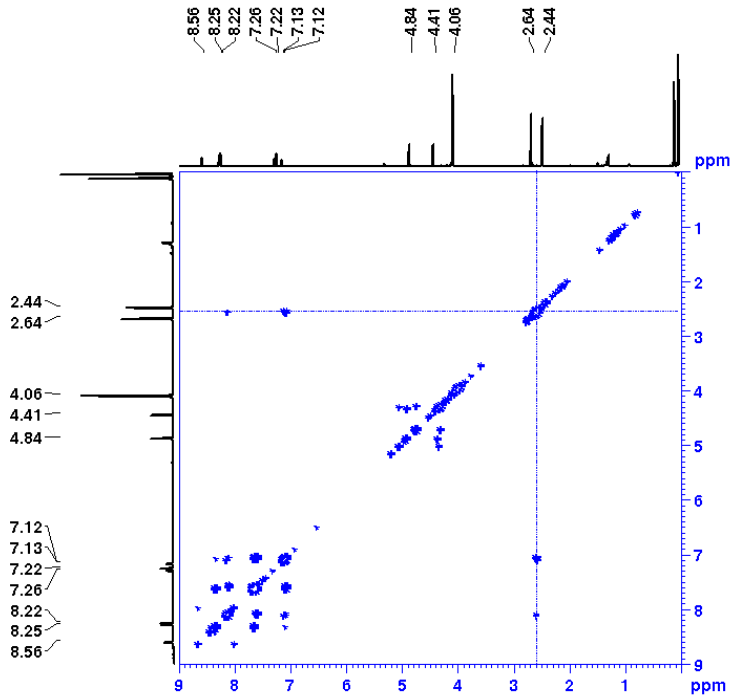

Figure S2u: $^{1}H–^{1}H$ correlation spectrum of **2b** (400 MHz, $CDCl_3$); shows the correlation between the methyl and aromatic protons.

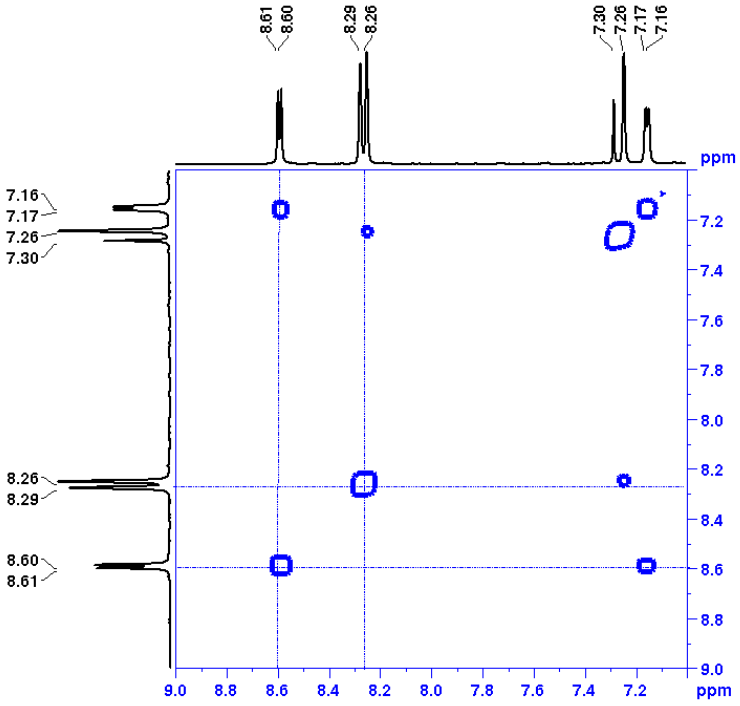

Figure S2v: $^{1}H–^{1}H$ correlation spectrum of **2b** showing correlations amongst the aromatic protons.

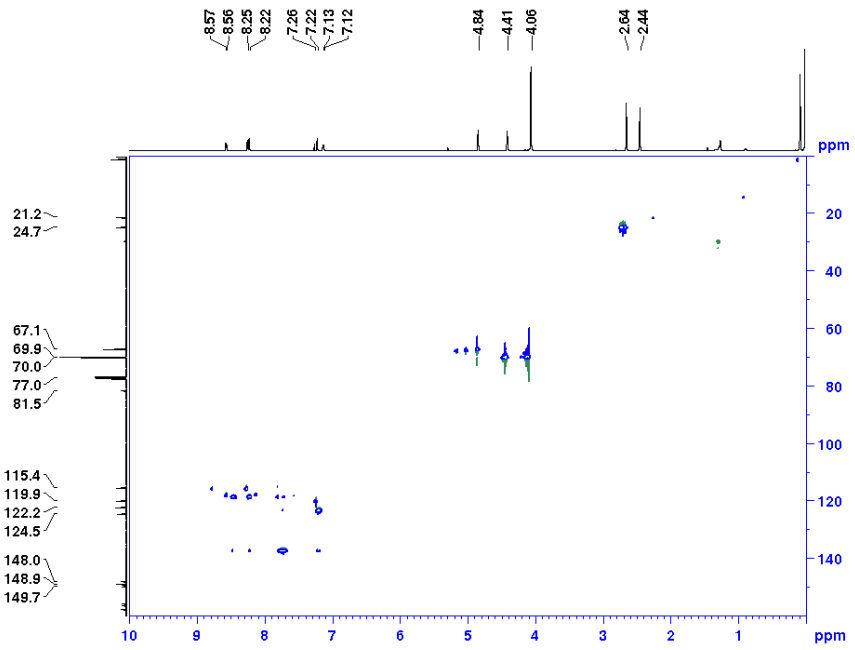

Figure S2w: HSQC spectrum of **2b** (400 MHz, $CDCl_3$).

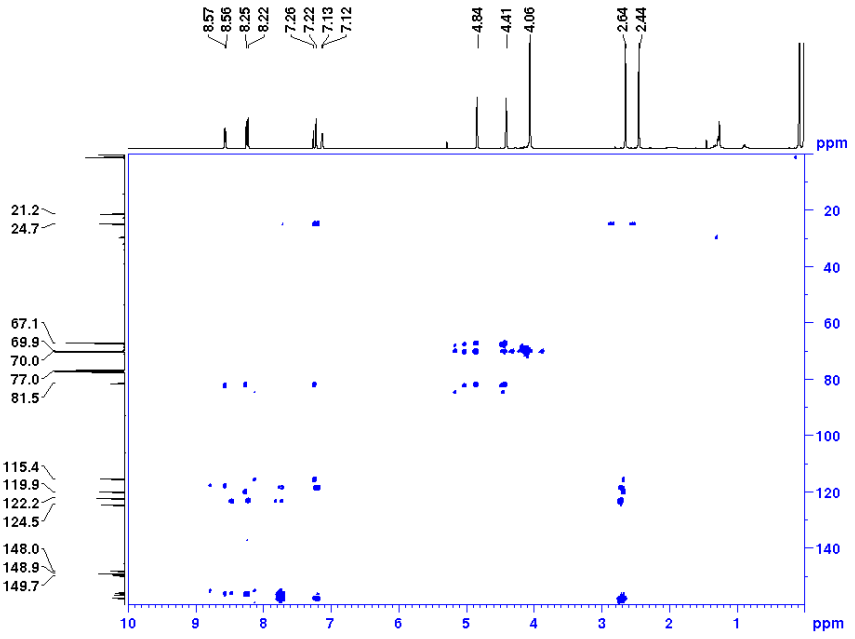

Figure S2x: HMBC spectrum of **2b** (400 MHz, $CDCl_3$).

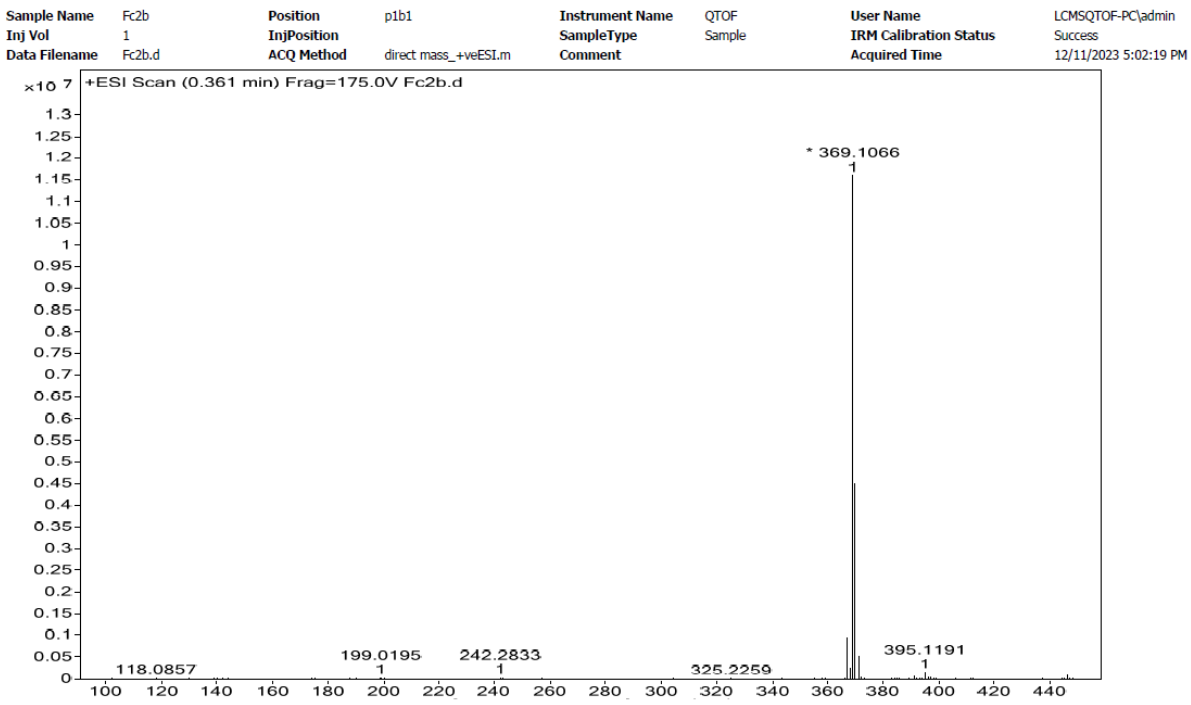

Figure S2y: HRMS spectrum of **2b** (M: $C_{22}H_{20}FeN_2$) *m/z* calcd for [M+H$^+$] 369.1095, *m/z* found for [M+H$^+$] 369.1066.

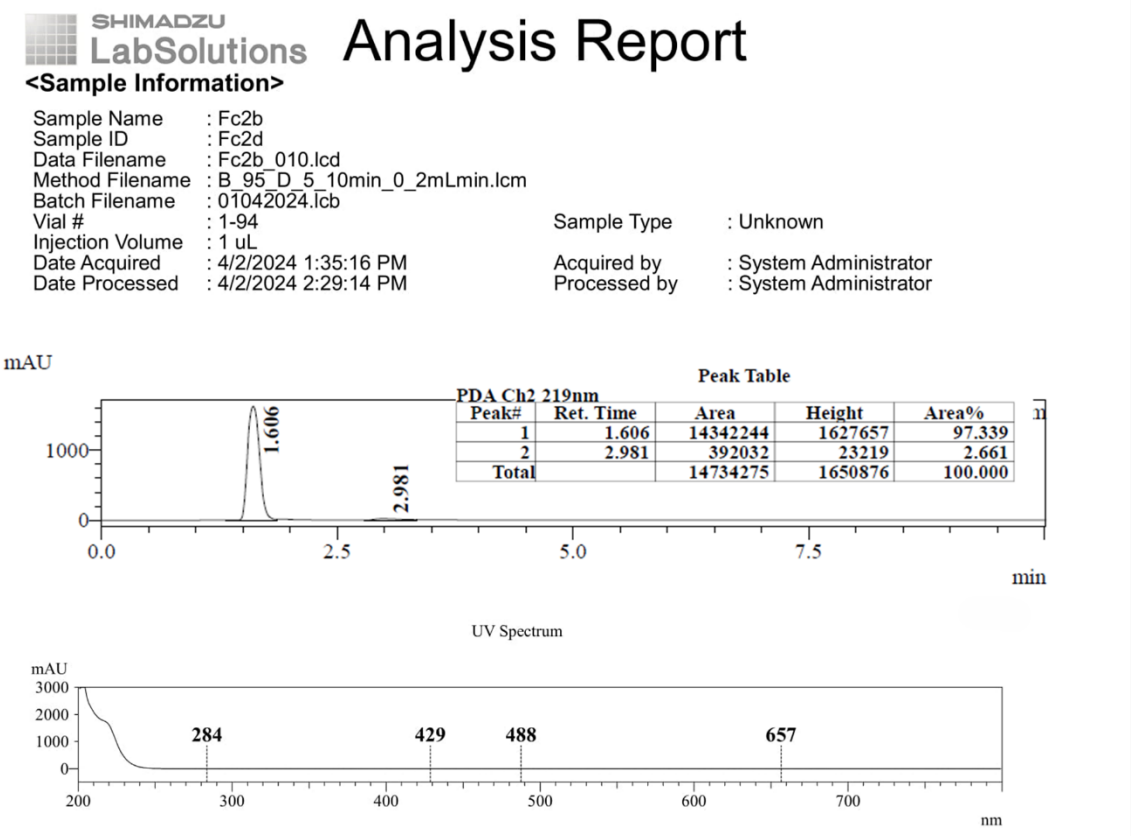

Figure S2z: RP–HPLC–MS of **2b**; HPLC purity 97%; UV–vis spectrum shown at Rt = 1.606 min.

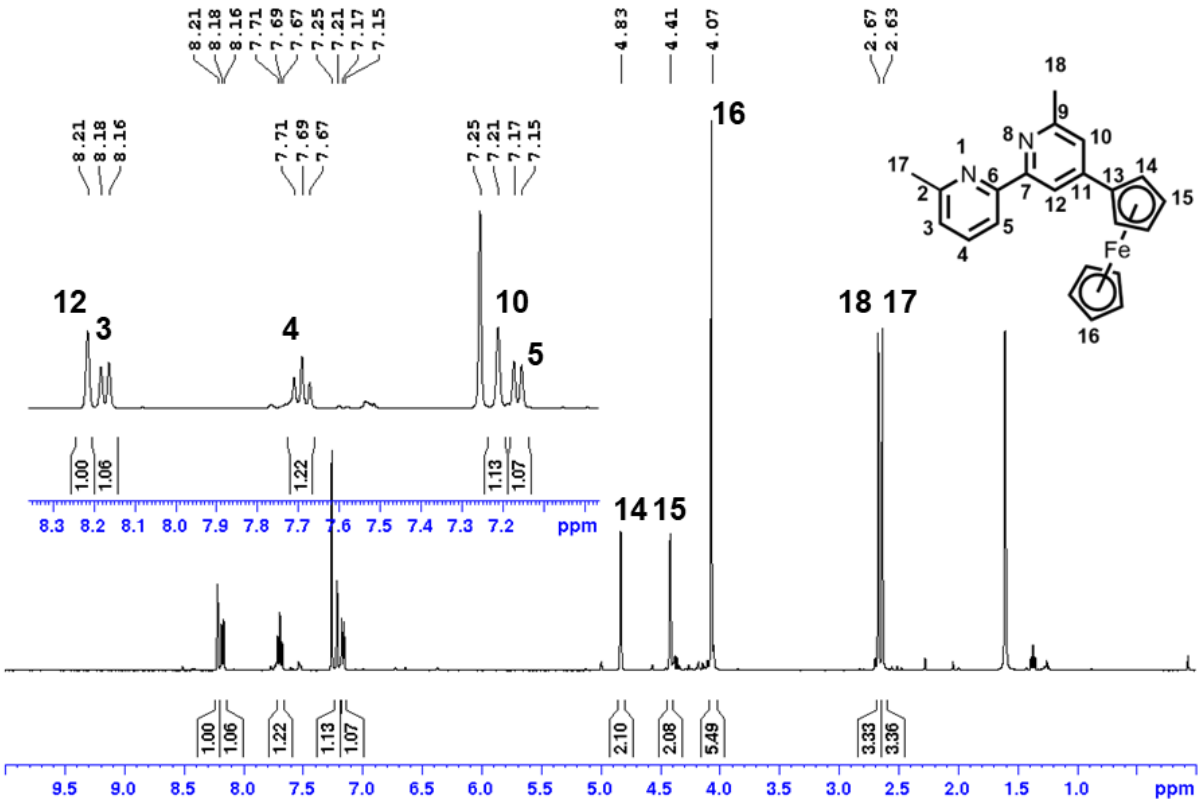

Figure S2aa: ^{1}H NMR ($CDCl_3$, 400 MHz) spectrum of **2c**.

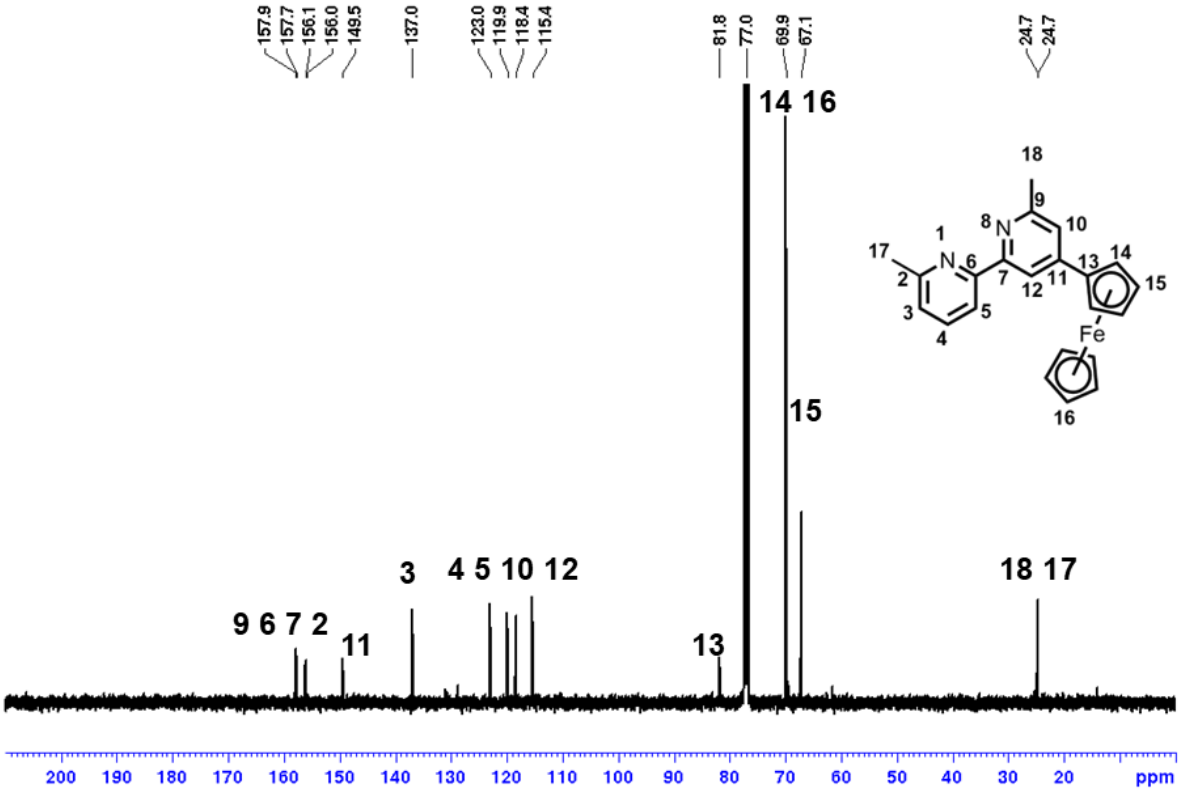

Figure S2ab: $^{13}C\{^{1}H\}$ NMR (101 MHz, $CDCl_3$) spectrum of **2c**.

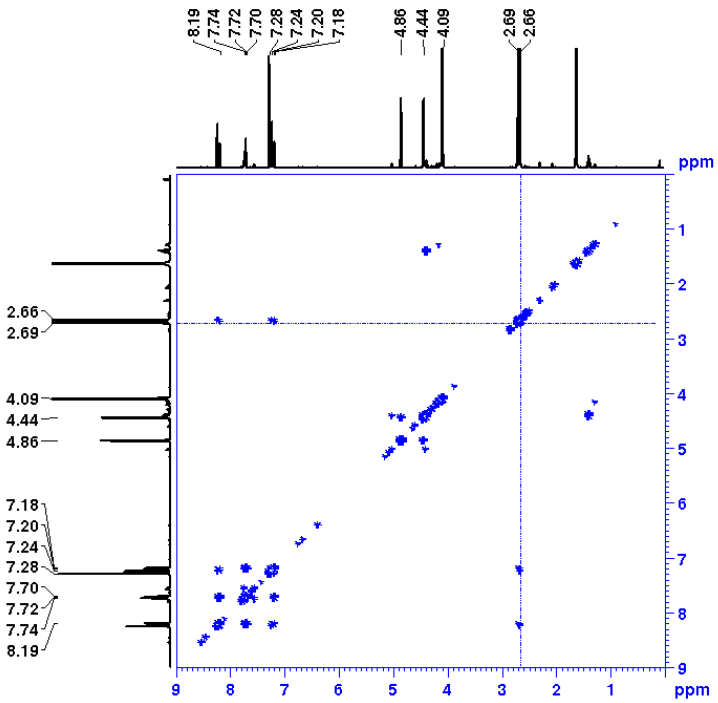

Figure S2ac: $^{1}H–^{1}H$ correlation spectrum of **2c** (400 MHz, $CDCl_3$); shows the correlation between methyl and aromatic protons.

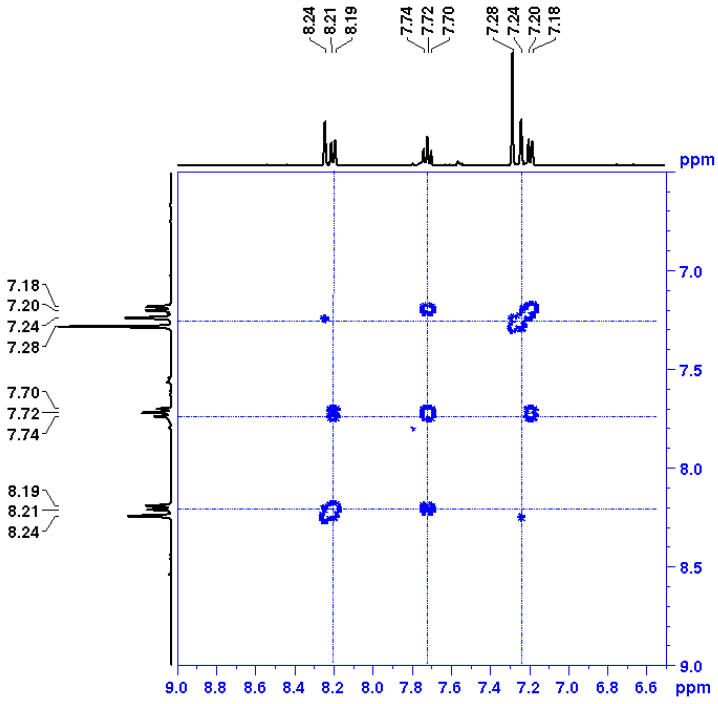

Figure S2ad: $^{1}H–^{1}H$ correlation spectrum of **2c**, showing the correlations amongst the aromatic protons.

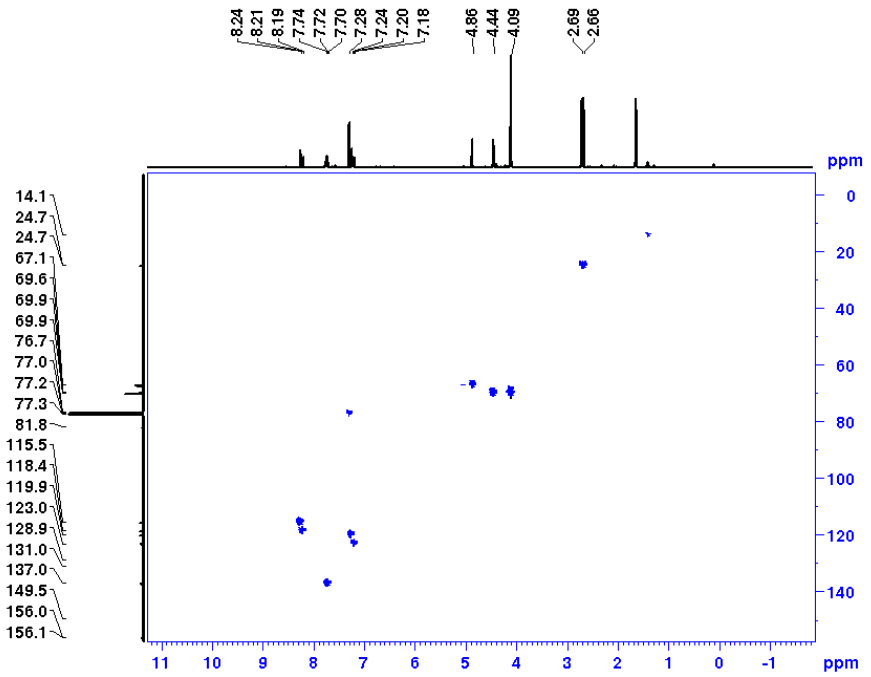

Figure S2ae: HSQC spectrum of **2c** (400 MHz, $CDCl_3$).

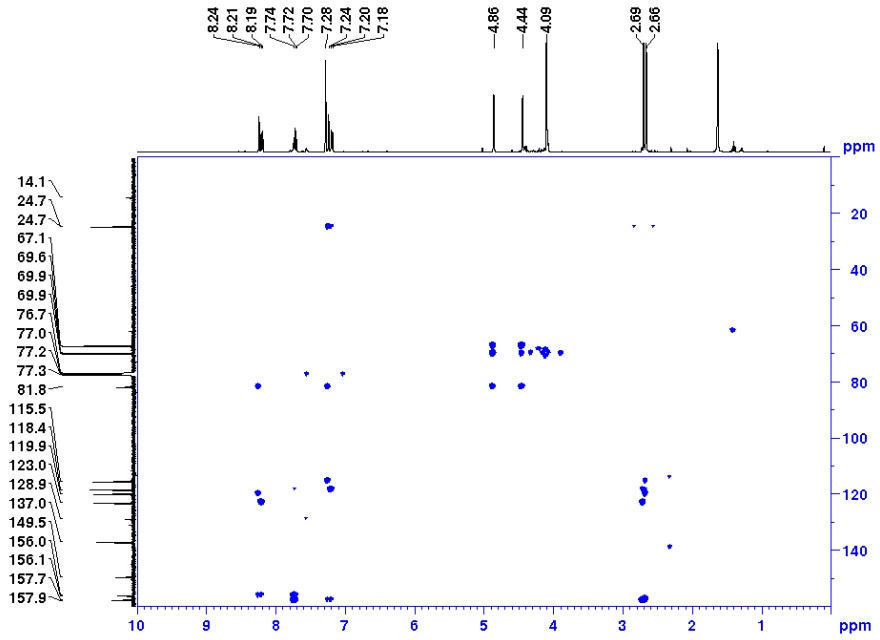

Figure S2af: HMBC spectrum of **2c** (400 MHz, $CDCl_3$).

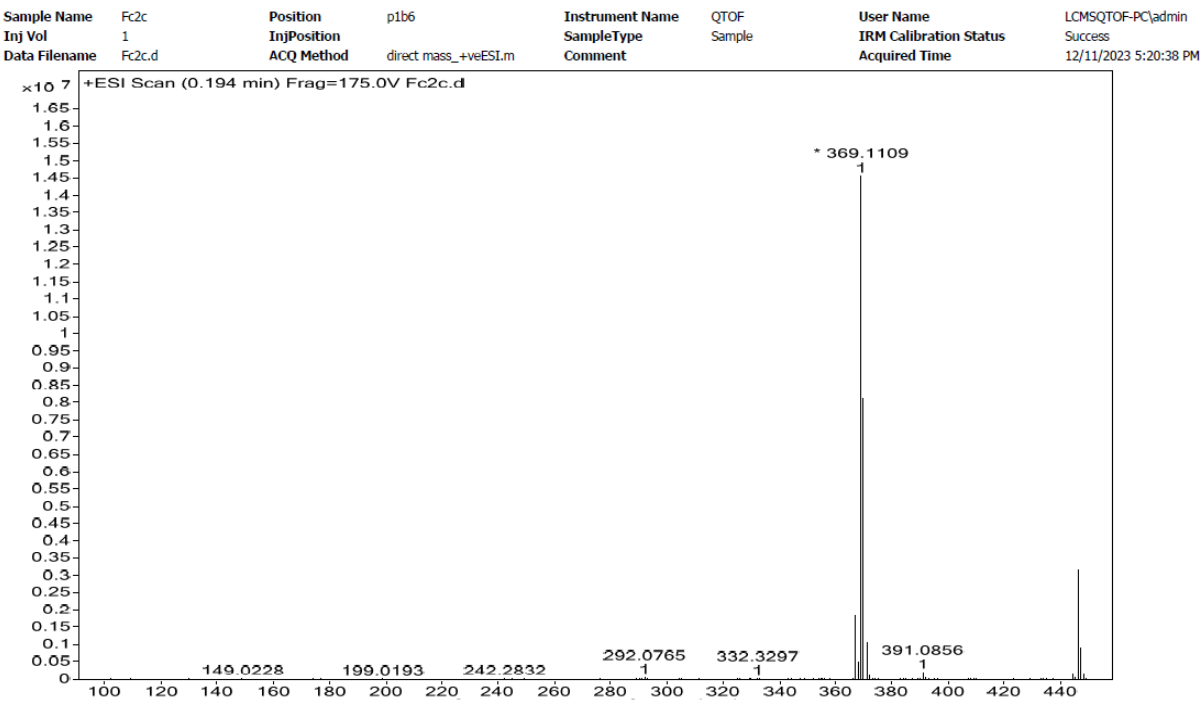

Figure S2ag: HRMS spectrum of **2c** (M: $C_{22}H_{20}FeN_2$) *m/z* calcd for [M+H$^+$] 369.1095, *m/z* found for [M+H$^+$] 369.1109.

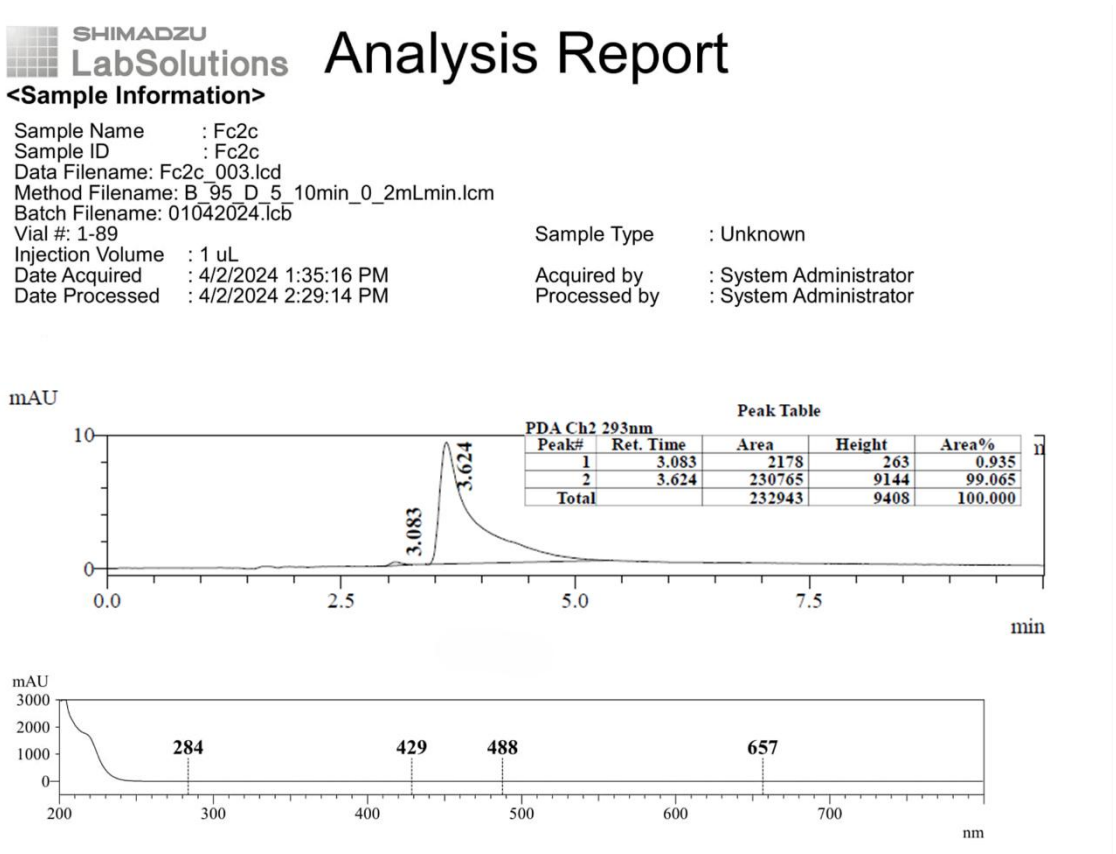

Figure S2ah: RP–HPLC–MS of **2c**; HPLC purity 99%; UV–vis spectrum shown at Rt = 3.634 min.

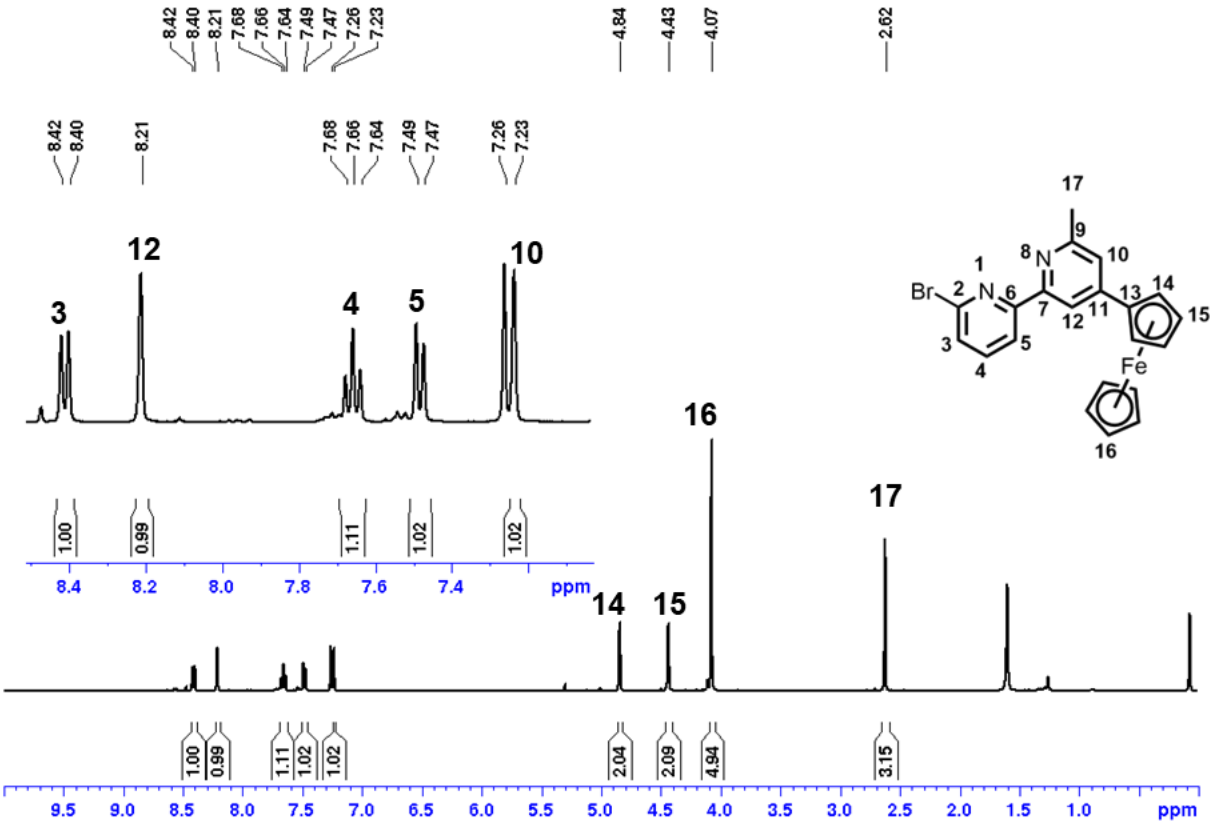

Figure S2ai: ^{1}H NMR ($CDCl_3$, 400 MHz) spectrum of **2d**.

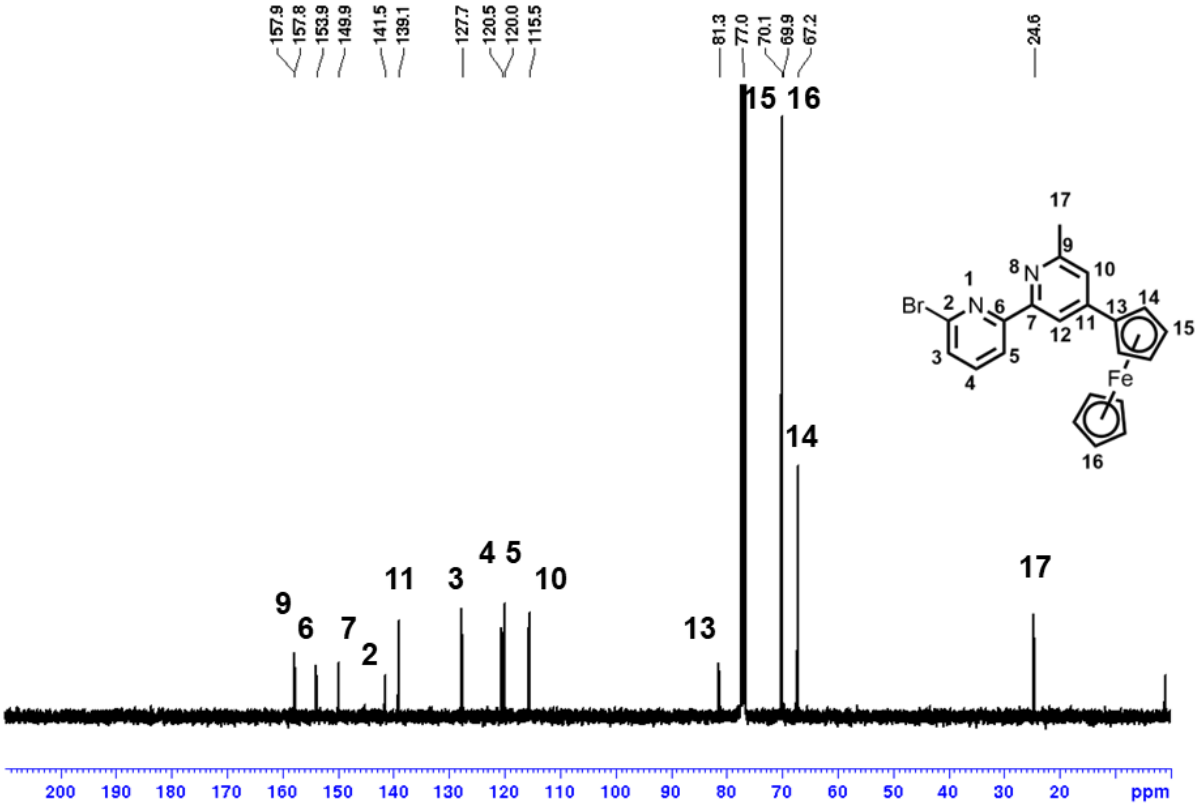

Figure S2aj: $^{13}C\{^{1}H\}$ NMR (101 MHz, $CDCl_3$) spectrum of **2d**.

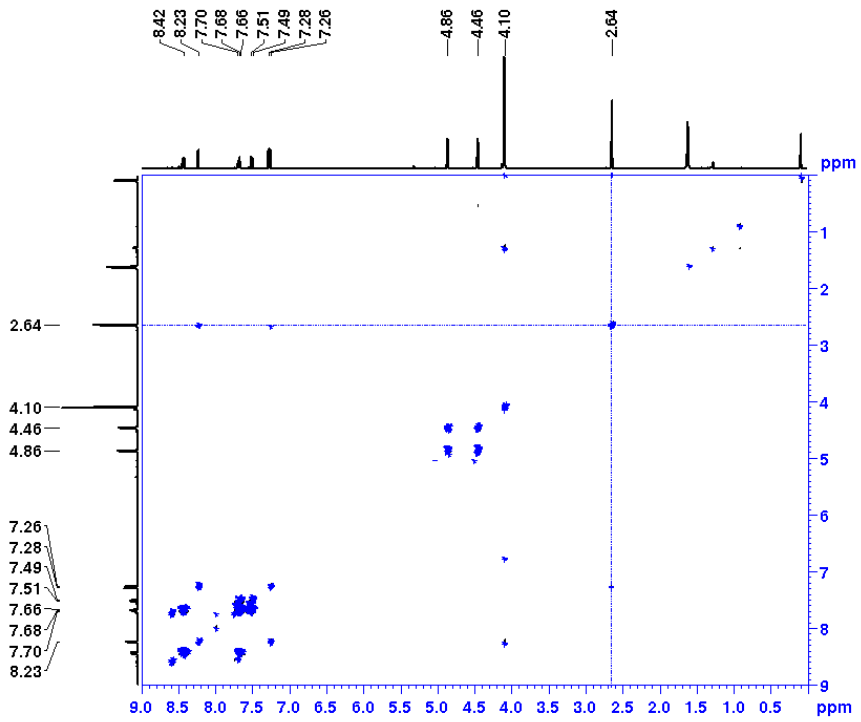

Figure S2ak: $^{1}H–^{1}H$ correlation spectrum of **2d** (400 MHz, $CDCl_3$); shows the correlation between methyl and aromatic protons.

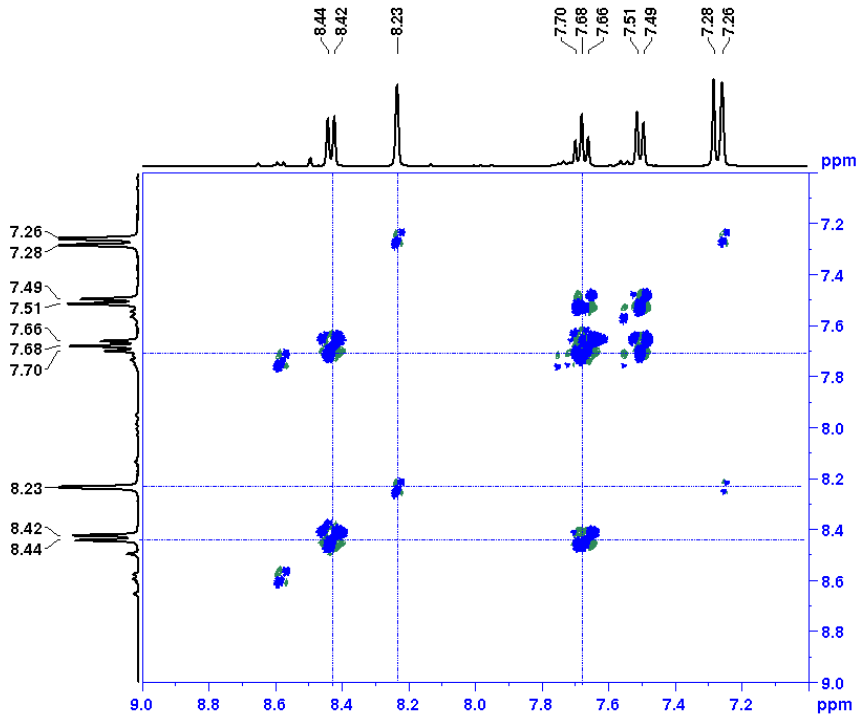

Figure S2al: $^{1}H–^{1}H$ correlation spectrum of **2d**, showing the correlations amongst the aromatic protons.

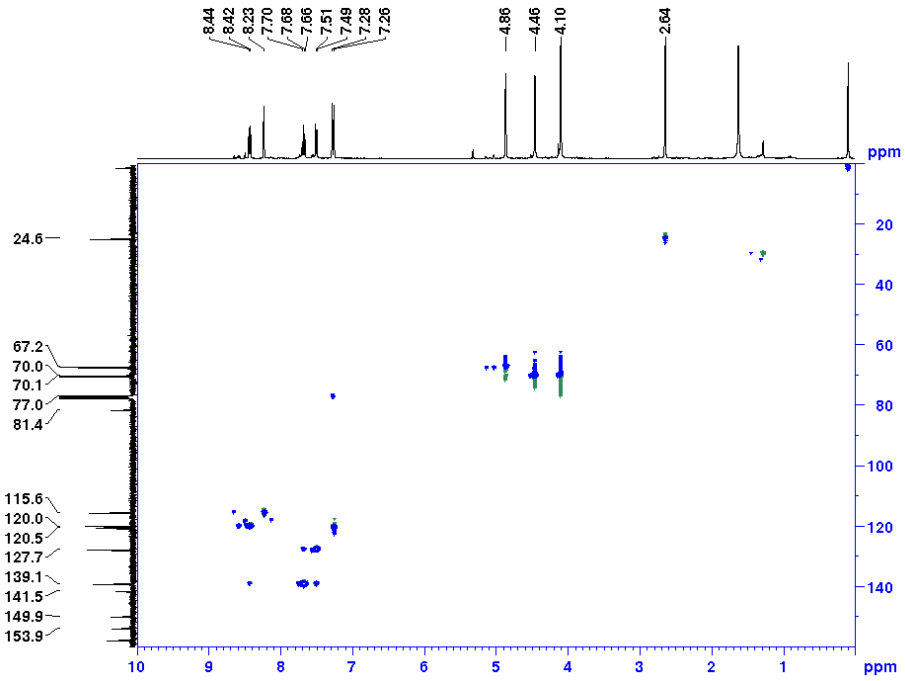

Figure S2am: HSQC spectrum of **2d** (400 MHz, $CDCl_3$).

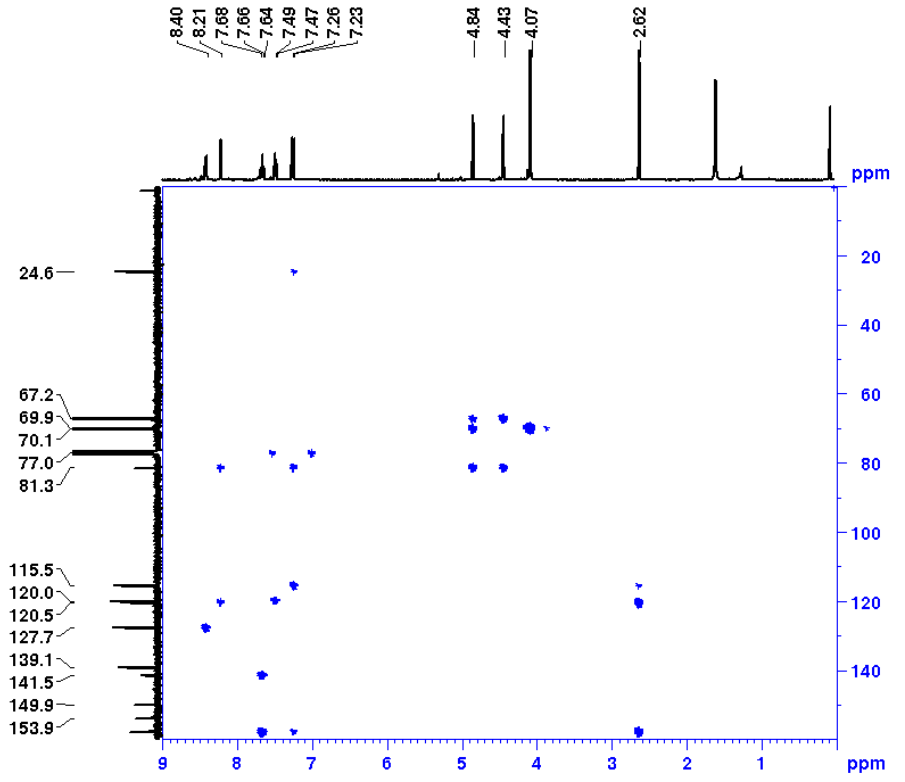

Figure S2an: HMBC spectrum of **2d** (400 MHz, $CDCl_3$).

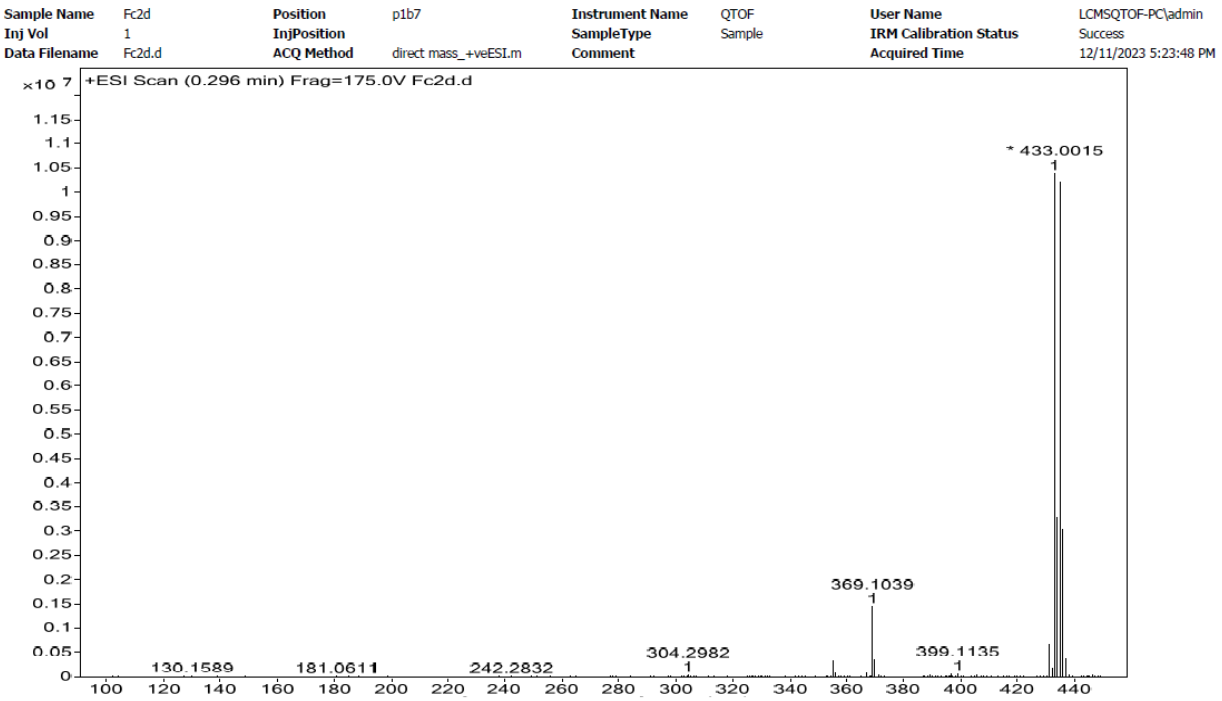

Figure S2ao: HRMS spectrum of **2d** (M: $C_{21}H_{17}BrFeN_2$) *m/z* calcd for [M+H$^+$] 433.0044, *m/z* found for [M+H$^+$] 433.0015.

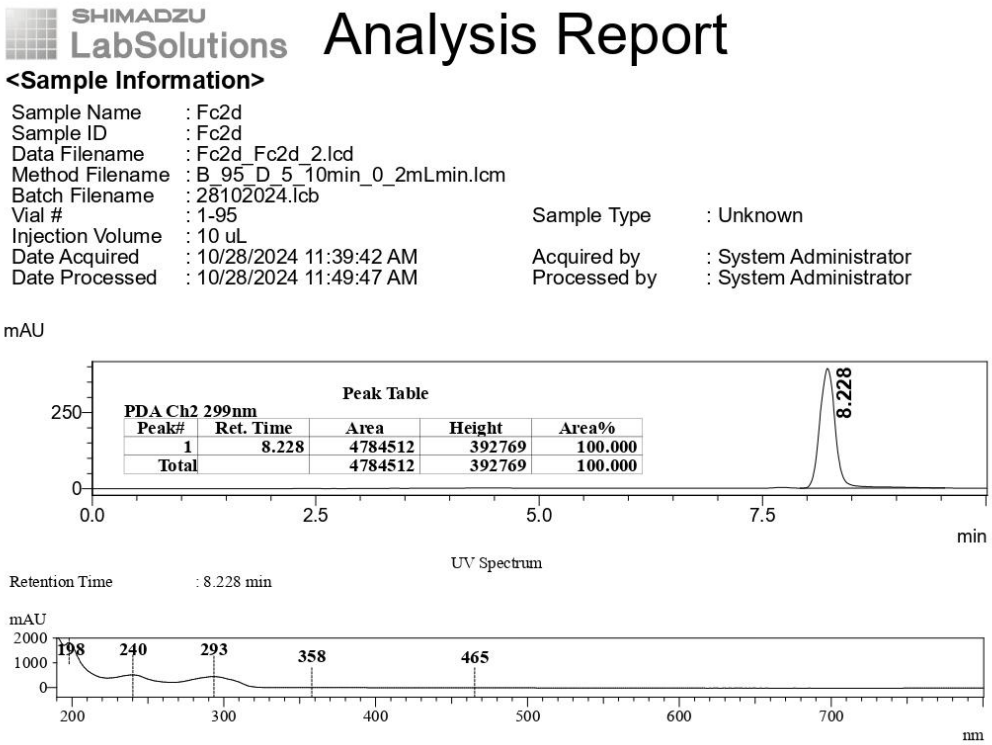

Figure S2ap: RP–HPLC–MS of **2d**; HPLC purity 100%; UV–vis spectrum shown at Rt = 8.228 min.

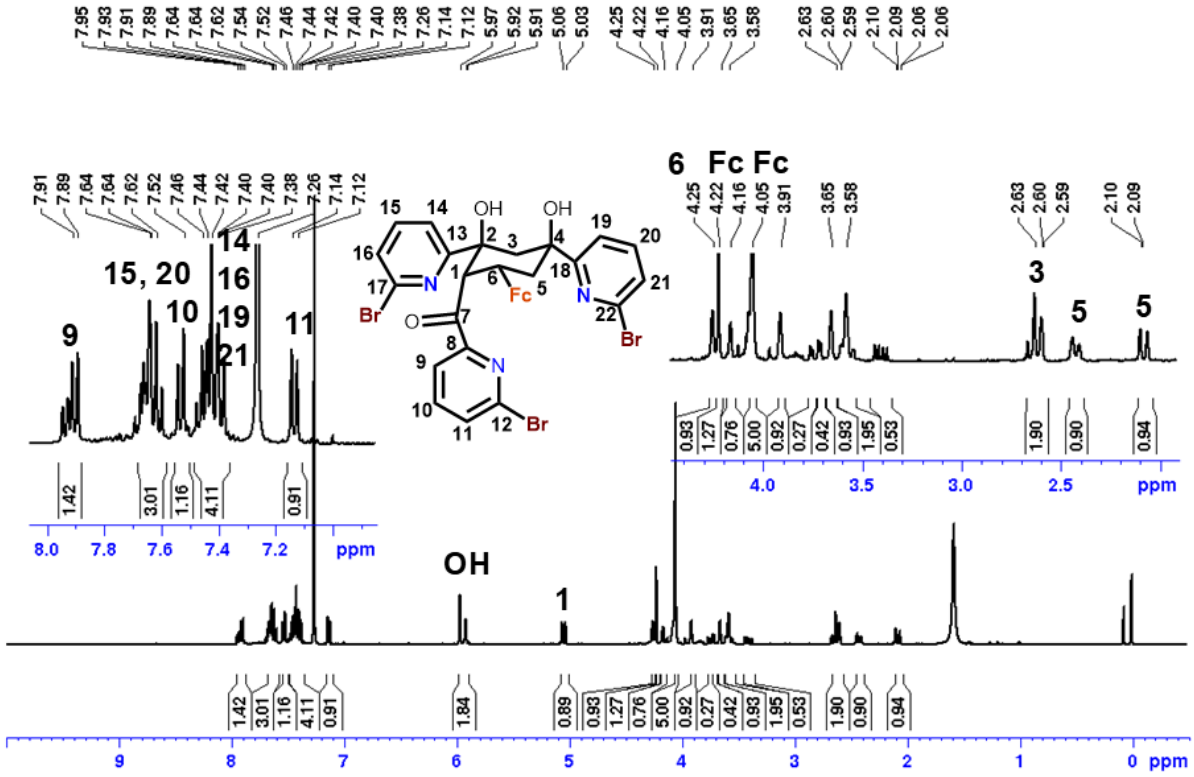

Figure S2aq: ^{1}H NMR (400 MHz, $CDCl_3$) spectrum of by-product **2d′**.

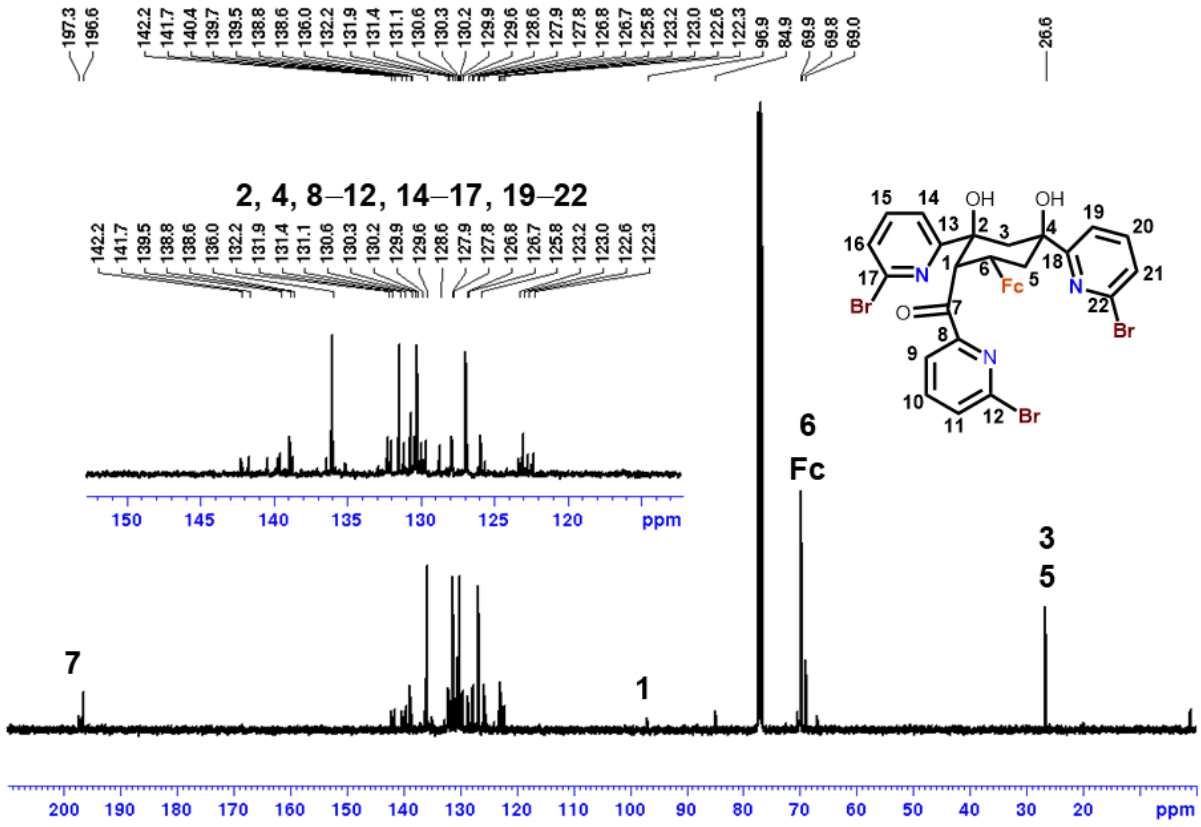

Figure S2ar: $^{13}C\{^{1}H\}$ NMR (101 MHz, $CDCl_3$) spectrum of by-product **2d′**.

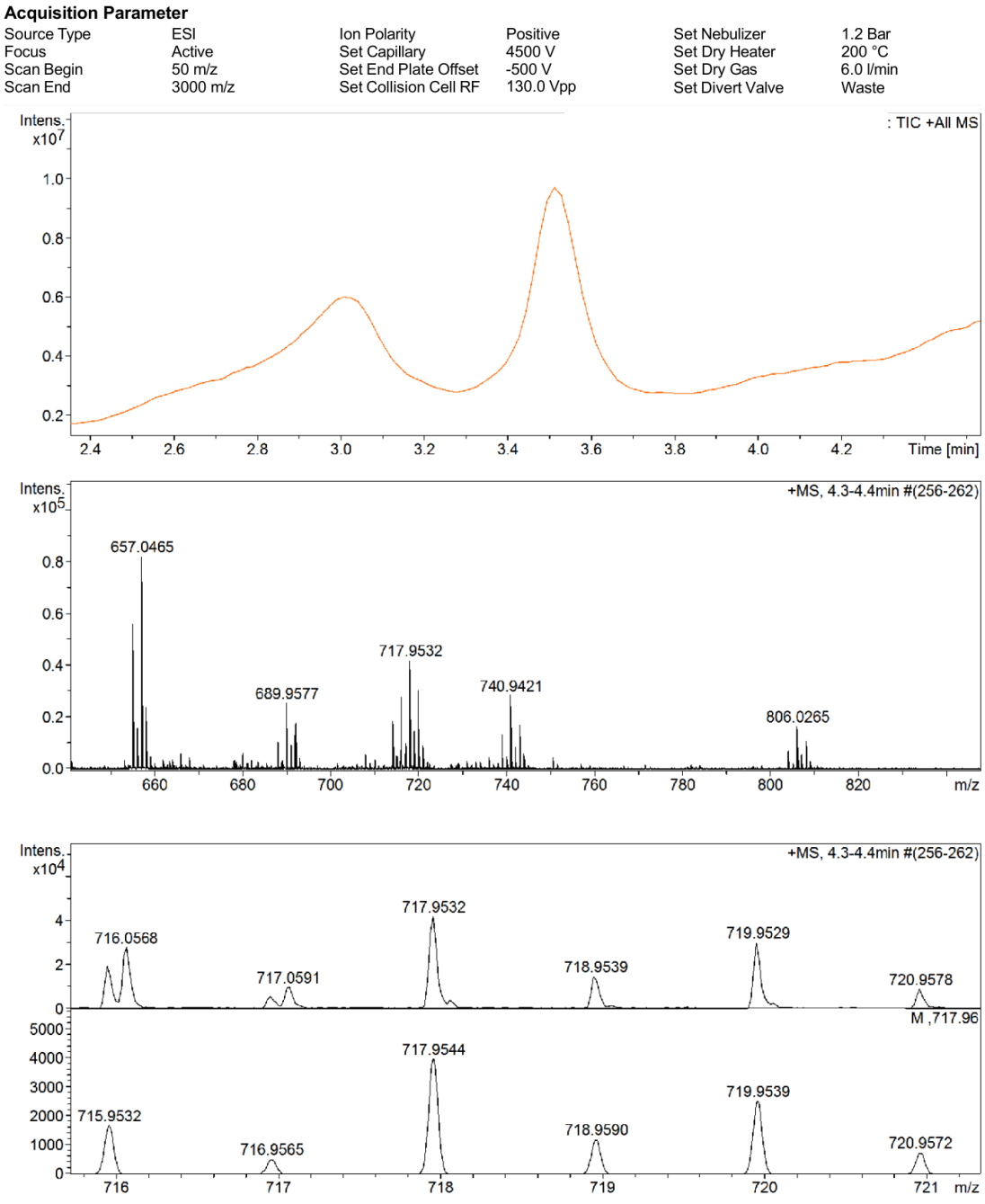

Figure S2as: HRMS spectrum of **2d′** (M: $C_{32}H_{26}Br_3FeN_3O_3$) *m/z* calcd for [M–Br+Na^+] 740.9635, *m/z* found for [M–Br+Na^+] 740.9421; *m/z* calcd for [M–Br^+] 717.9737, *m/z* found for [M–Br^+] 717.9544.

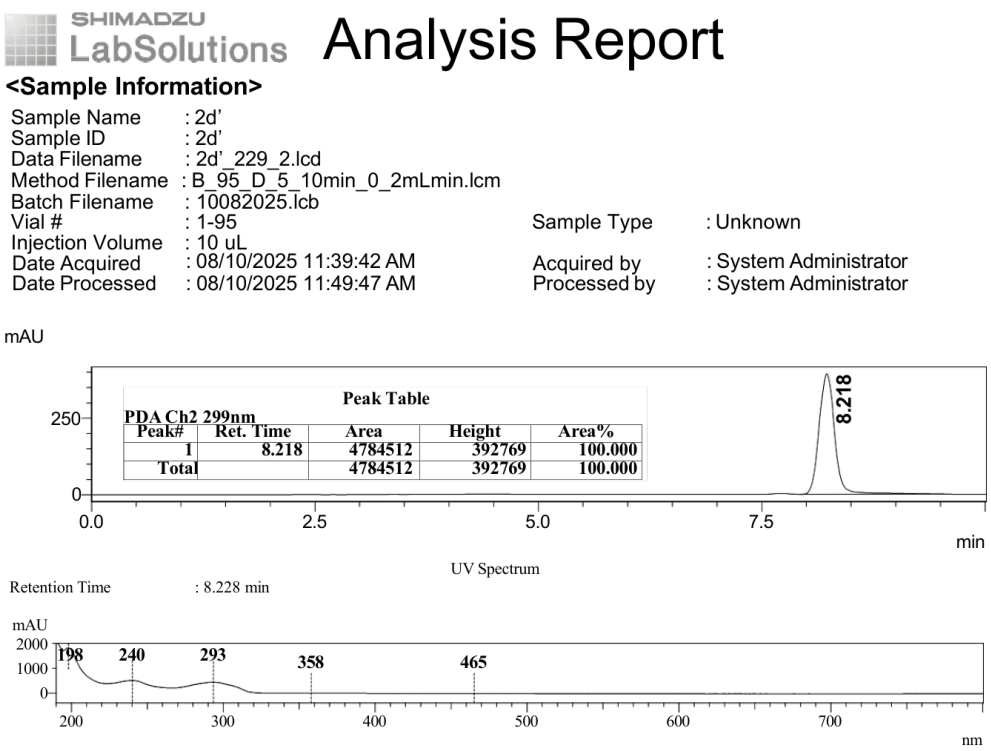

Figure S2at: RP–HPLC–MS of **2d′**; HPLC purity 80%; UV–vis spectrum shown at Rt = 8.218 min.

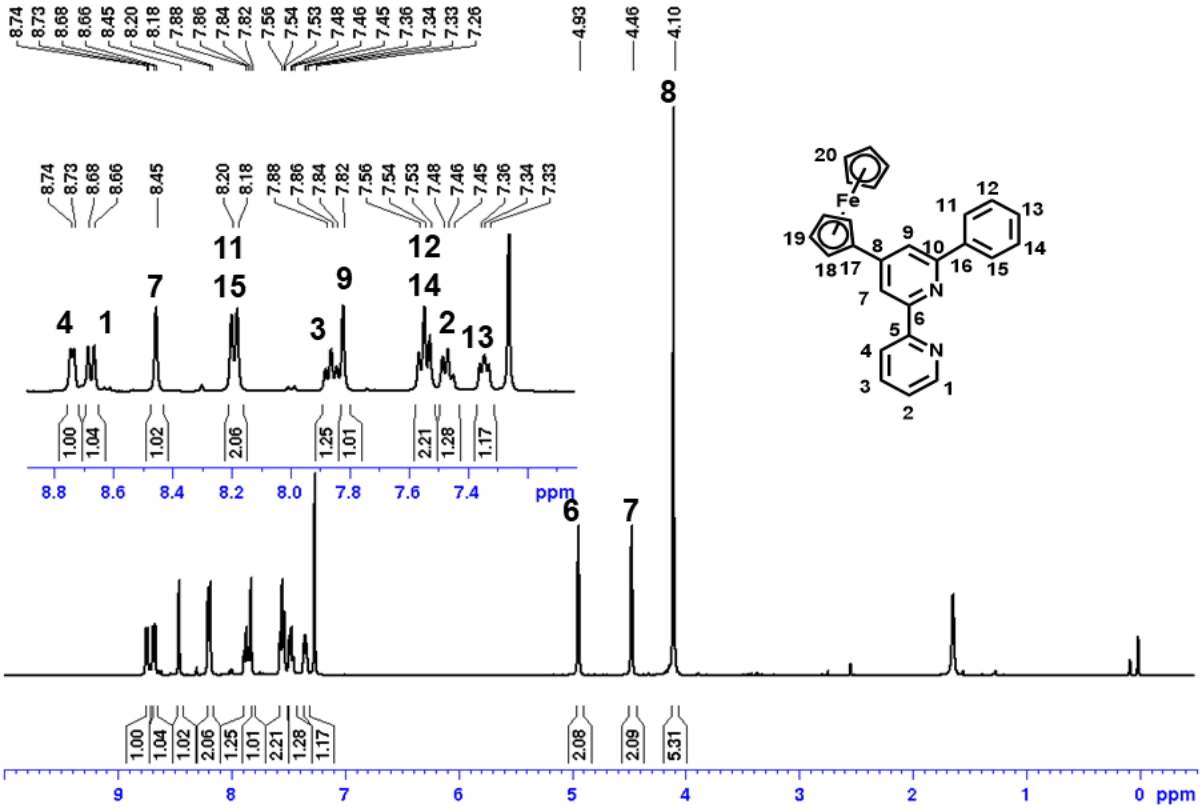

Figure S2au: ^{1}H NMR (400 MHz, $CDCl_3$) spectrum of ligand **2e**.

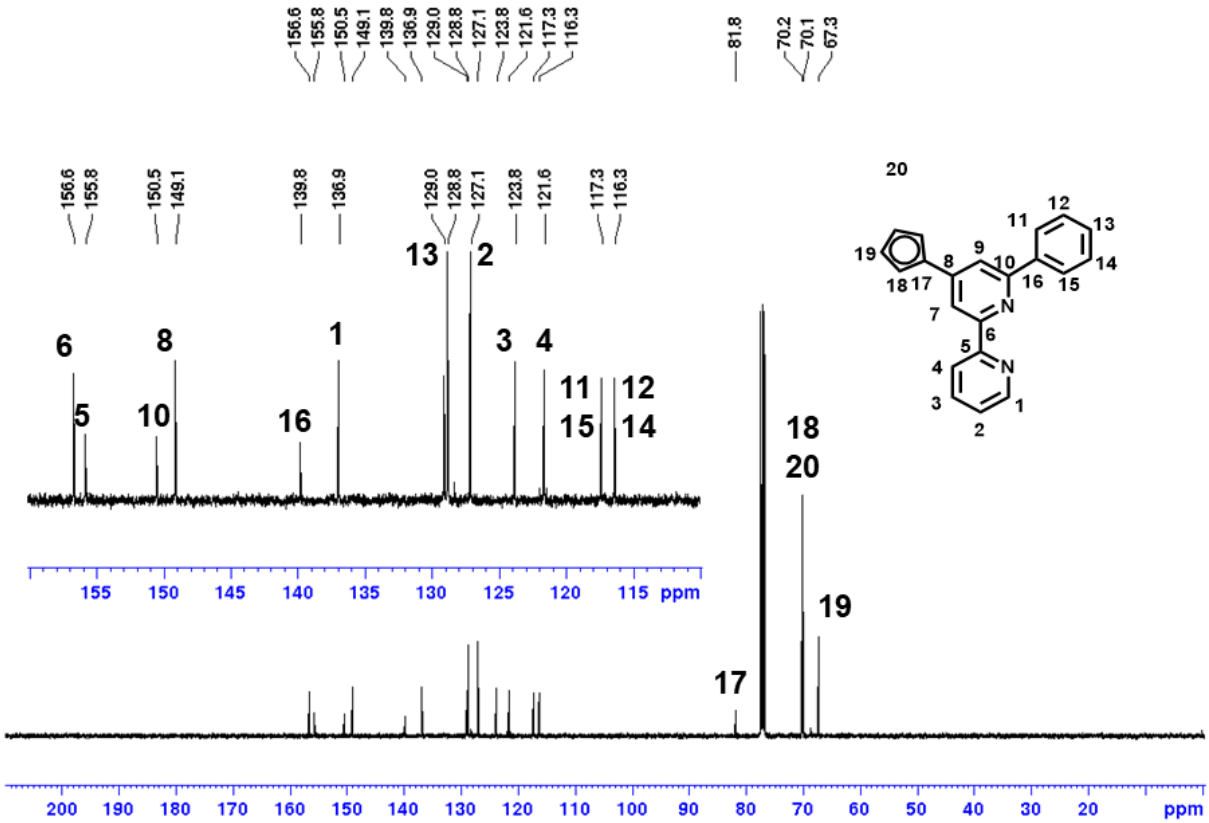

Figure S2av: $^{13}C\{^{1}H\}$ NMR (101 MHz, $CDCl_3$) spectrum of ligand **2e**.

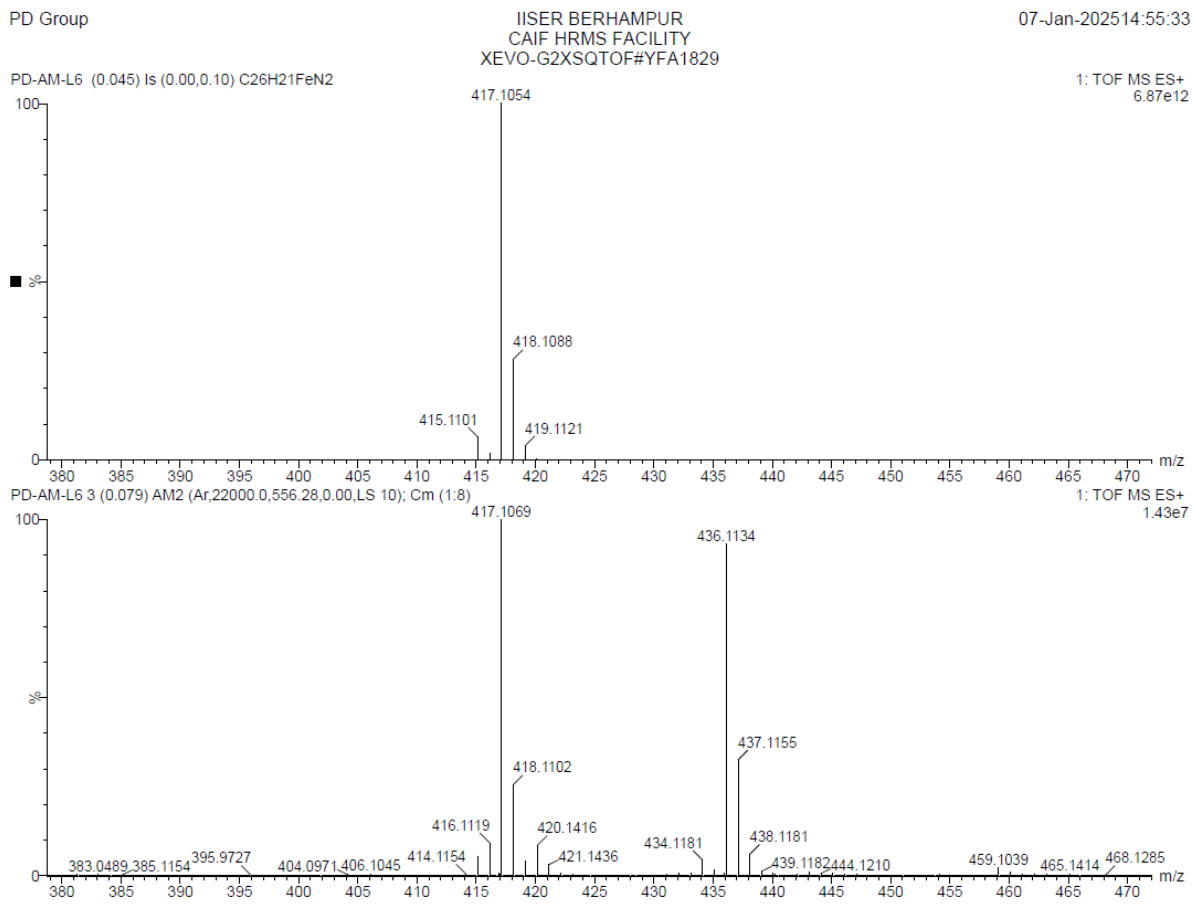

Figure S2aw: HRMS spectrum of **2e** (M: $C_{26}H_{20}FeN_2$) *m/z* calcd for [M+H$^+$] 417.1095, *m/z* found for [M+H$^+$] 417.1069.

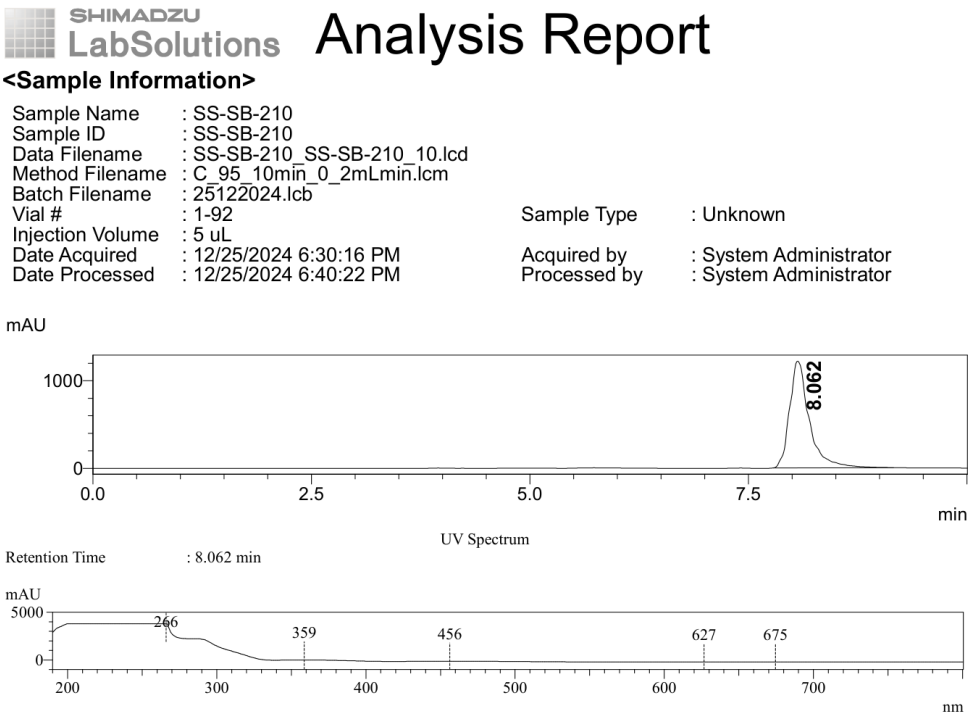

Figure S2ax: RP–HPLC–MS of **2e**; HPLC purity 100%; UV–vis spectrum shown at Rt = 8.062 min.

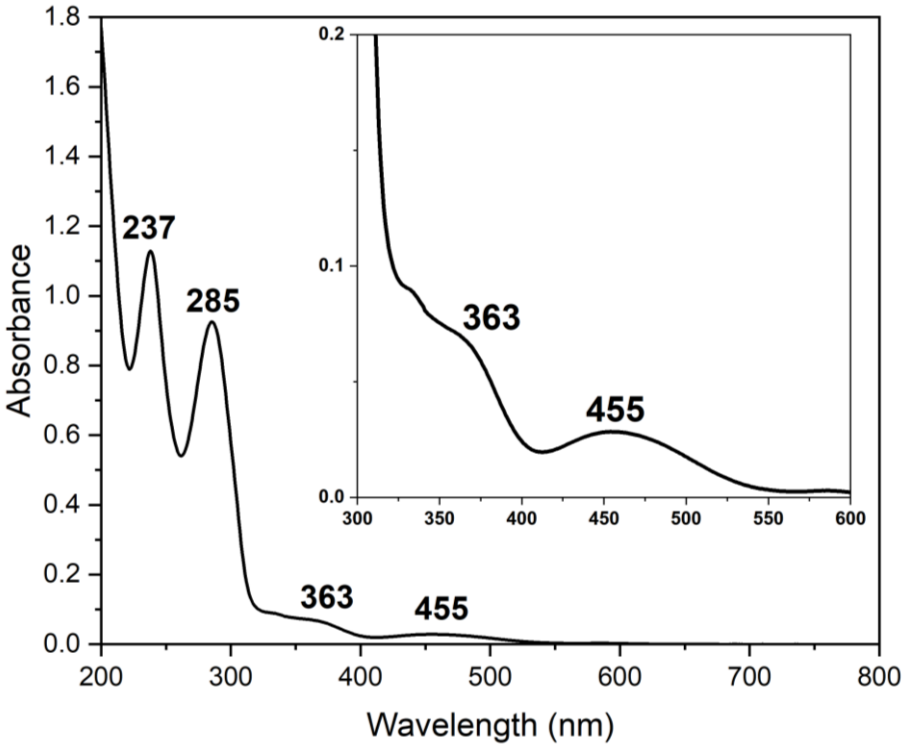

Figure S2ay: Absorbance spectrum of **2a** (0.1 μM) in acetonitrile; inset shows the zoomed region of 300–600 nm.

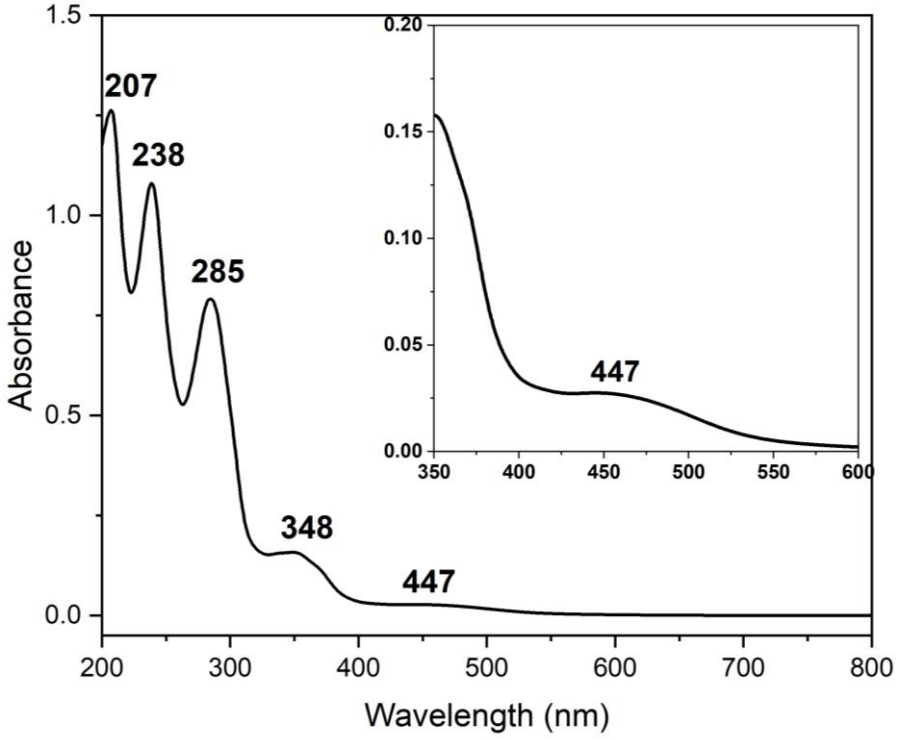

Figure S2az: Absorbance spectrum of **2b** (0.1 μM) in acetonitrile; inset shows the zoomed region of 350–600 nm.

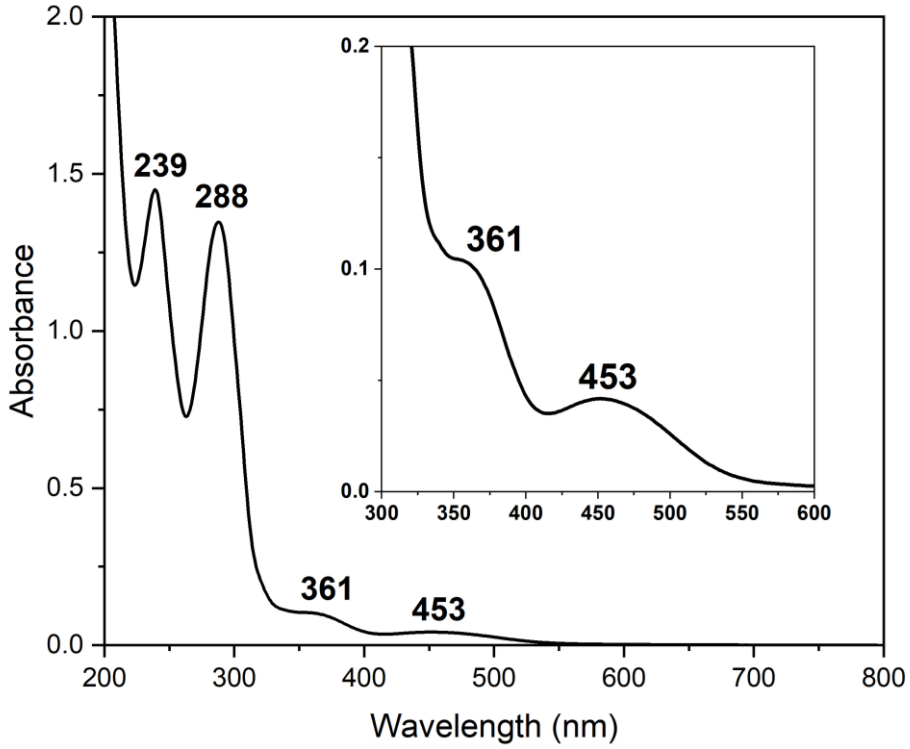

Figure S2ba: Absorbance spectrum of **2c** (0.1 μM) in acetonitrile; inset shows the zoomed region of 300–600 nm.

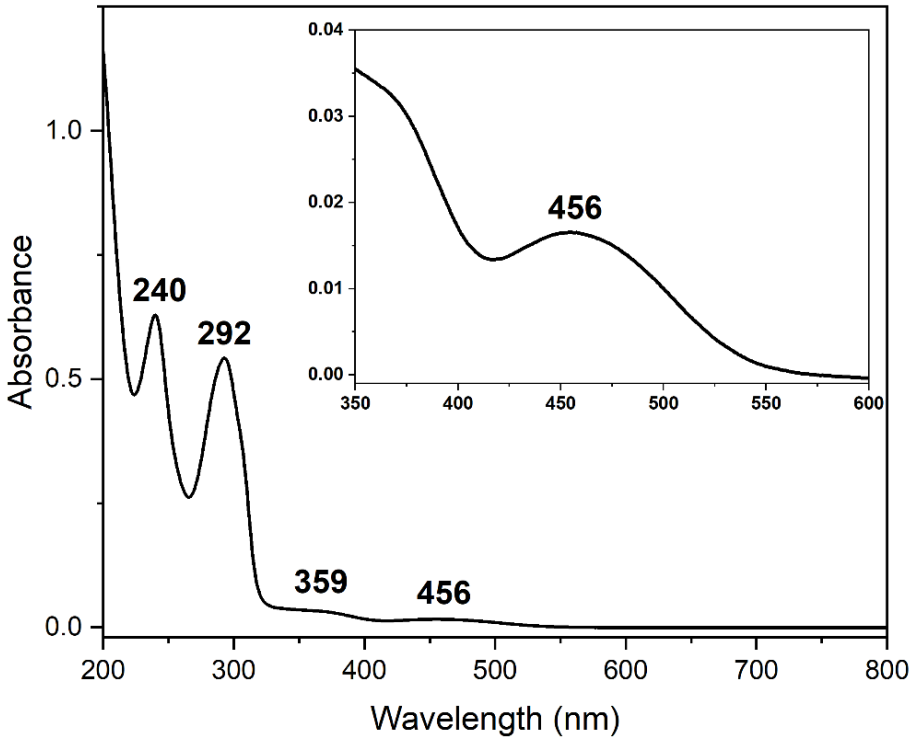

Figure S2bb: Absorbance spectrum of **2d** (0.1 μM) in acetonitrile; inset shows the zoomed region of 350–600 nm.

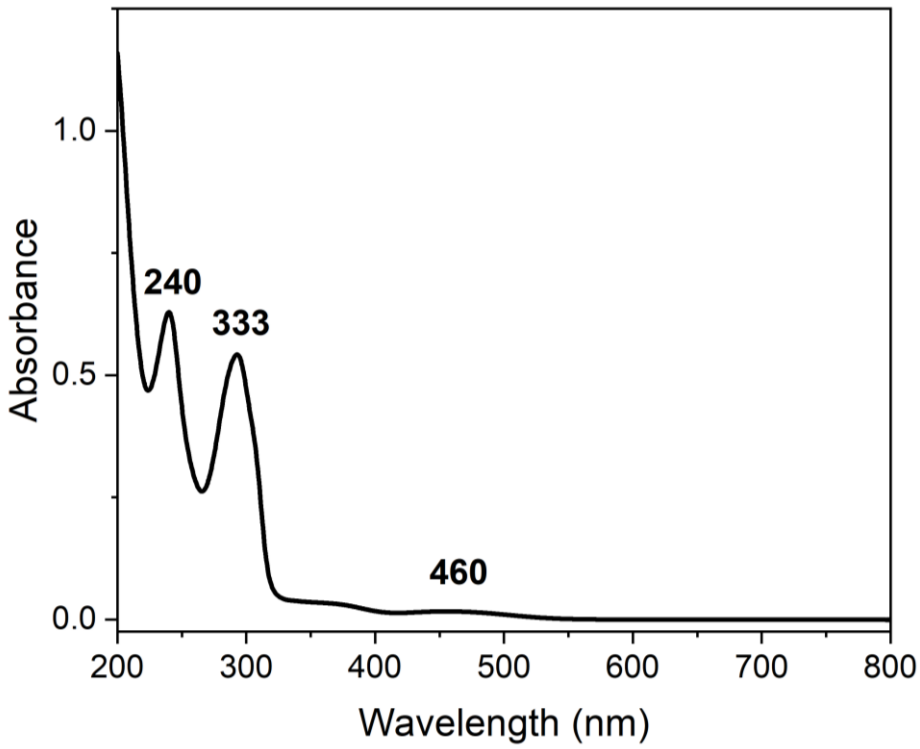

Figure S2bc: Absorbance spectrum of **2d′** (0.1 μM) in acetonitrile.

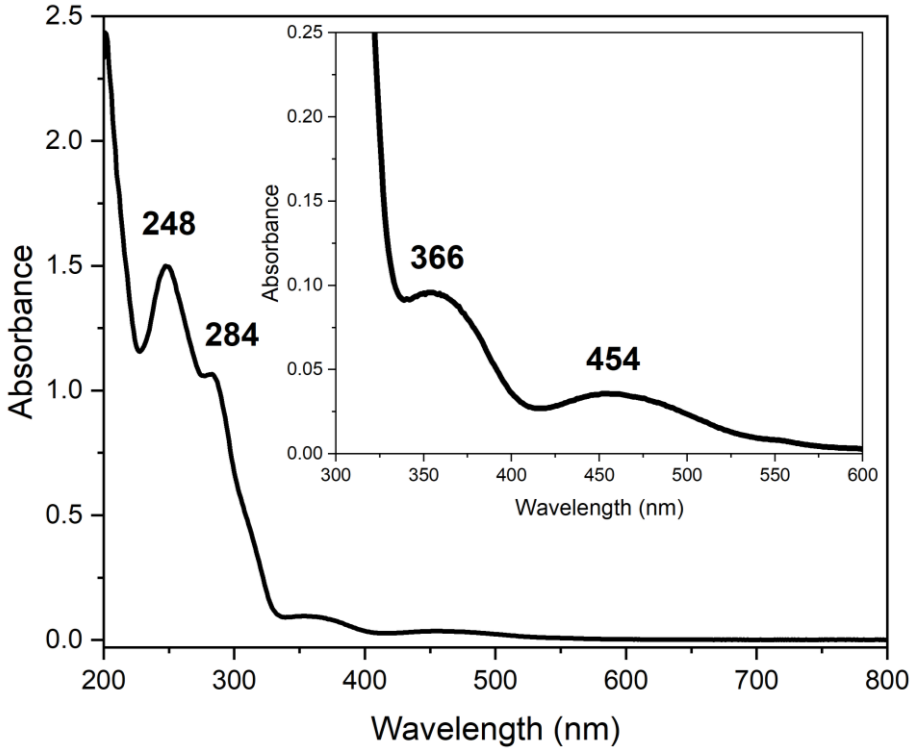

Figure S2bd: Absorbance spectrum of **2e** (0.1 μM) in acetonitrile; inset shows the zoomed region of 300–600 nm.

Characterisation of complexes

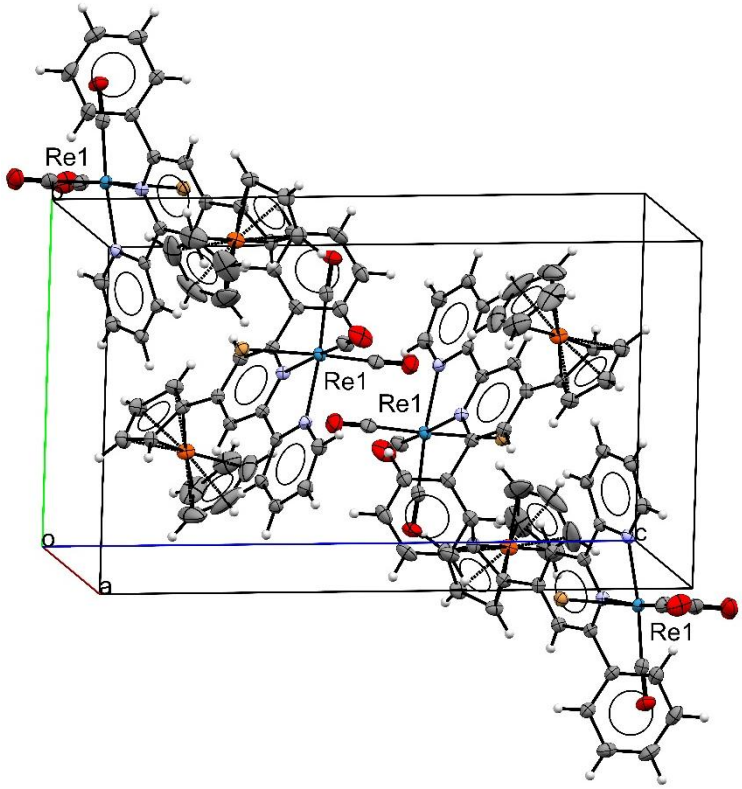

Figure S3a: 3e in the lattice unit cell.

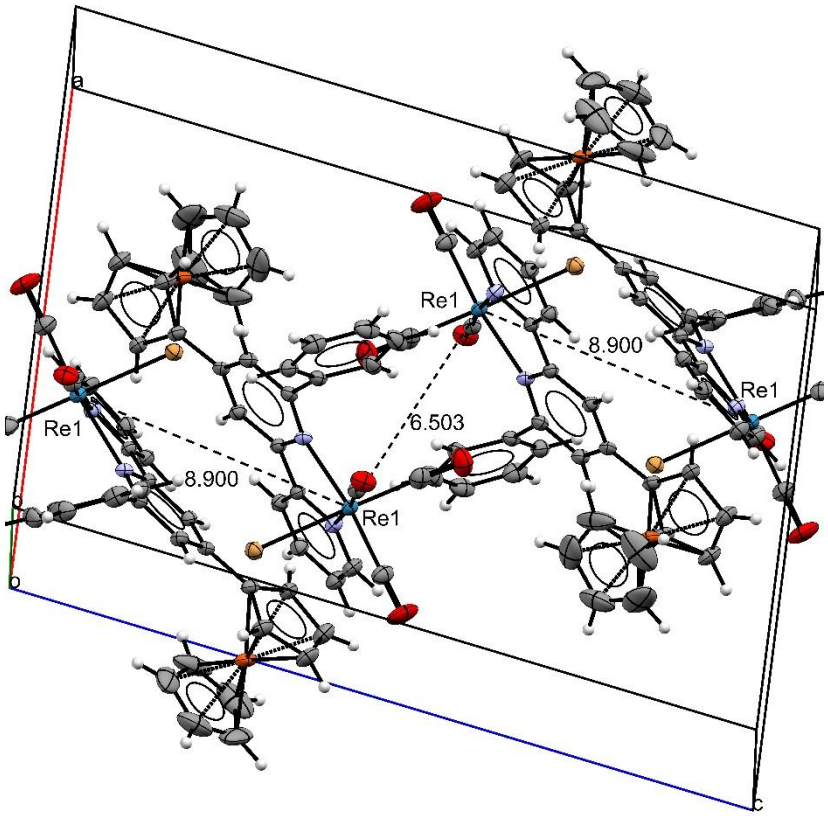

Figure S3b: The weak interactions shown between the Re(I) centers in the unit cell of **3e**.

Table S4: Crystal data and structure refinement of **3e**.

Identification code	**3e**
CCDC deposition number	2443100
Empirical formula	$C_{29}H_{20}FeN_2O_3ReBr$
Formula weight	766.449
Temperature/K	140.00
Crystal system	monoclinic
Space group	$P2_1/n$
a/Å	12.7797(11)
b/Å	10.8637(8)
c/Å	19.3382(15)
α/°	90
β/°	99.810(3)
γ/°	90
Volume/Å^3	2645.6(4)
Z	4
ρ_{calc} g/cm^3	1.924
μ/mm^{-1}	6.664
F(000)	1471.2
Crystal size/mm^3	0.2 × 0.1 × 0.05
Radiation	Mo Kα (λ = 0.71073)
2Θ range for data collection/°	4.28 to 59.14
Index ranges	$-17 \le h \le 17$, $-15 \le k \le 15$, $-26 \le l \le 26$
Reflections collected	62962
Independent reflections	7329 [R_{int} = 0.0654, R_{sigma} = 0.0367]
Data/restraints/parameters	7329/0/334
Goodness-of-fit on F^2	1.052
Final R indexes [I>=2σ (I)]	R_1 = 0.0228, wR_2 = 0.0542
Final R indexes [all data]	R_1 = 0.0275, wR_2 = 0.0579
Largest diff. peak/hole / e Å^{-3}	0.90/−1.26

Table S5: Bond lengths and angles for **3e**.

Bond lengths for 3e					
Atom	**Atom**	**Length/Å**	**Atom**	**Atom**	**Length/Å**
Re1	N1	2.2019(18)	C8	C14	1.481(3)
Re1	N2	2.173(2)	C4	C9	1.478(3)
Re1	C3	1.916(3)	C14	C15	1.393(3)
Re1	C2	1.907(3)	C13	C12	1.377(3)
Re1	C1	1.921(3)	C4	C5	1.384(3)
Re1	Br1	2.6223(3)	C6	C20	1.462(3)
N1	C8	1.363(3)	Fe1	C20	2.030(2)
N1	C4	1.354(3)	Fe1	C25	2.031(3)
N2	C9	1.353(3)	C20	C21	1.434(3)
N2	C13	1.350(3)	C25	C26	1.379(6)

Bond angles for 3e							
Atom	**Atom**	**Atom**	**Angle/°**	**Atom**	**Atom**	**Atom**	**Angle/°**
N2	Re1	N1	75.01(7)	Br1	Re1	N1	82.45(5)
C3	Re1	N1	171.25(9)	Br1	Re1	N2	80.39(5)
C3	Re1	N2	98.49(9)	Br1	Re1	C3	90.76(9)
C2	Re1	N1	97.90(9)	Br1	Re1	C2	176.84(7)
C2	Re1	N2	96.65(9)	Br1	Re1	C1	95.46(7)
C2	Re1	C3	88.58(12)	C20	C6	C5	122.8(2)
C1	Re1	N1	100.68(8)	C6	C20	Fe1	124.87(16)
C1	Re1	N2	174.31(8)	C6	C20	C21	126.6(2)
C1	Re1	C3	85.40(10)	C6	C20	C24	125.8(2)
C1	Re1	C2	87.57(10)	C7	C6	C20	120.8(2)

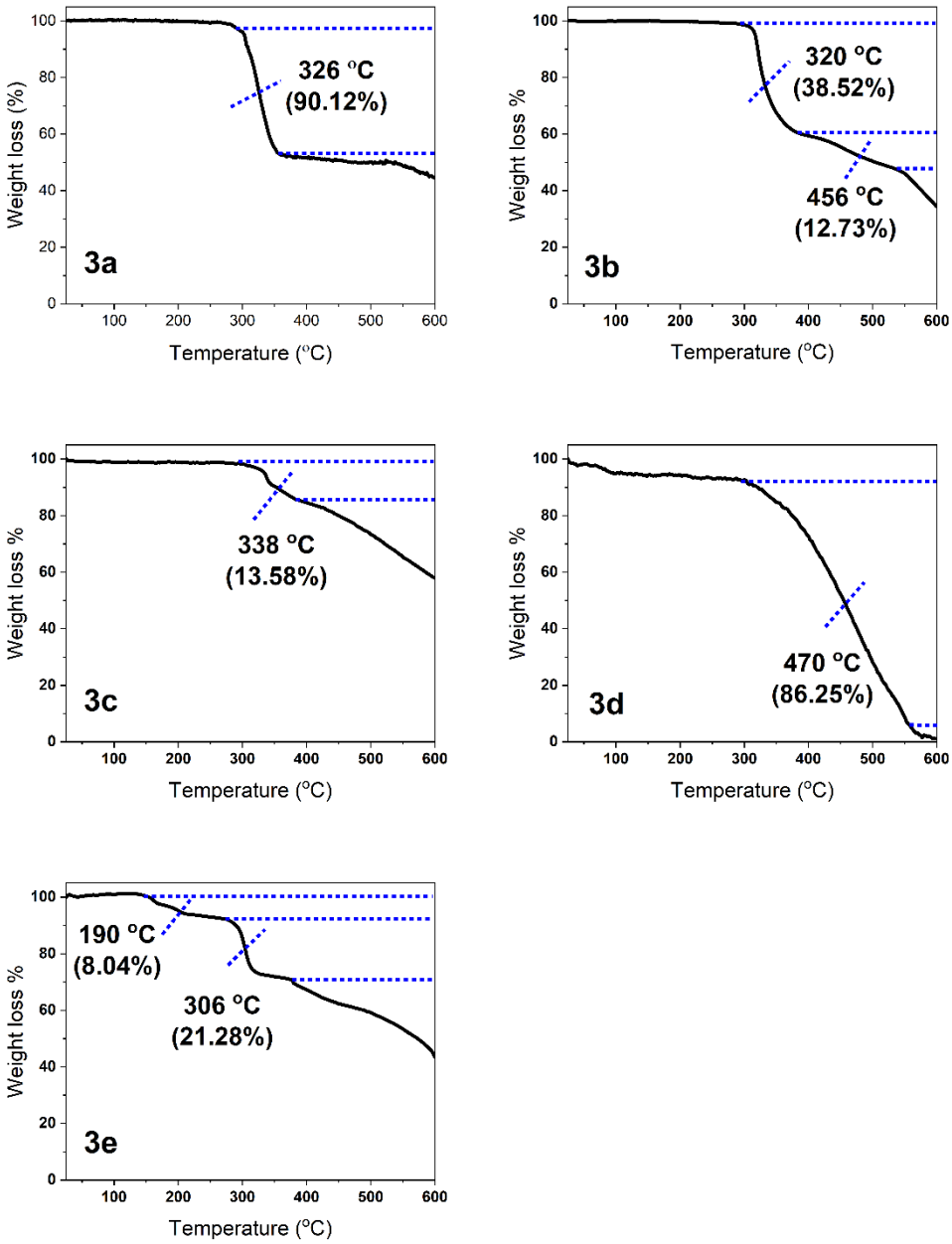

Figure S3c: Thermogravimetric profile of the rhenium complexes, measured from 25–600 °C, with a heating rate of 10K/min under N_2 flow.

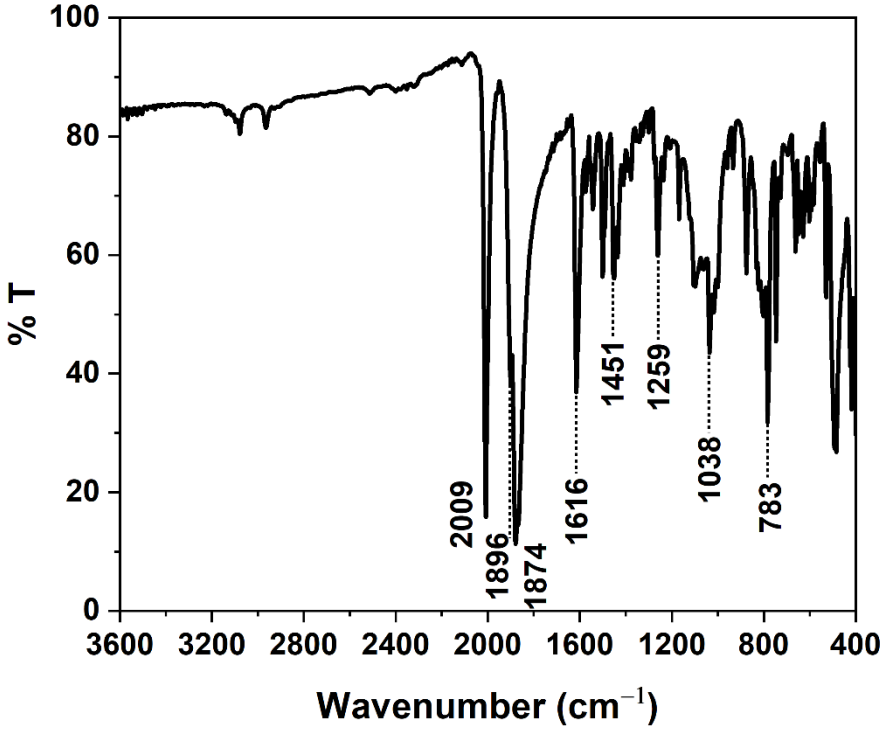

Figure S3d: ATR-IR spectrum of **3a**.

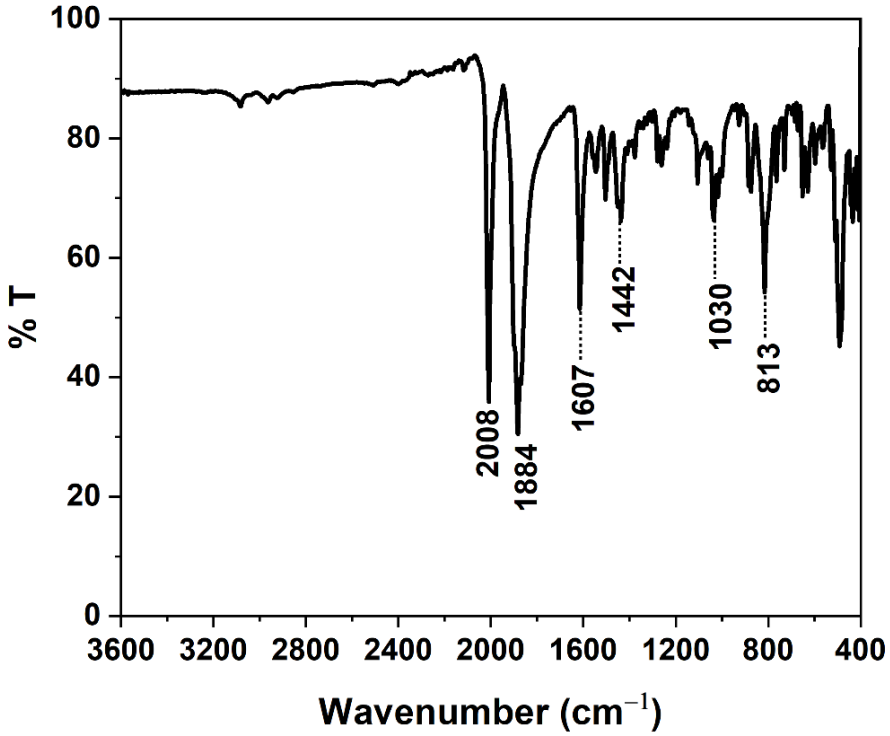

Figure S3e: ATR-IR spectrum of **3b**.

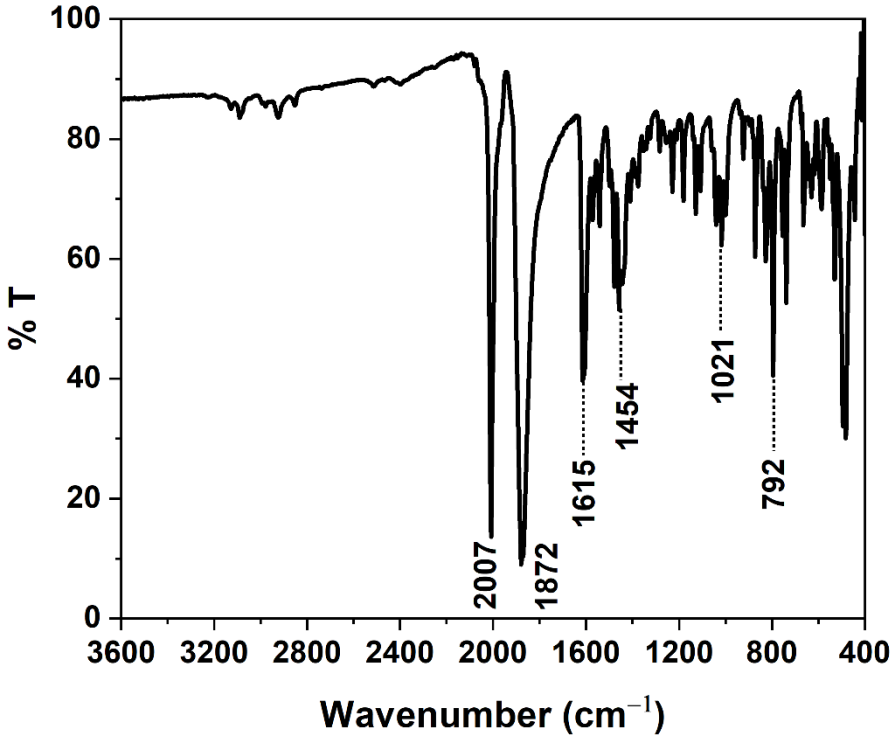

Figure S3f: ATR-IR spectrum of **3c**.

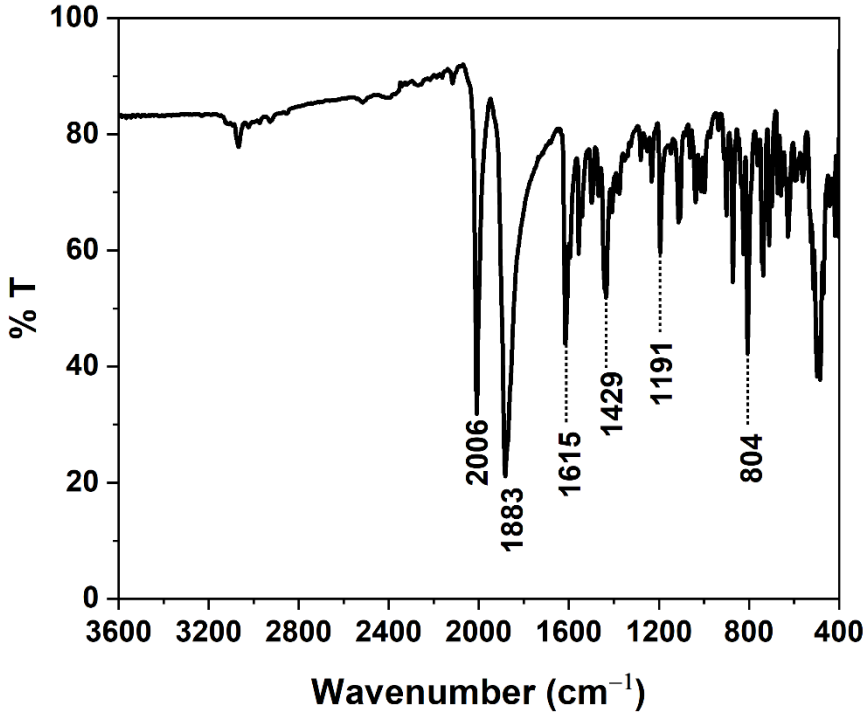

Figure S3g: ATR-IR spectrum of **3d**.

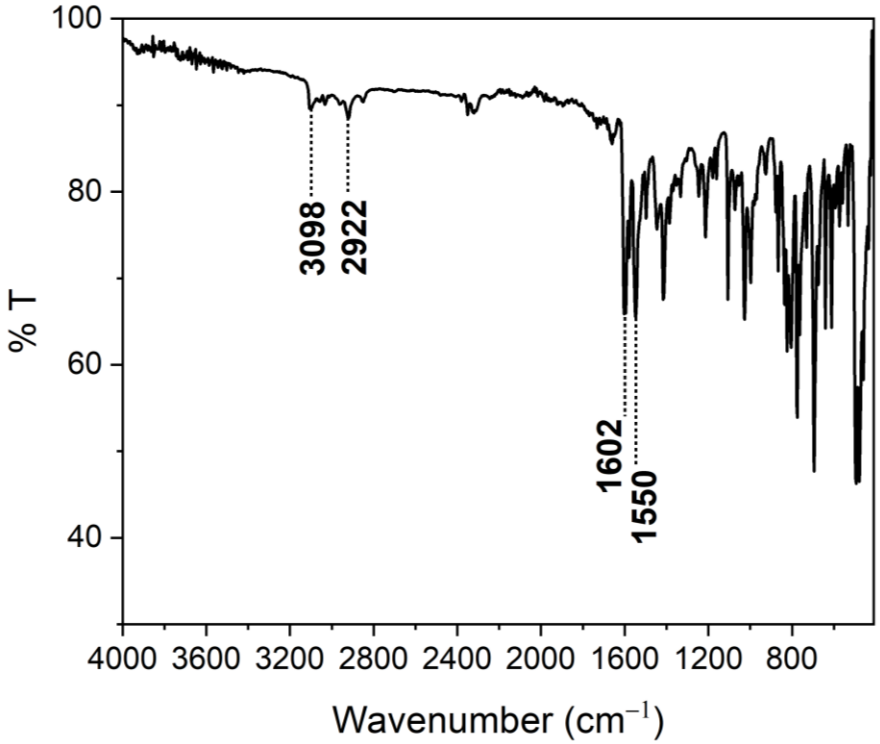

Figure S3h: ATR-IR spectrum of **3e**.

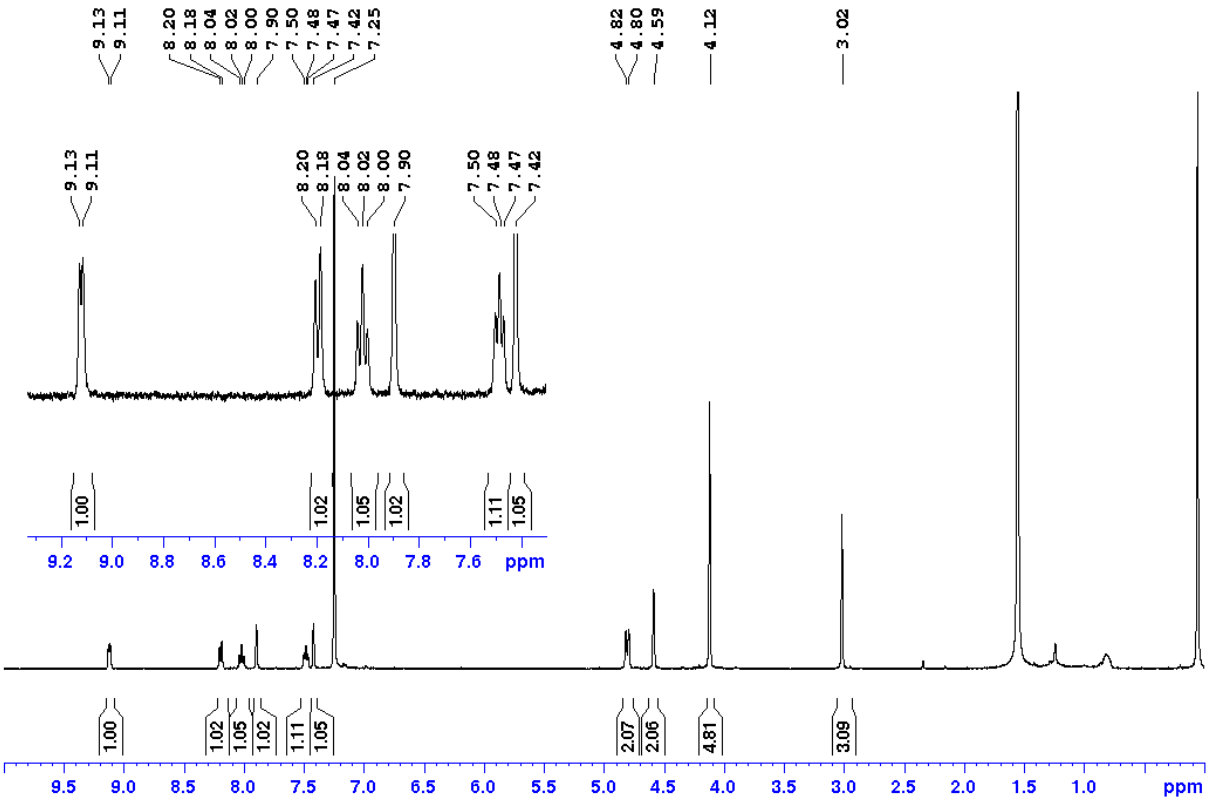

Figure S3i: ^{1}H NMR ($CDCl_3$, 400 MHz) spectrum of **3a**.

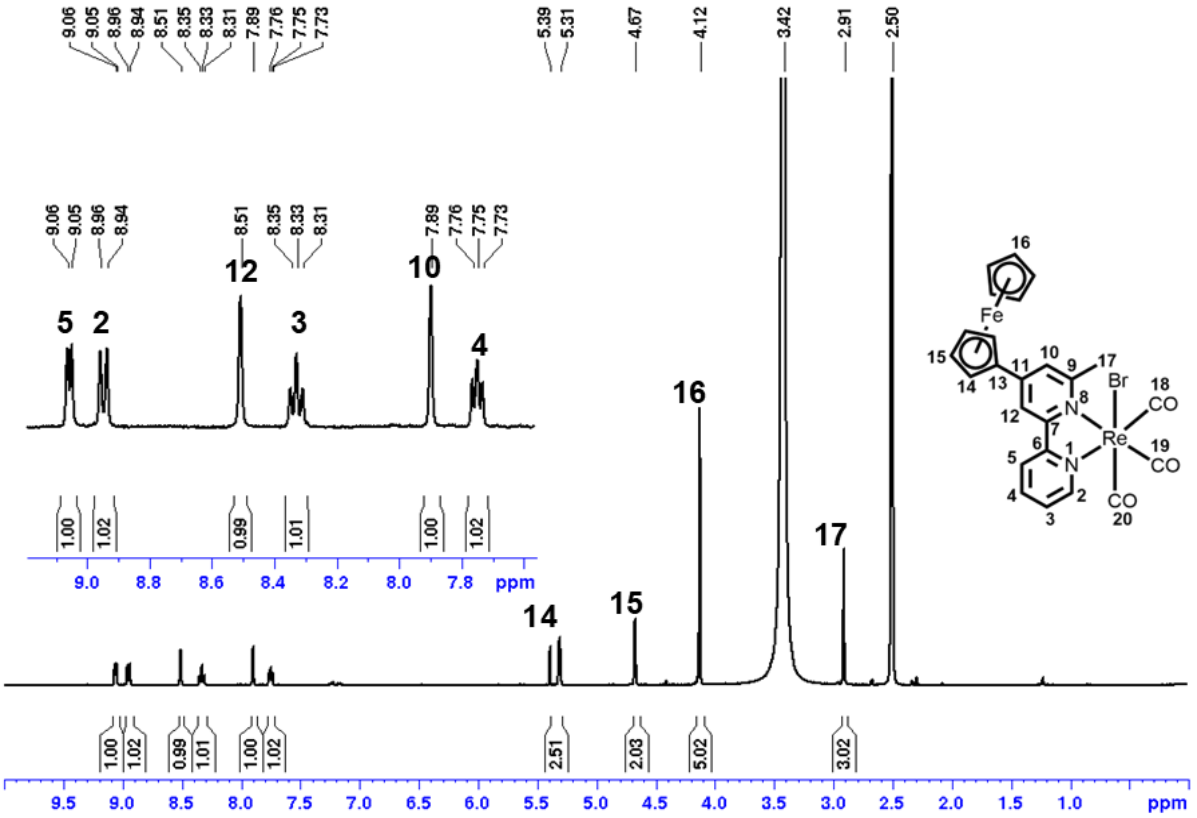

Figure S3j: ^{1}H NMR (DMSO-D_6, 400 MHz) spectrum of **3a**.

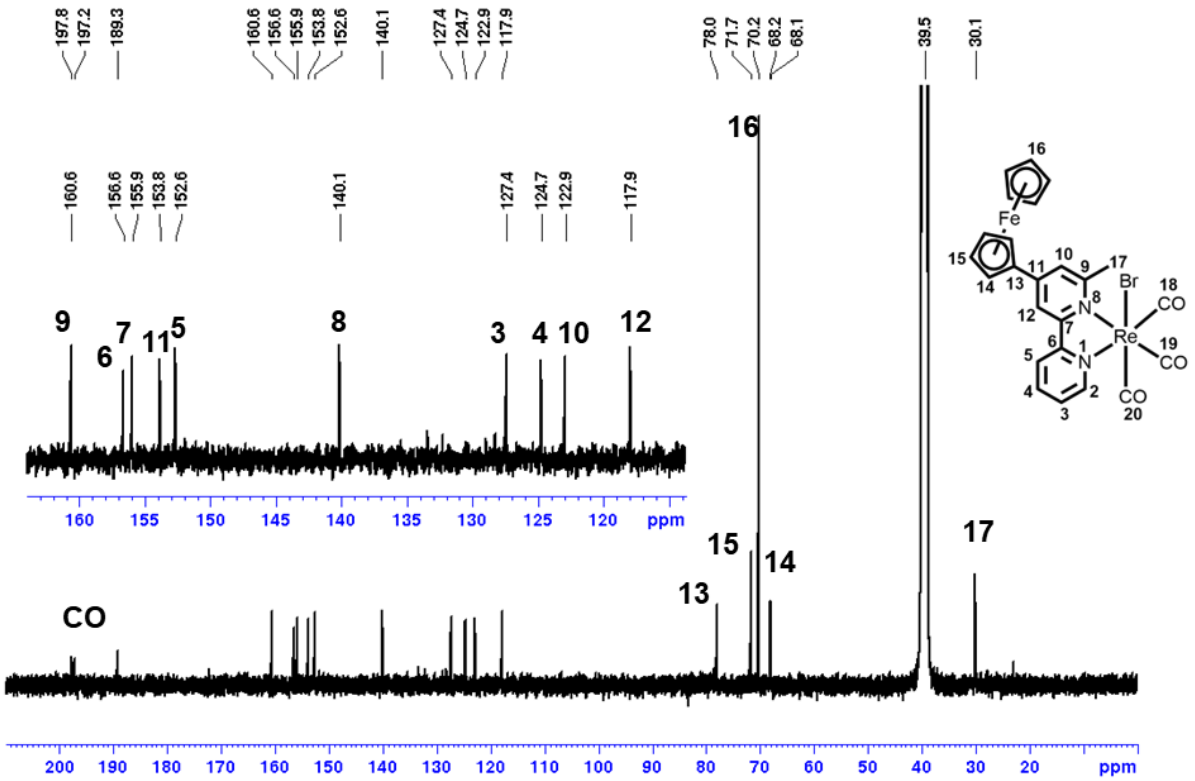

Figure S3k: $^{13}C\{^{1}H\}$ NMR (101 MHz, DMSO-D_6) spectrum of **3a**, with 13203 scans.

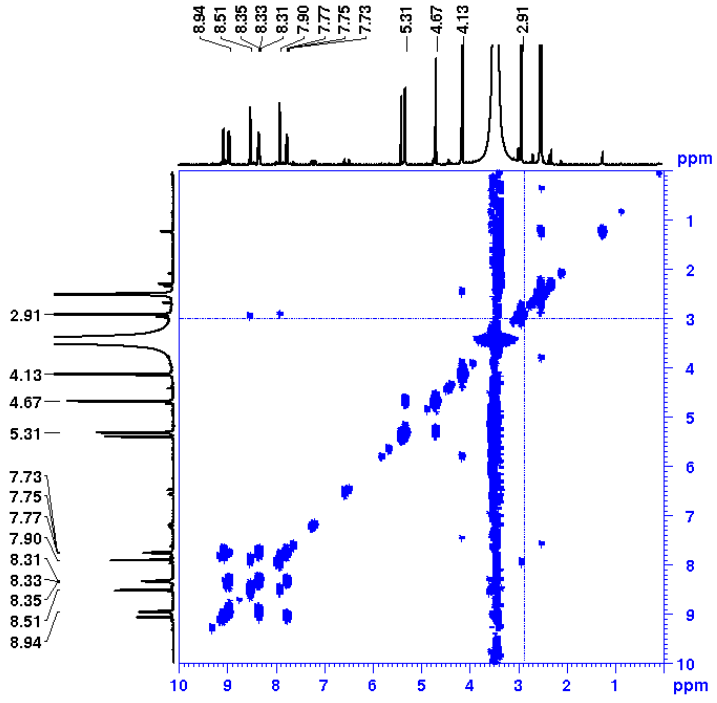

Figure S3l: $^{1}H–^{1}H$ correlation spectrum of **3a** (400 MHz, DMSO-D_6); shows the correlations between the methyl and aromatic protons.

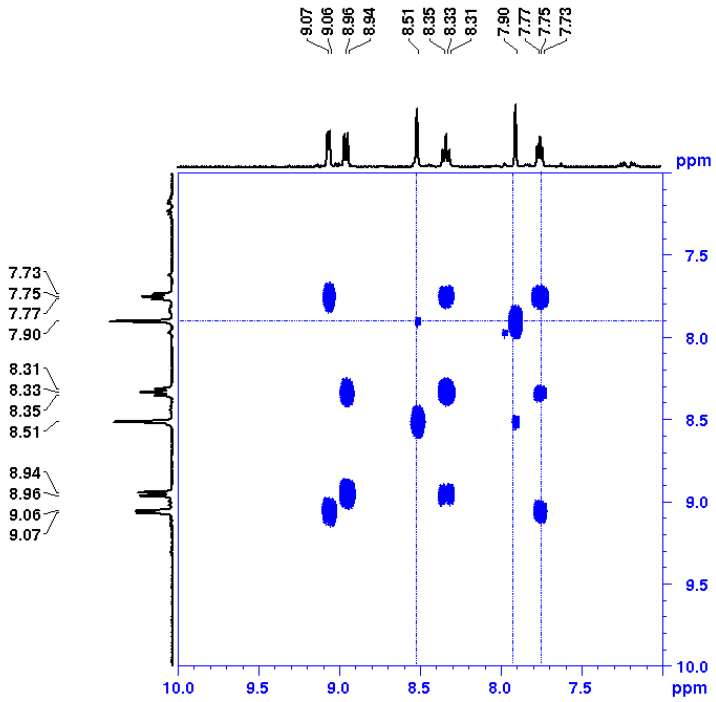

Figure S3m: $^{1}H–^{1}H$ correlation spectrum of **3a**, showing the correlations amongst the aromatic protons.

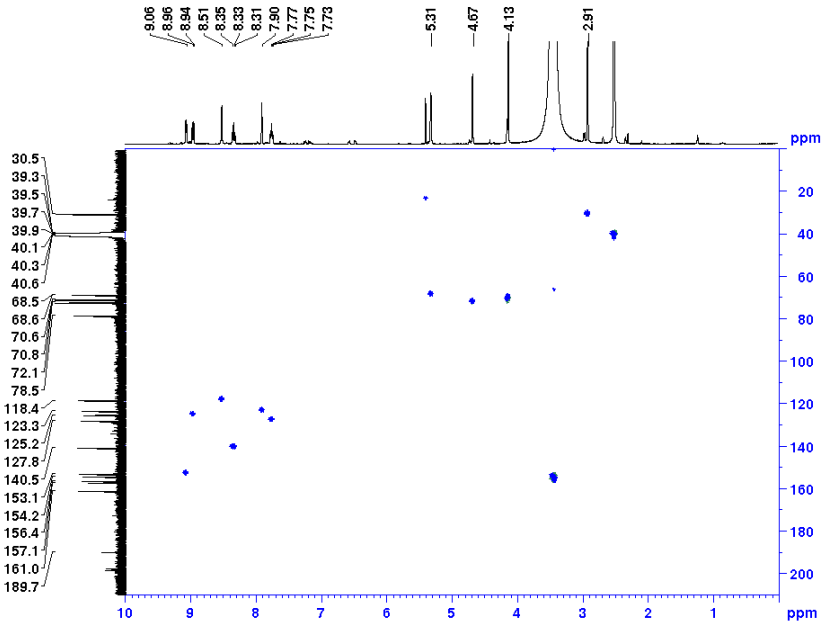

Figure S3n: HSQC spectrum of **3a** (400 MHz, DMSO-D_6).

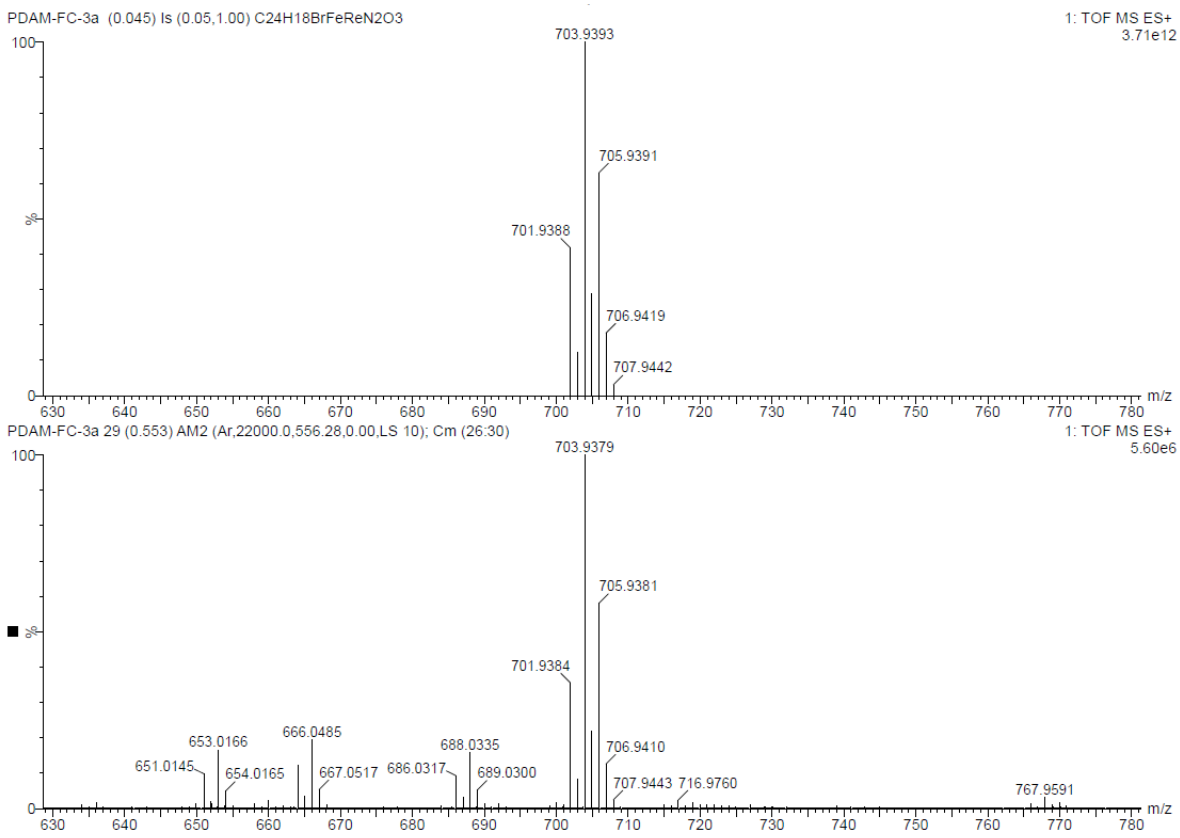

Figure S3o: HRMS spectrum of **3a** (M: $C_{24}H_{18}BrFeN_2O_3Re$) *m/z* calcd for [M^+] 703.9426, *m/z* found [M^+] 703.9379.

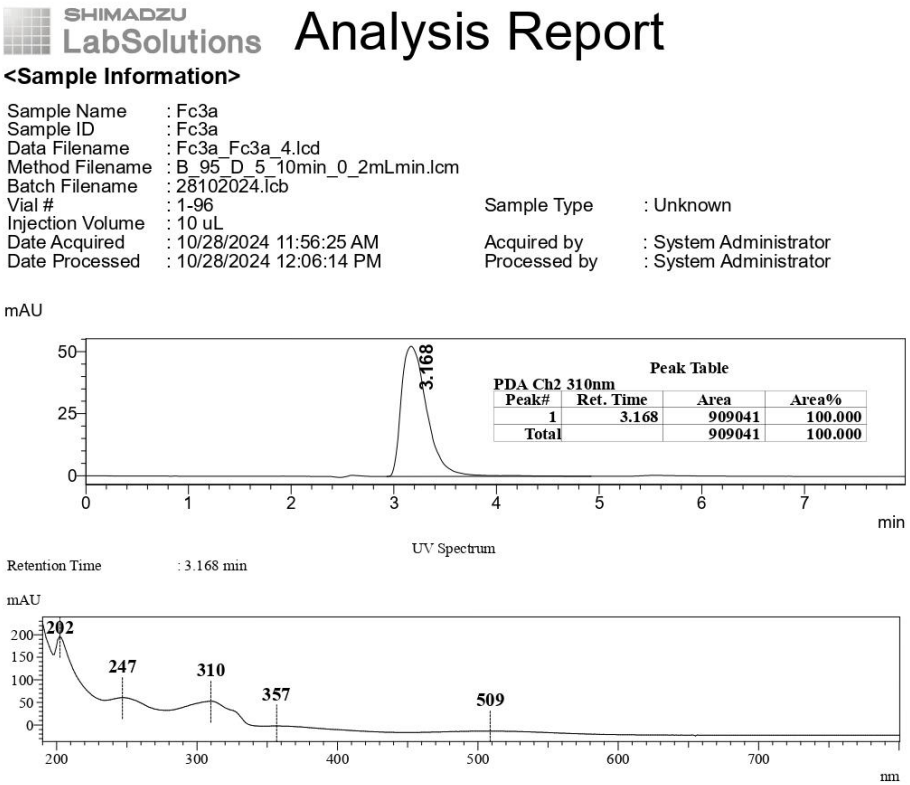

Figure S3p: RP–HPLC–MS of **3a**; HPLC purity 100%; UV–vis spectrum shown at Rt = 3.168 min.

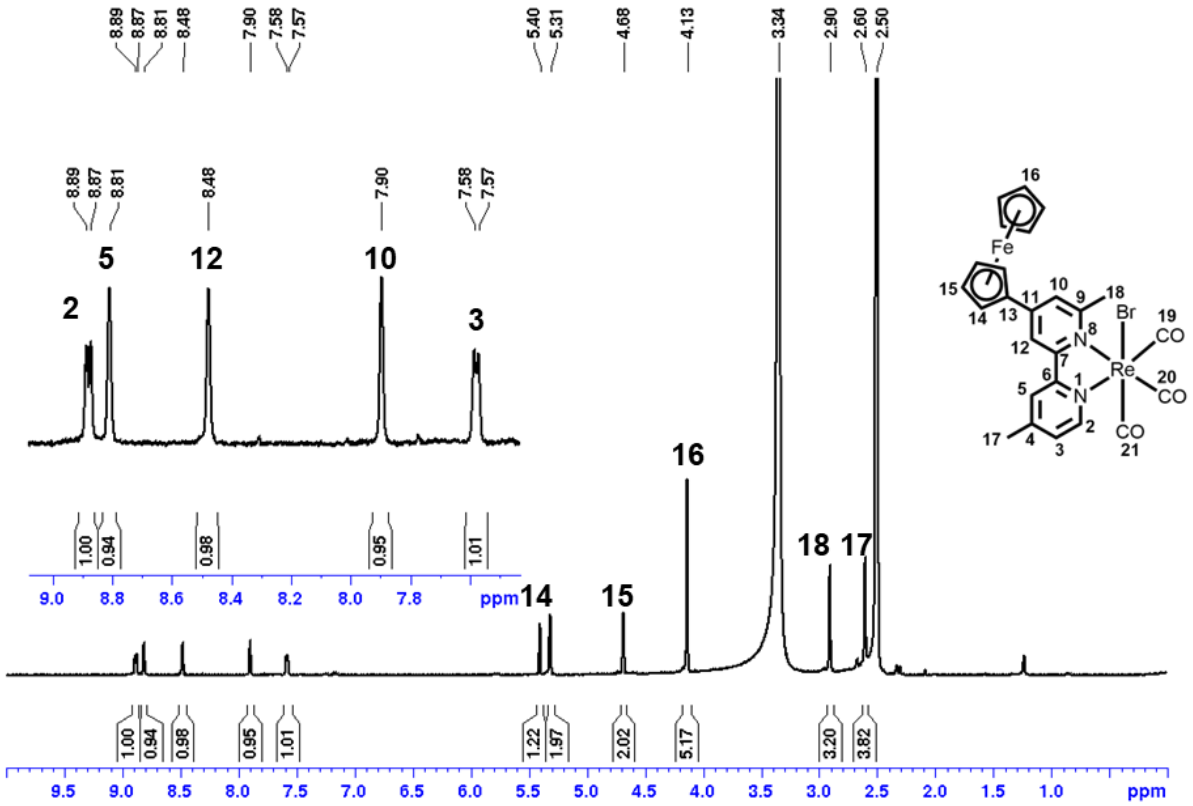

Figure S3q: ^{1}H NMR (DMSO-D$_6$, 400 MHz) spectrum of **3b**.

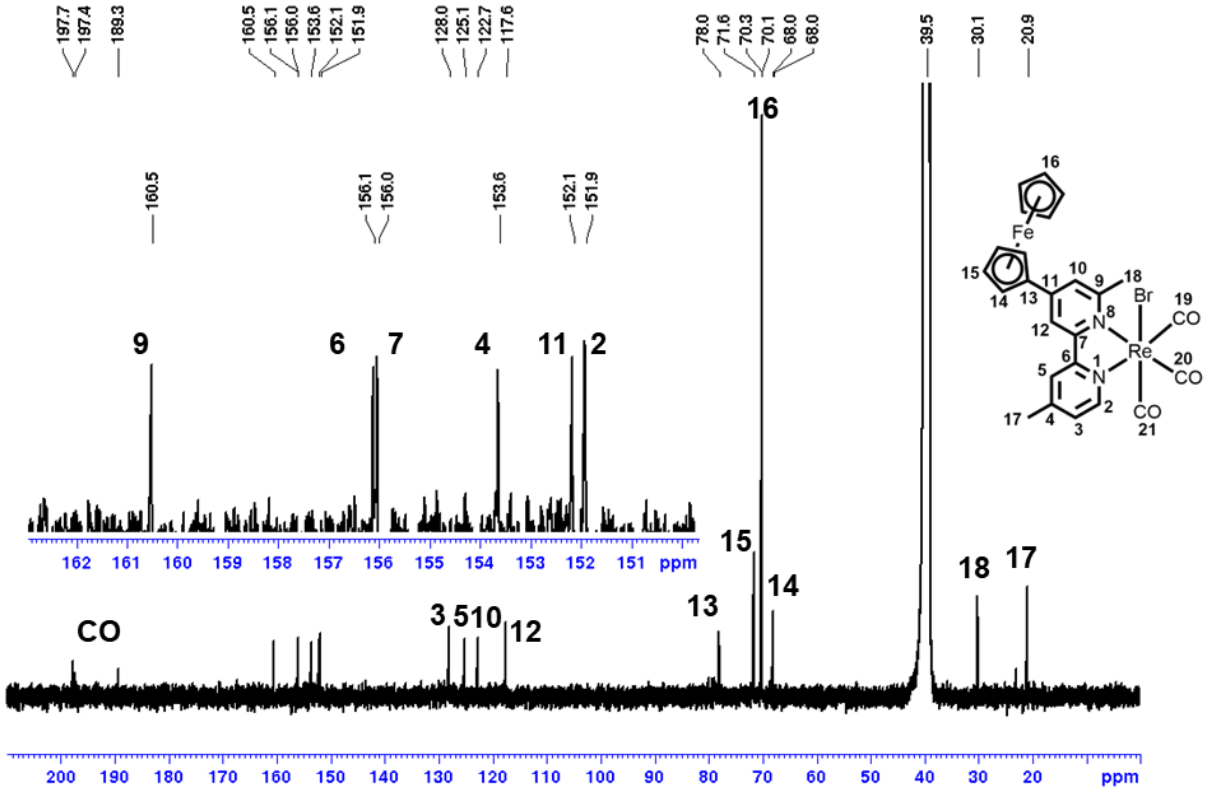

Figure S3r: ^{13}C{^{1}H} NMR (101 MHz, DMSO-D$_6$) spectrum of **3b**, with 12630 scans.

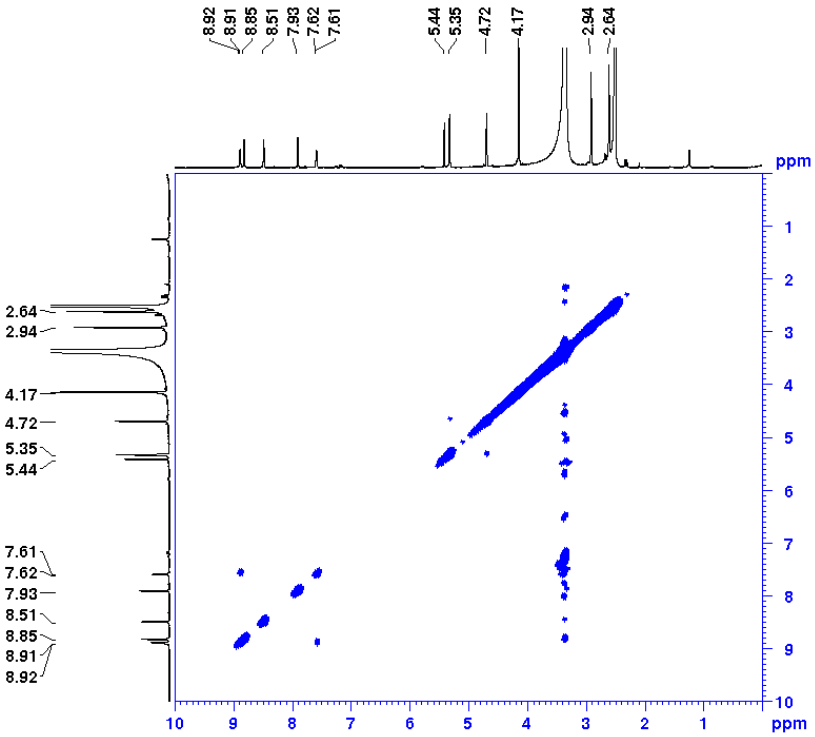

Figure S3s: $^{1}H–^{1}H$ correlation spectrum of **3b** (400 MHz, DMSO-D_6).

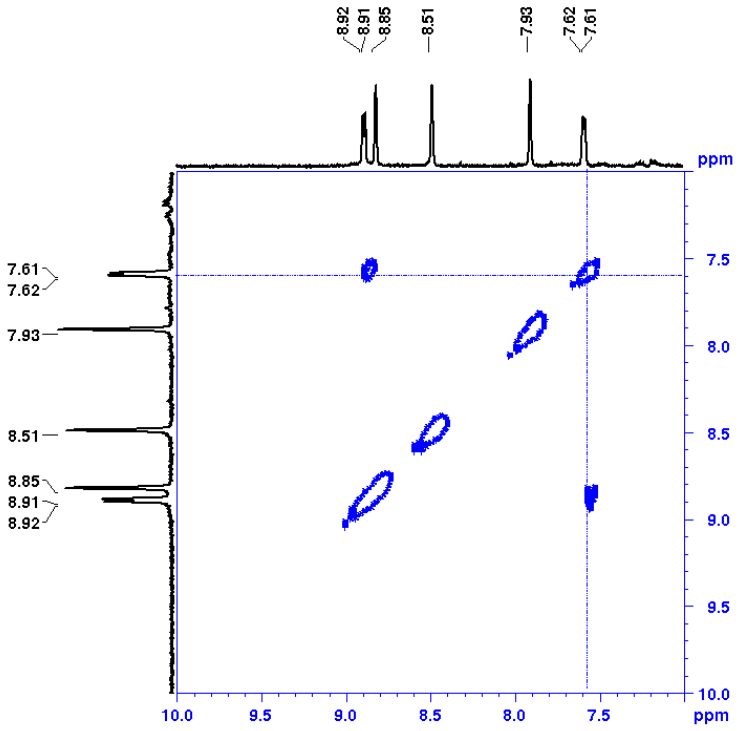

Figure S3t: $^{1}H–^{1}H$ correlation spectrum of **3b**, showing the correlations amongst the aromatic protons.

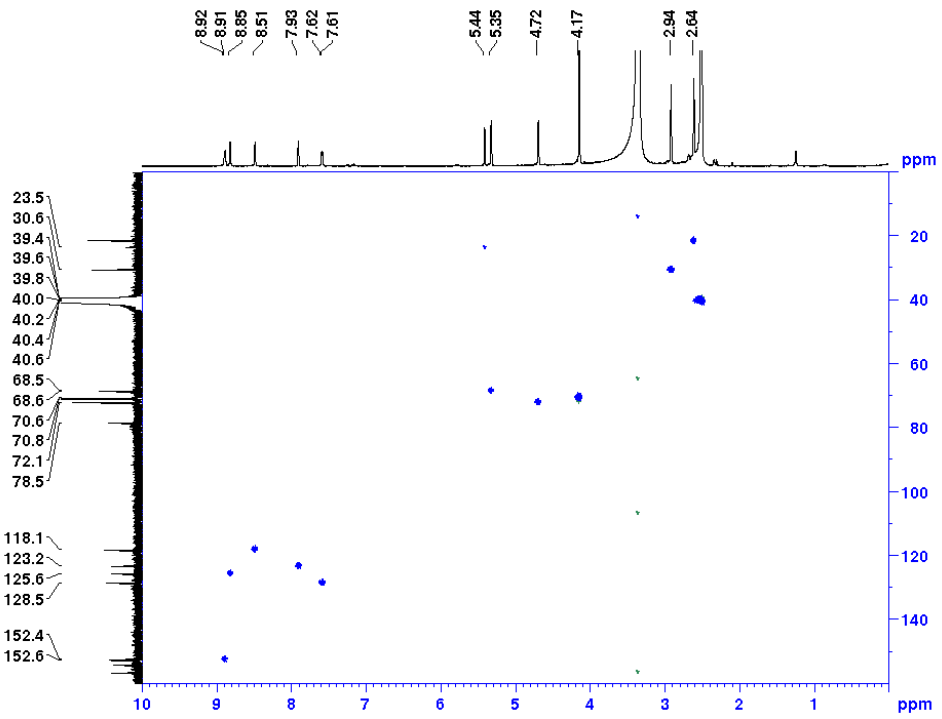

Figure S3u: HSQC spectrum of **3b** (400 MHz, DMSO-D_6).

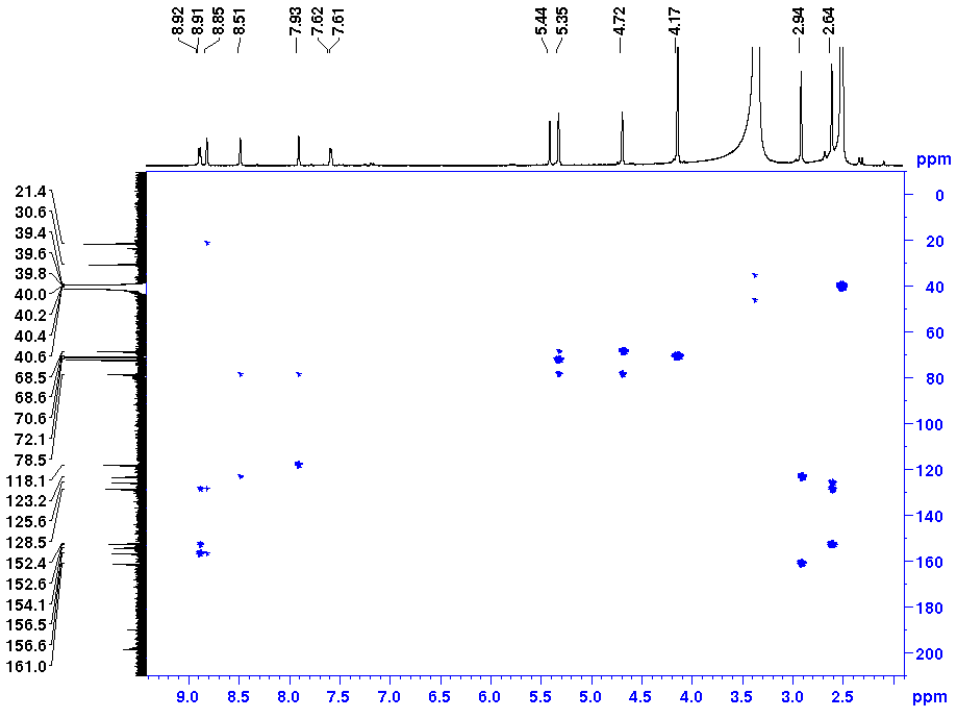

Figure S3v: HMBC spectrum of **3b** (400 MHz, DMSO-D_6).

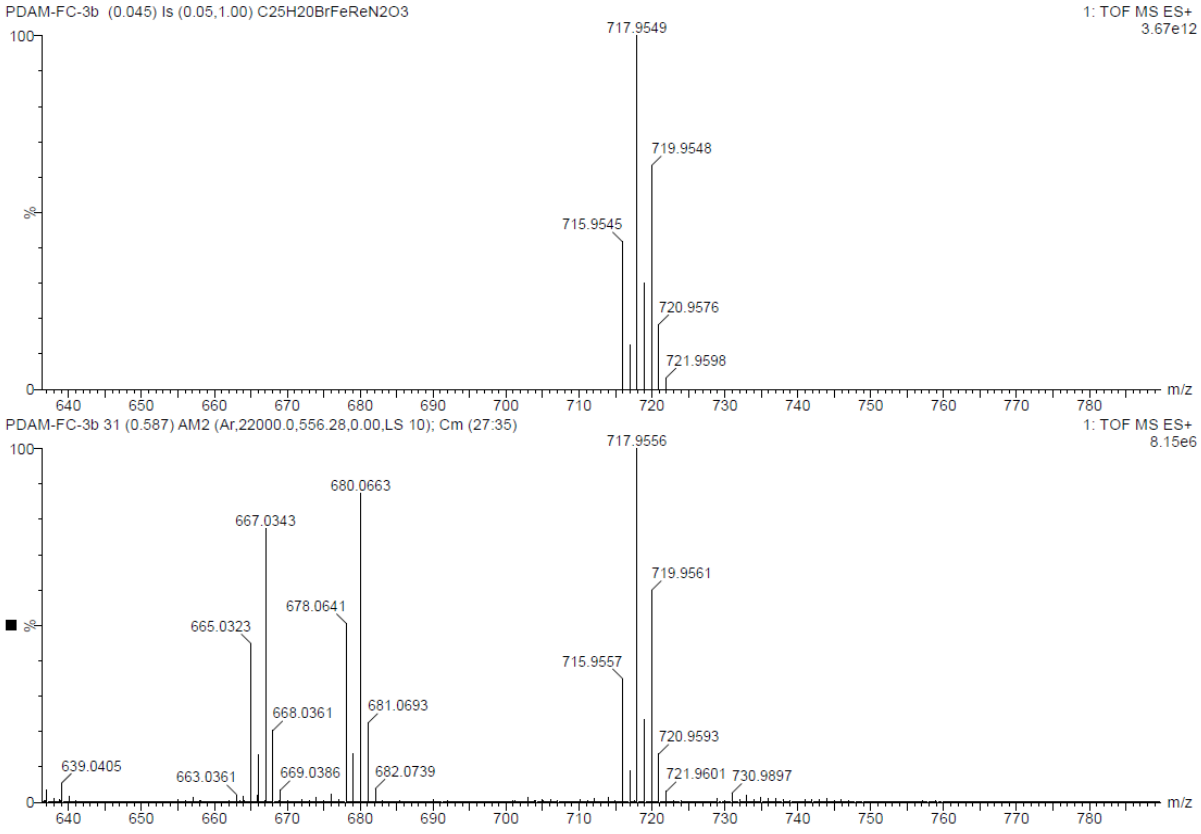

Figure S3w: HRMS spectrum of **3b** (M: $C_{25}H_{20}BrFeN_2O_3Re$) m/z calcd for [M^+] 717.9583, m/z found [M^+] 717.9556.

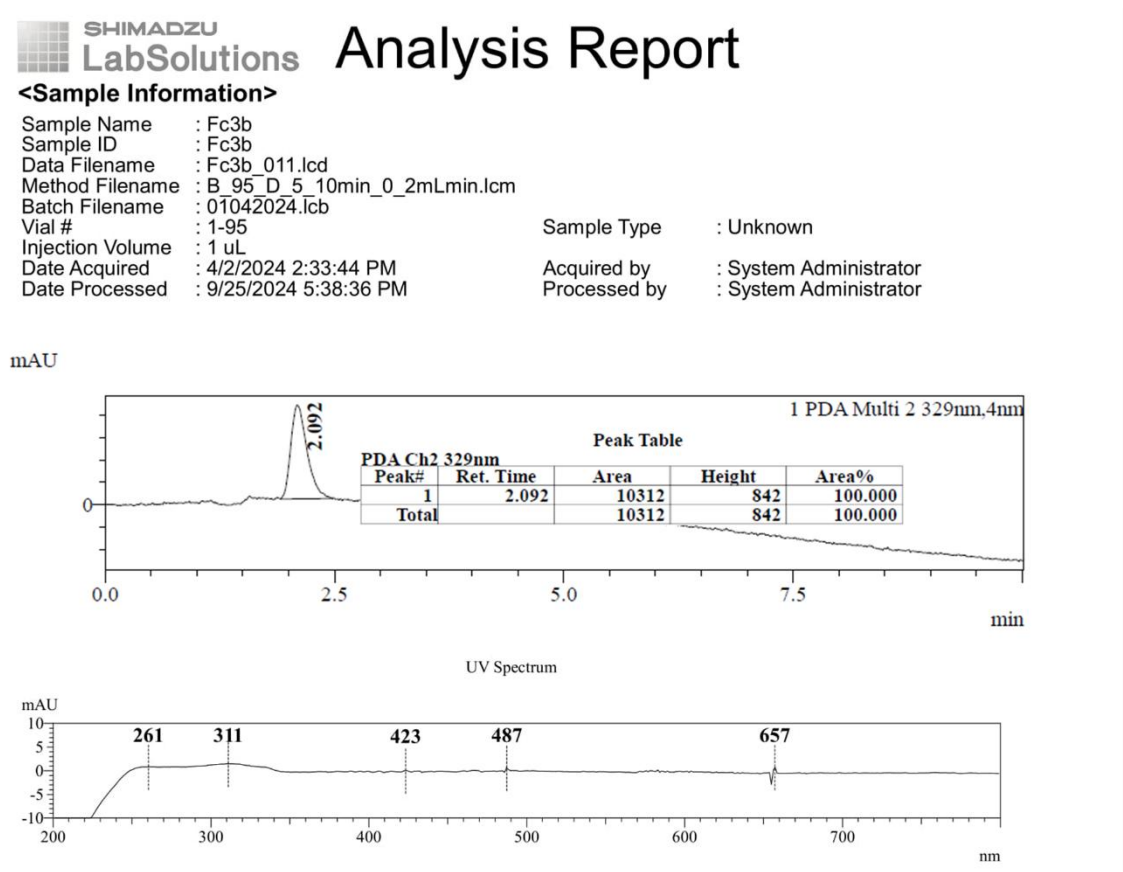

Figure S3x: RP–HPLC–MS of **3b**; HPLC purity 100%; UV–vis spectrum shown at Rt = 2.092 min.

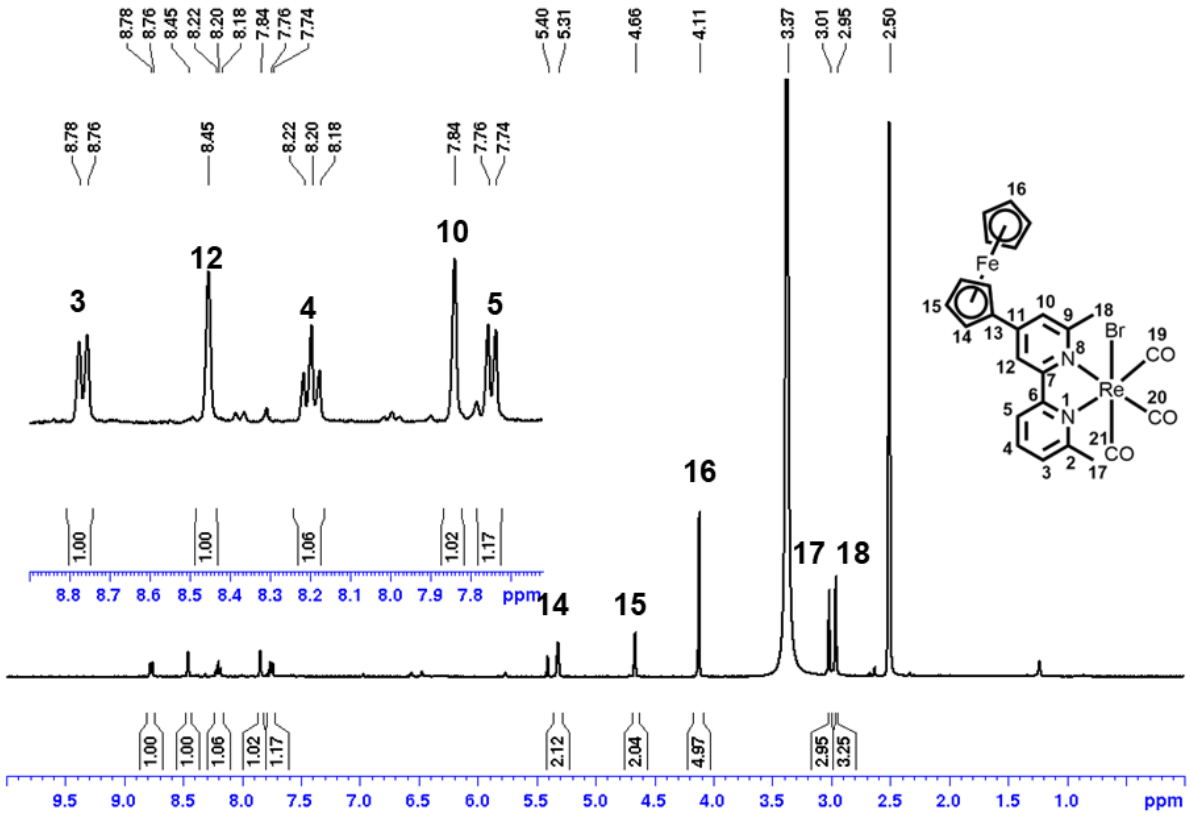

Figure S3y: ^{1}H NMR (DMSO-D$_6$, 400 MHz) spectrum of **3c**.

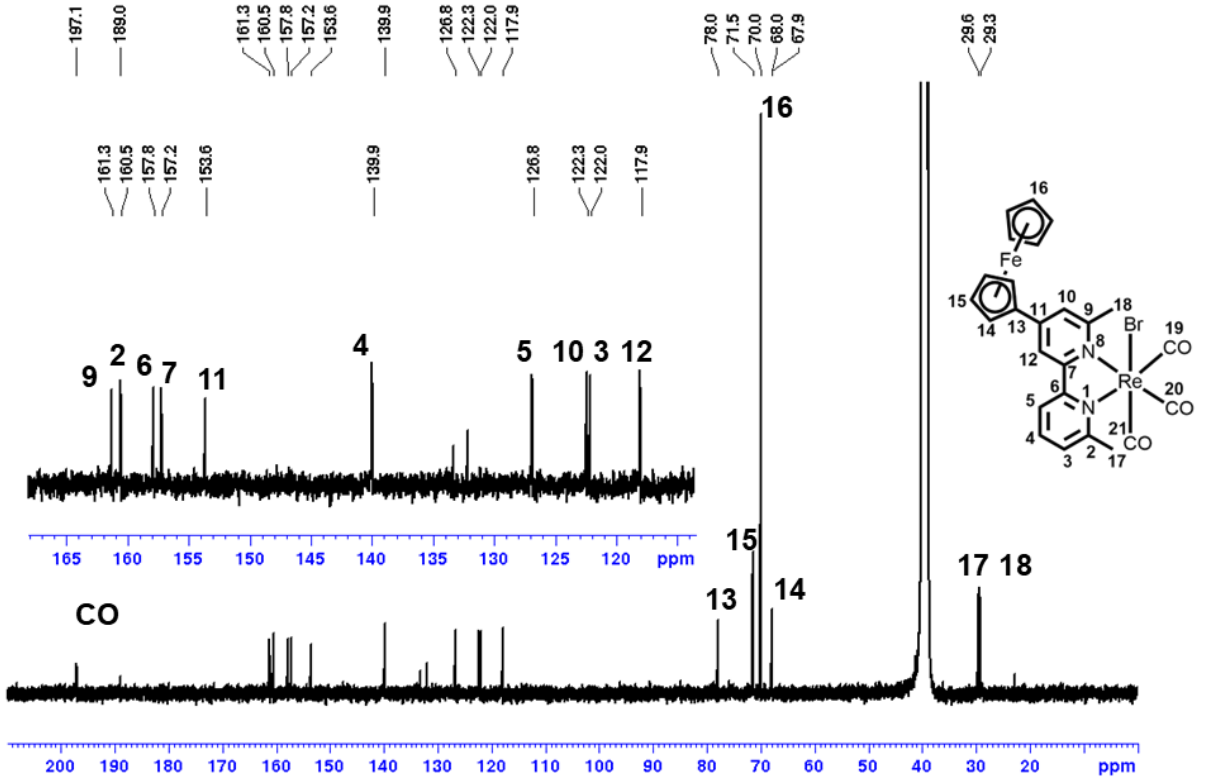

Figure S3z: ^{13}C{^{1}H} NMR (101 MHz, DMSO-D$_6$) spectrum of **3c**, with 12325 scans.

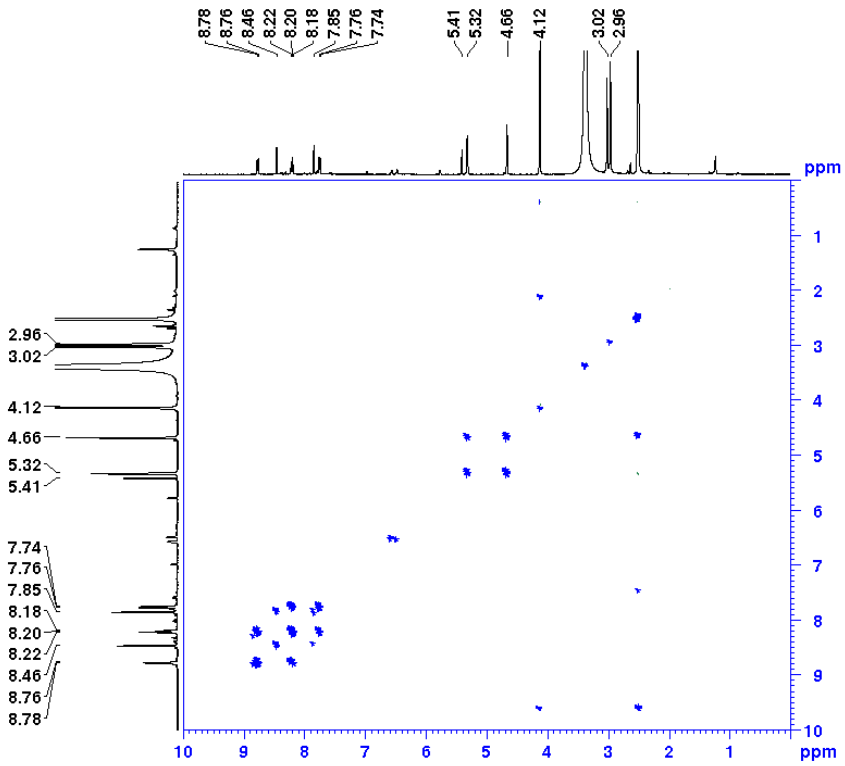

Figure S3aa: $^{1}H–^{1}H$ correlation spectrum of **3c** (400 MHz, DMSO-D_6).

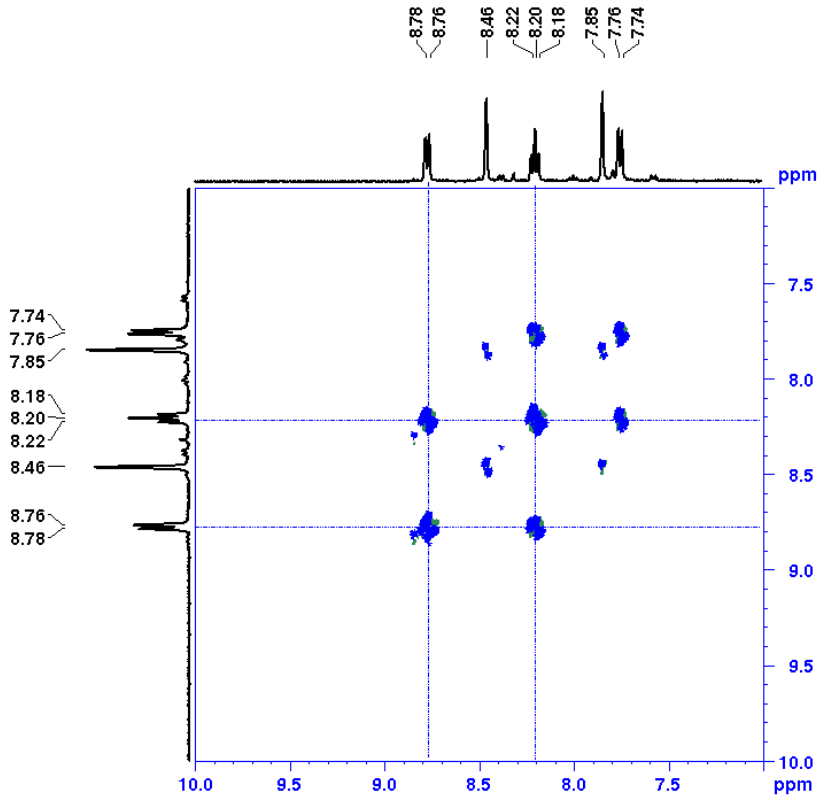

Figure S3ab: $^{1}H–^{1}H$ correlation spectrum of **3c**, showing the correlations amongst the aromatic protons.

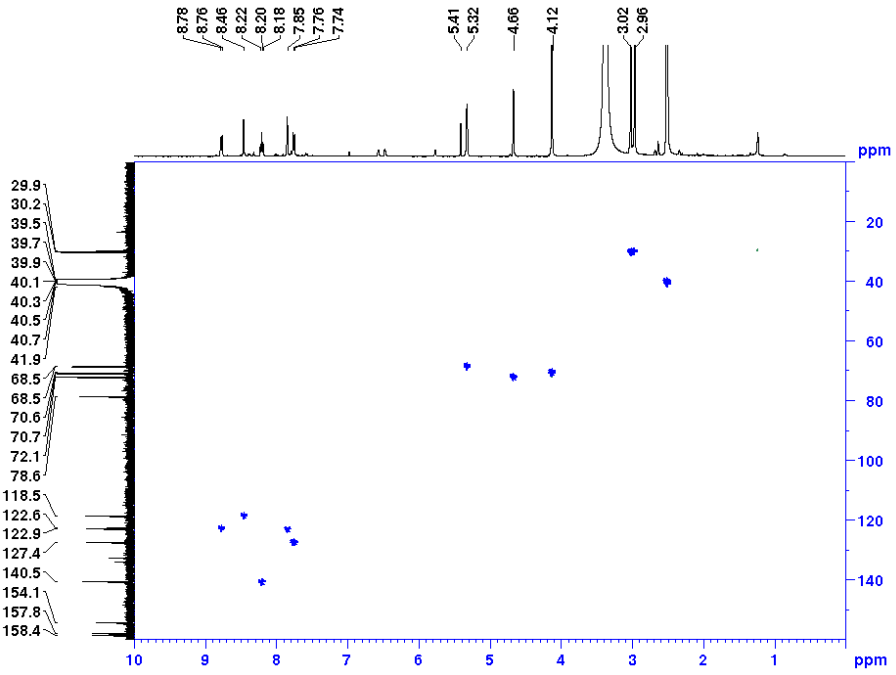

Figure S3ac: HSQC spectrum of **3c** (400 MHz, DMSO-D_6).

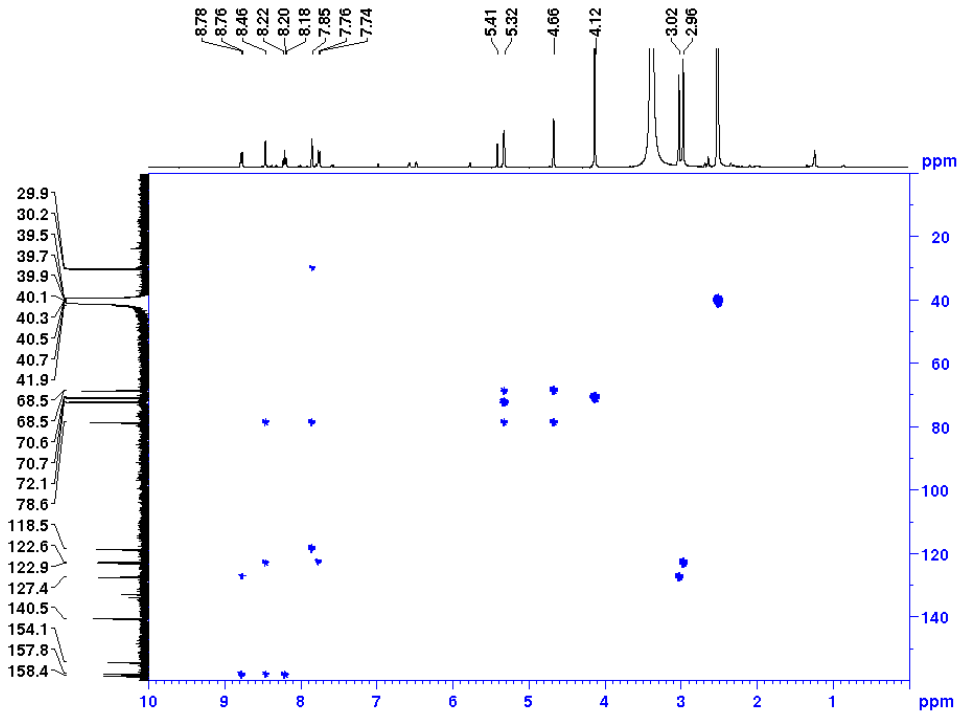

Figure S3ad: HMBC spectrum of **3c** (400 MHz, DMSO-D_6).

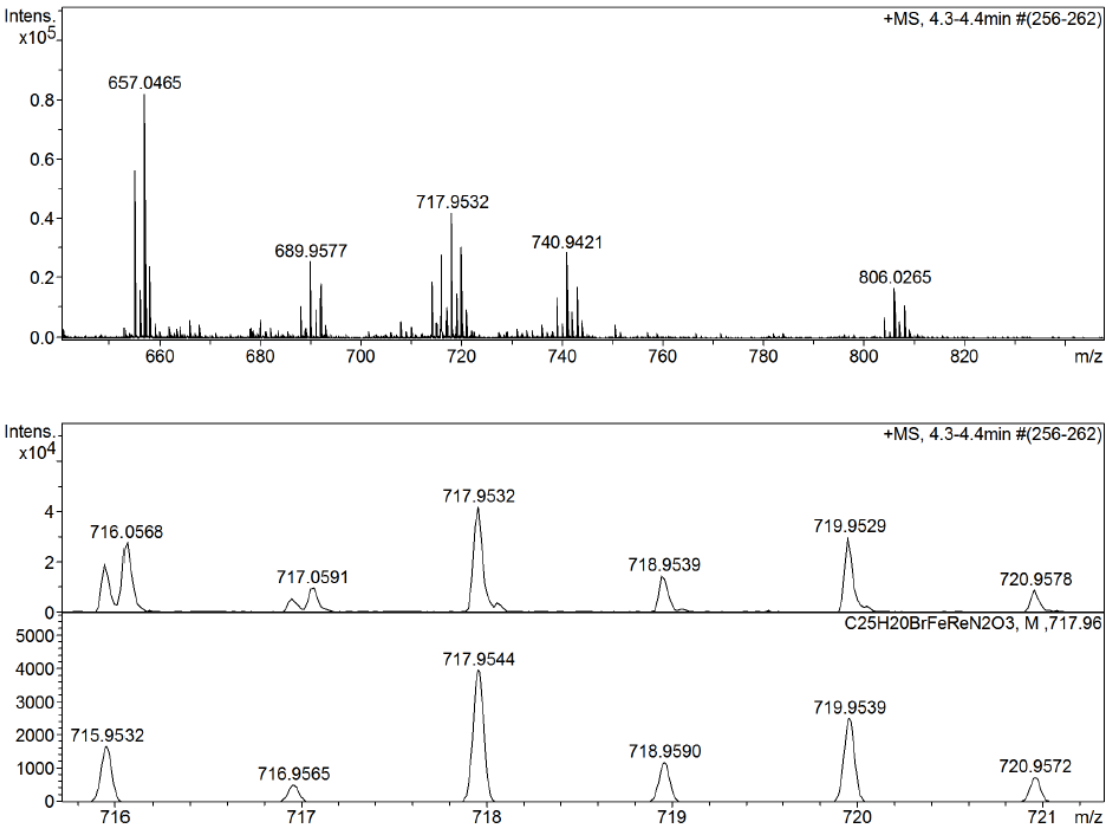

Figure S3ae: HRMS spectrum of **3c** (M: $C_{25}H_{20}BrFeN_2O_3Re$) *m/z* calcd for [M^+] 717.9583, *m/z* found [M^+] 717.9532.

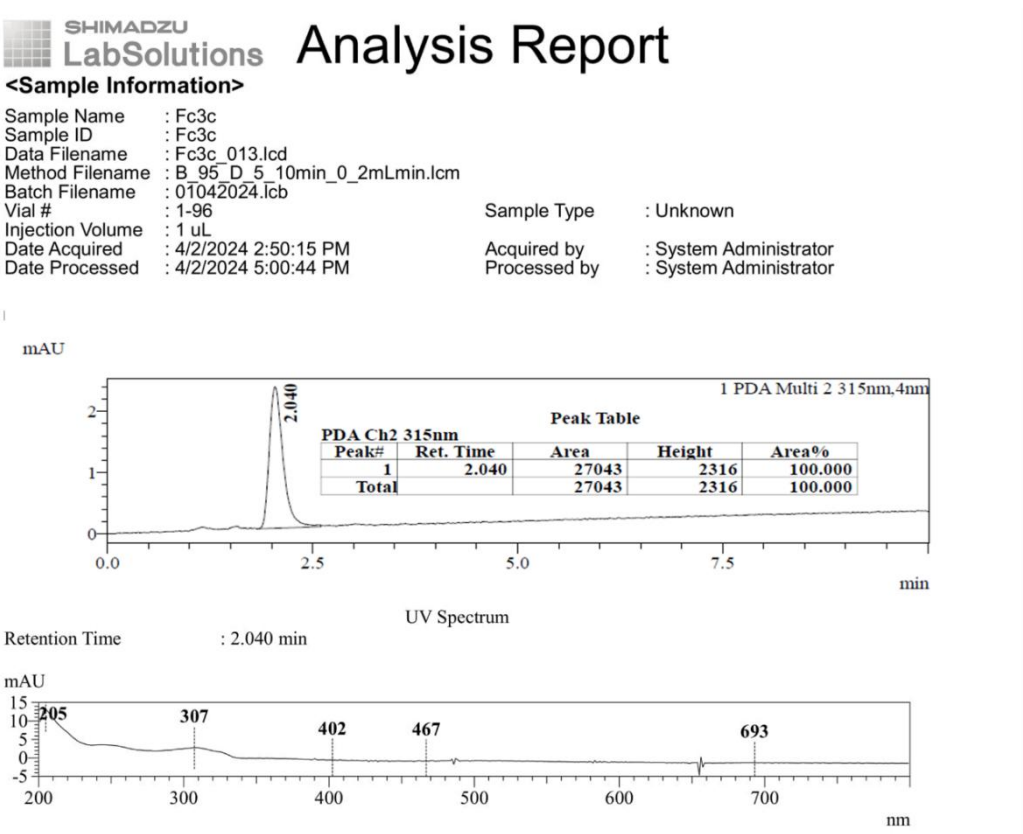

Figure S3af: RP–HPLC–MS of **3c**; HPLC purity 100%; UV–vis spectrum shown at Rt = 2.040 min.

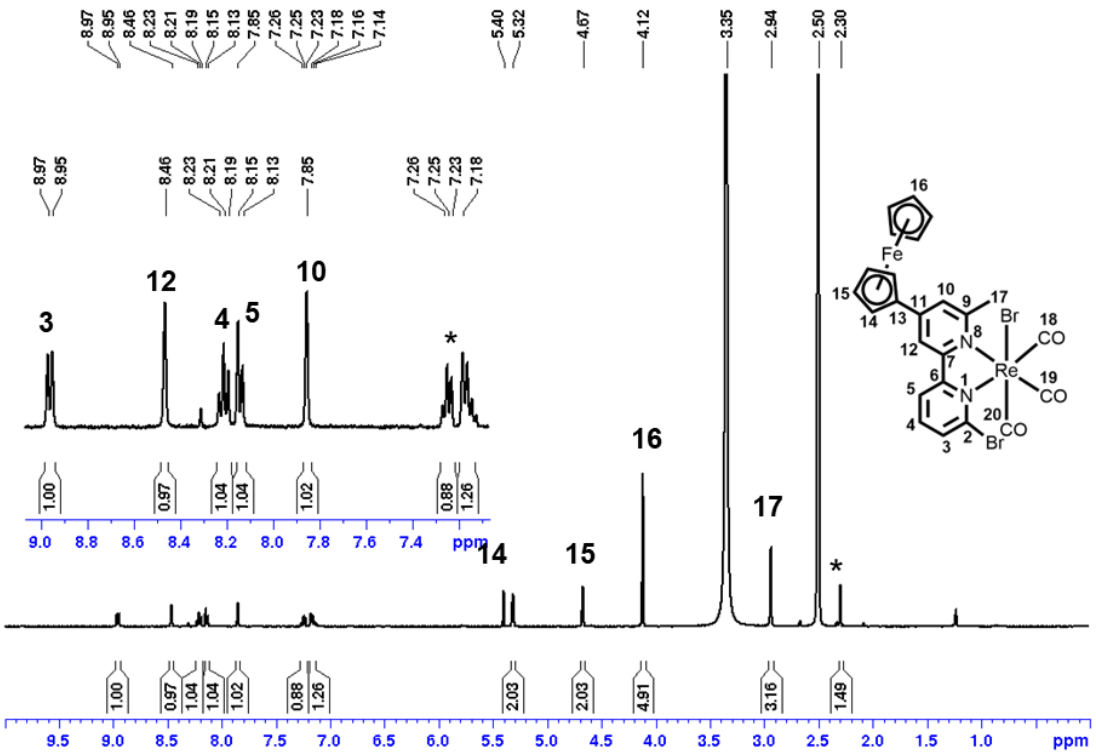

Figure S3ag: ^{1}H NMR (DMSO-D$_6$, 400 MHz) spectrum of **3d**; toluene peaks marked with *; observed at 7.25, 7.18 & 2.30 ppm; reported[14] at 7.25, 7.18 & 2.30 ppm; ~0.5 molecules of toluene as solvent of crystallization, verified by thermogravimetric analysis.

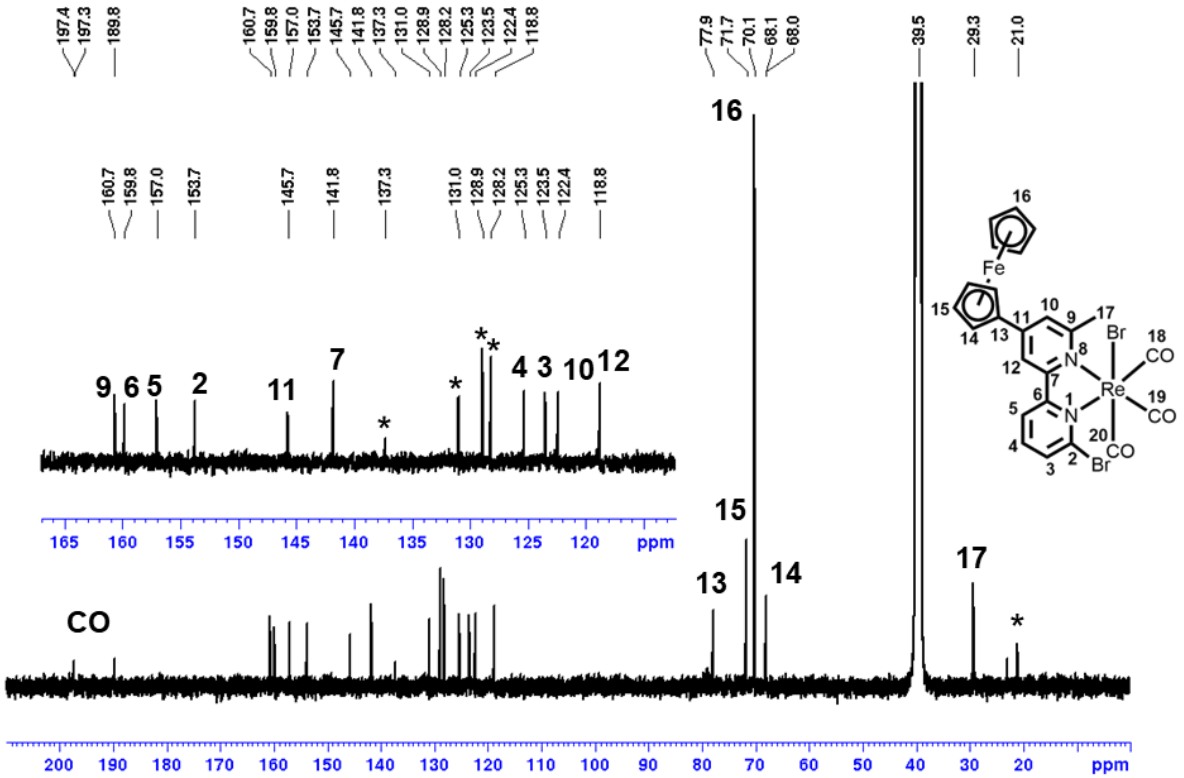

Figure S3ah: ^{13}C{^{1}H} NMR (101 MHz, DMSO-D$_6$) spectrum of **3d**, with 13329 scans; toluene peaks marked with *; observed at 137.3, 131.0, 128.9, 128.2 & 21.0 ppm; reported at[14] 137.4, 128.9, 128.2, 125.3 & 21.0 ppm.

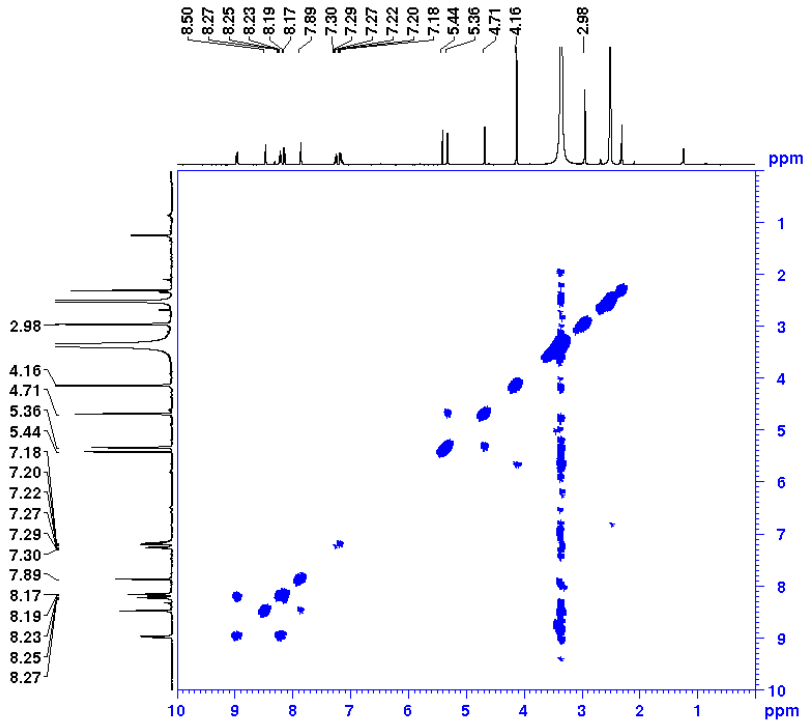

Figure S3ai: $^{1}H–^{1}H$ correlation spectrum of **3d** (400 MHz, DMSO-D_6).

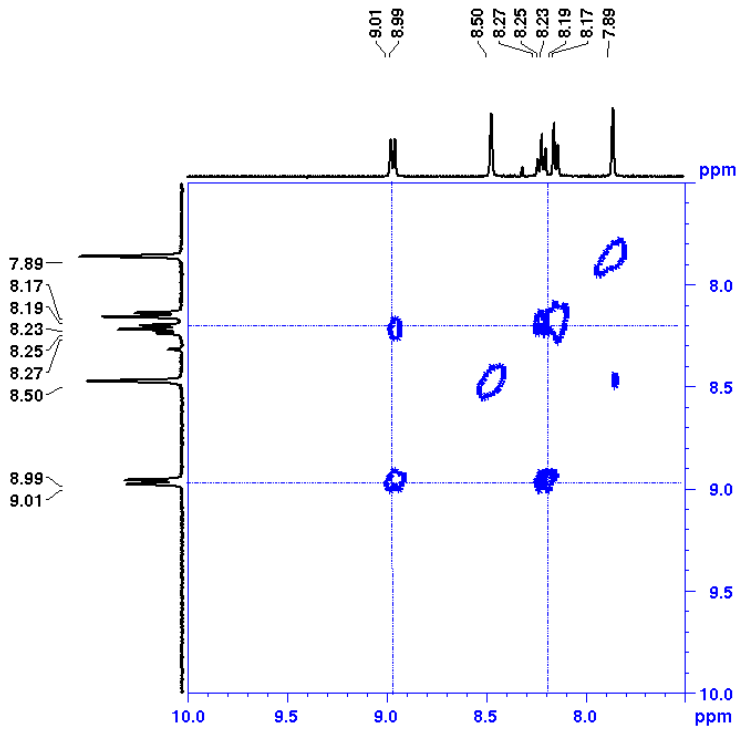

Figure S3aj: $^{1}H–^{1}H$ correlation spectrum of **3d**, showing the correlations amongst the aromatic protons.

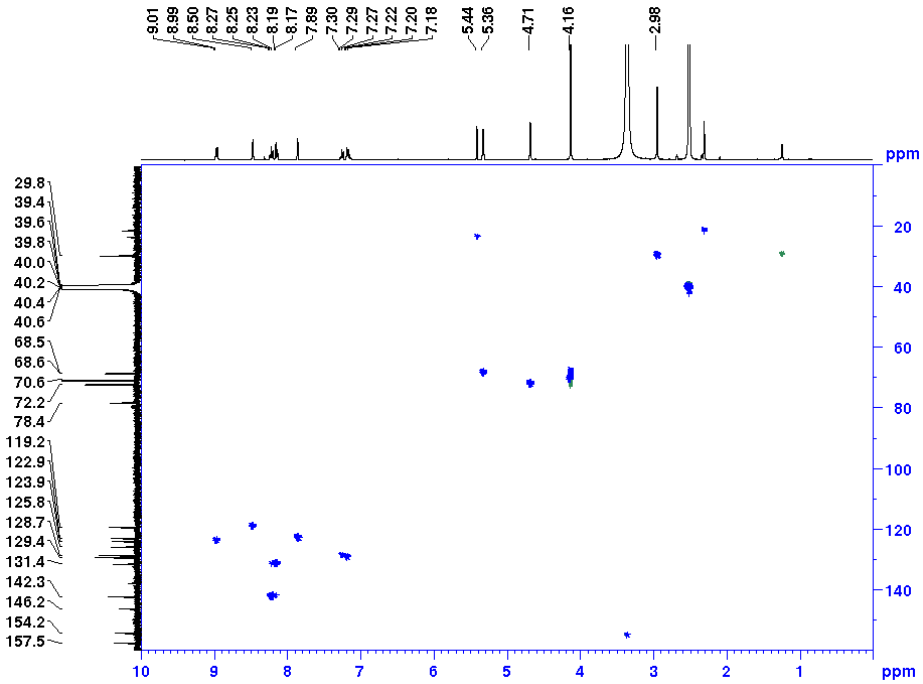

Figure S3ak: HSQC spectrum of **3d** (400 MHz, DMSO-D_6).

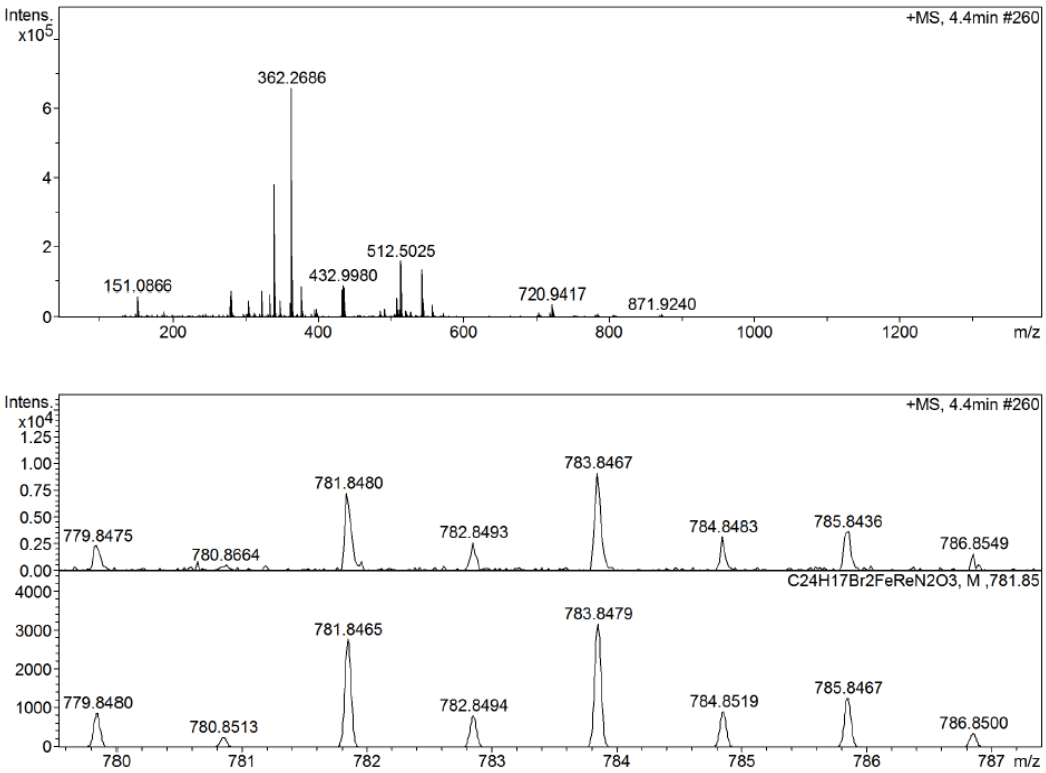

Figure S3al: HRMS spectrum of **3d** (M: $C_{24}H_{17}Br_2FeN_2O_3Re$) *m/z* calcd for [$M^+$] 783.8531, *m/z* found [M^+] 783.8467.

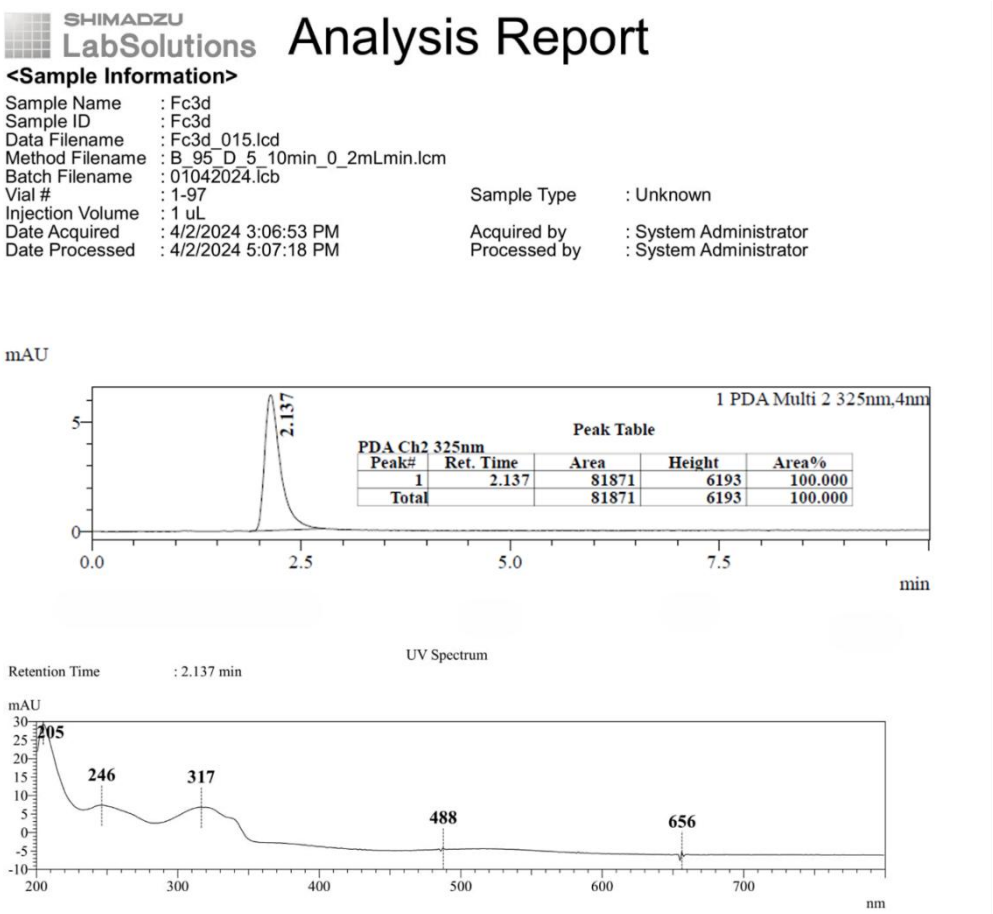

Figure S3am: RP–HPLC–MS of **3d;** HPLC purity 100%; UV–vis spectrum shown at Rt = 2.137 min.

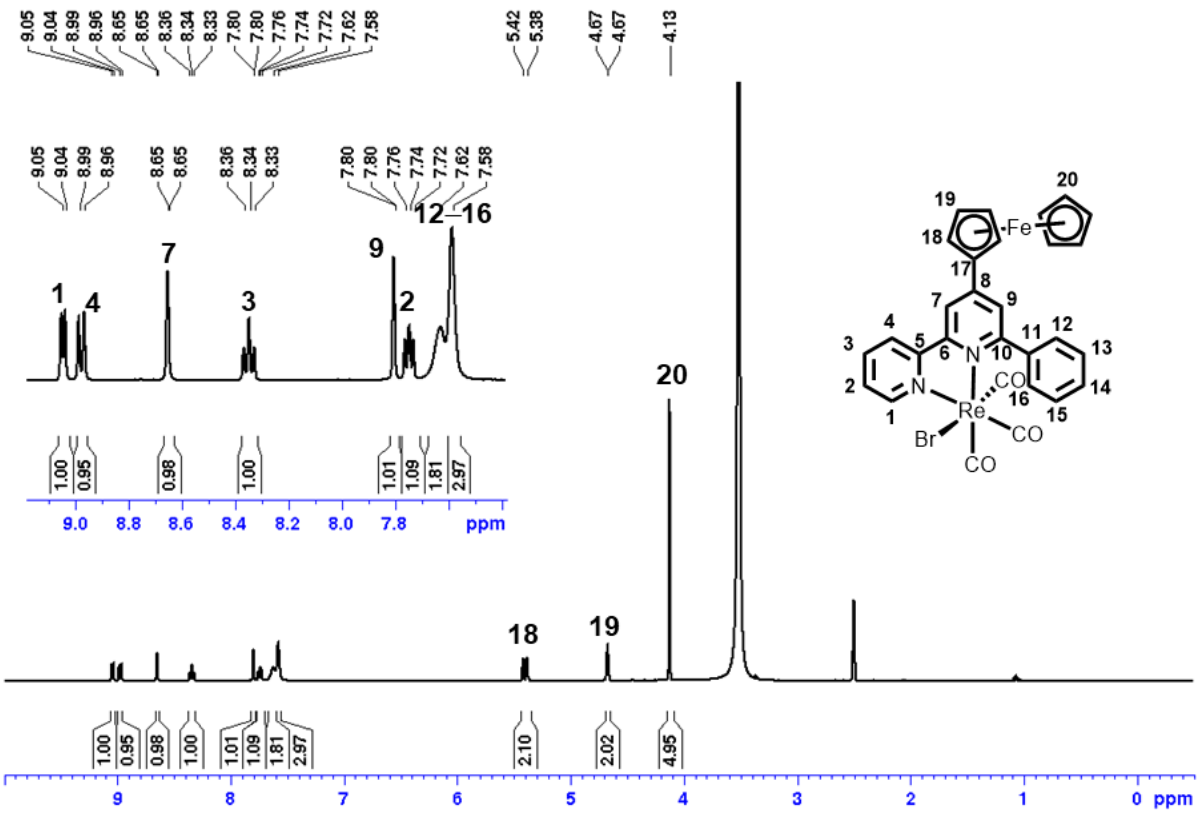

Figure S3an: ^{1}H NMR (400 MHz, DMSO-D_6) spectrum of **3e**.

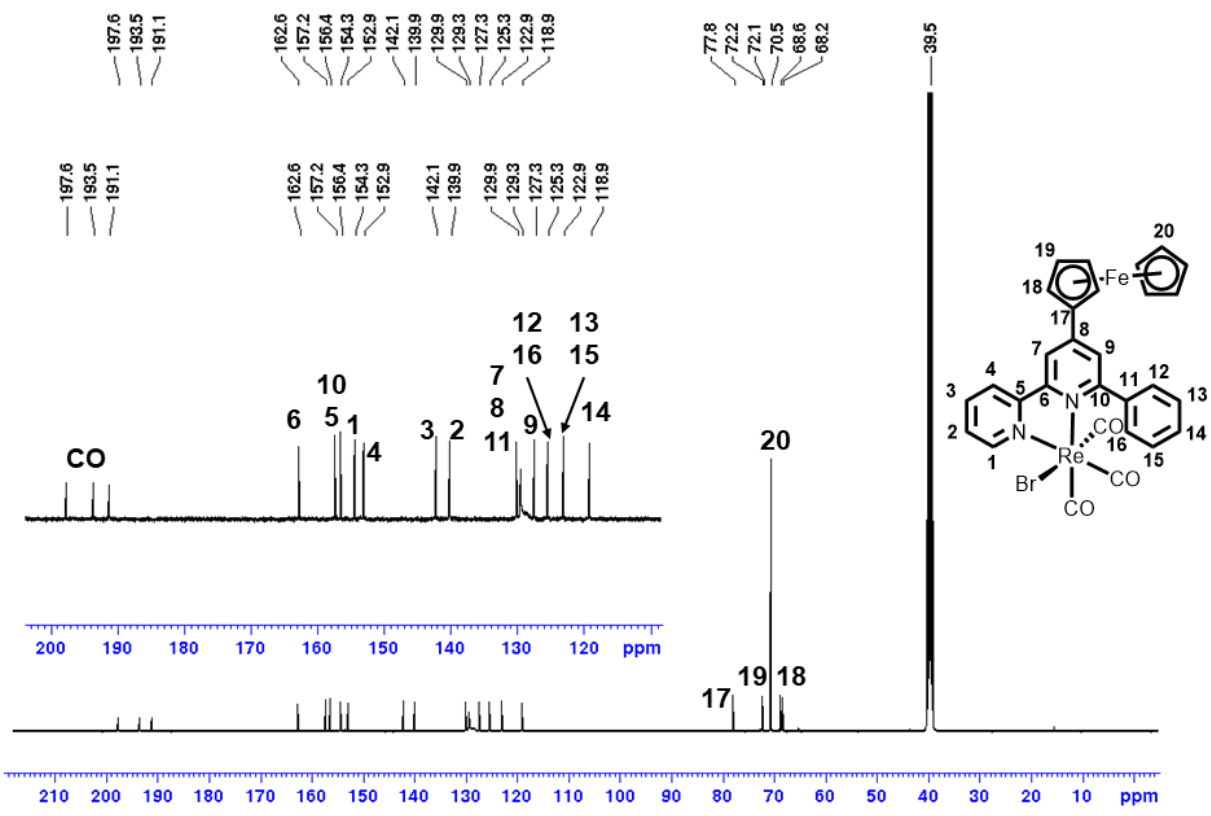

Figure S3ao: $^{13}C\{^{1}H\}$ NMR (101 MHz, DMSO-D_6) spectrum of **3e**, with 12914 scans.

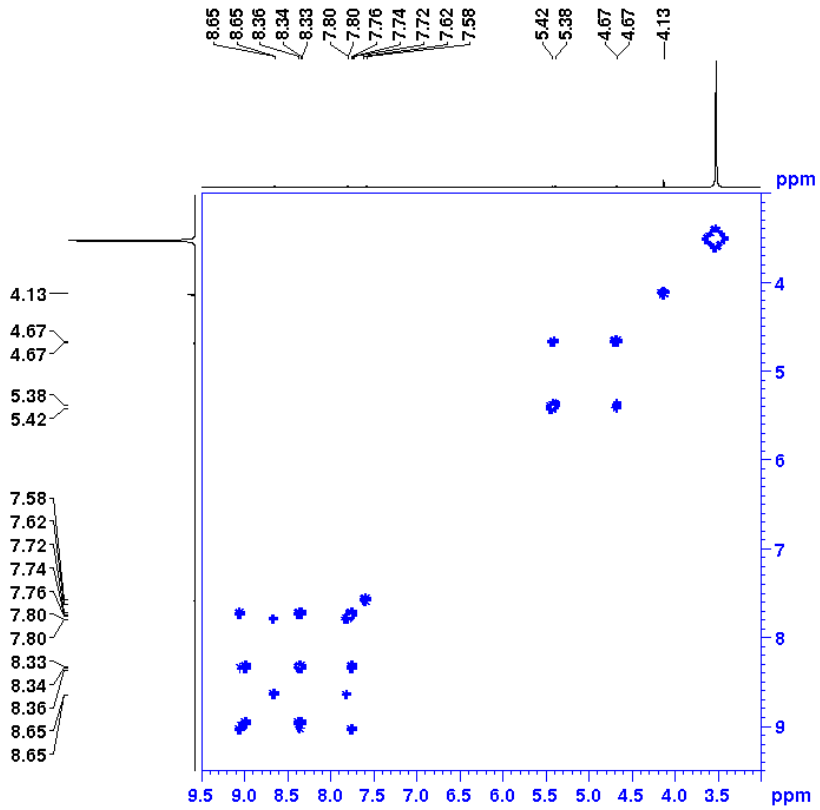

Figure S3ap: $^{1}H–^{1}H$ correlation spectrum of **3e** (400 MHz, DMSO-D_6).

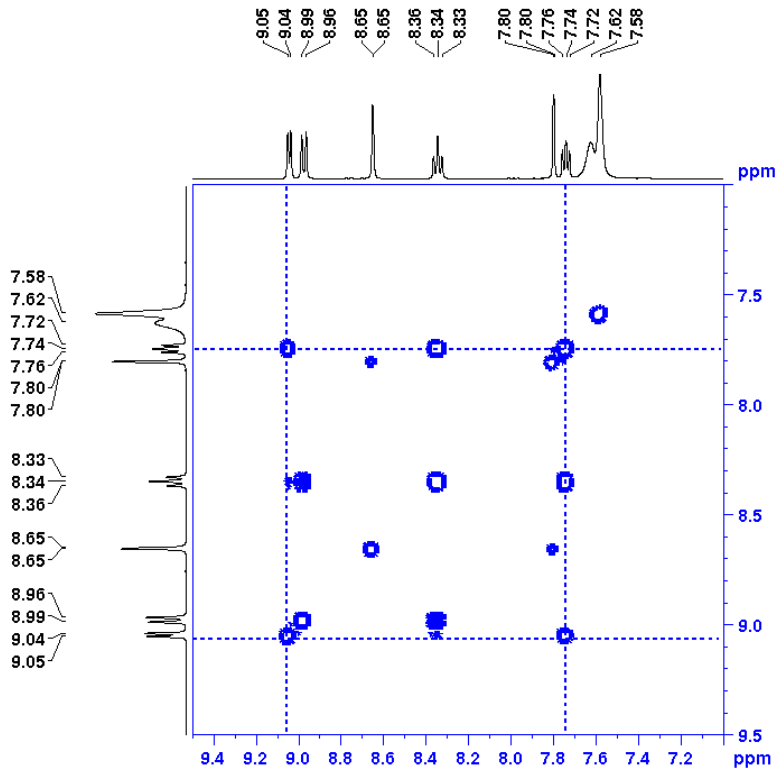

Figure S3aq: $^{1}H–^{1}H$ correlation spectrum of **3e** (400 MHz, DMSO-D_6), showing the correlations amongst the aromatic protons.

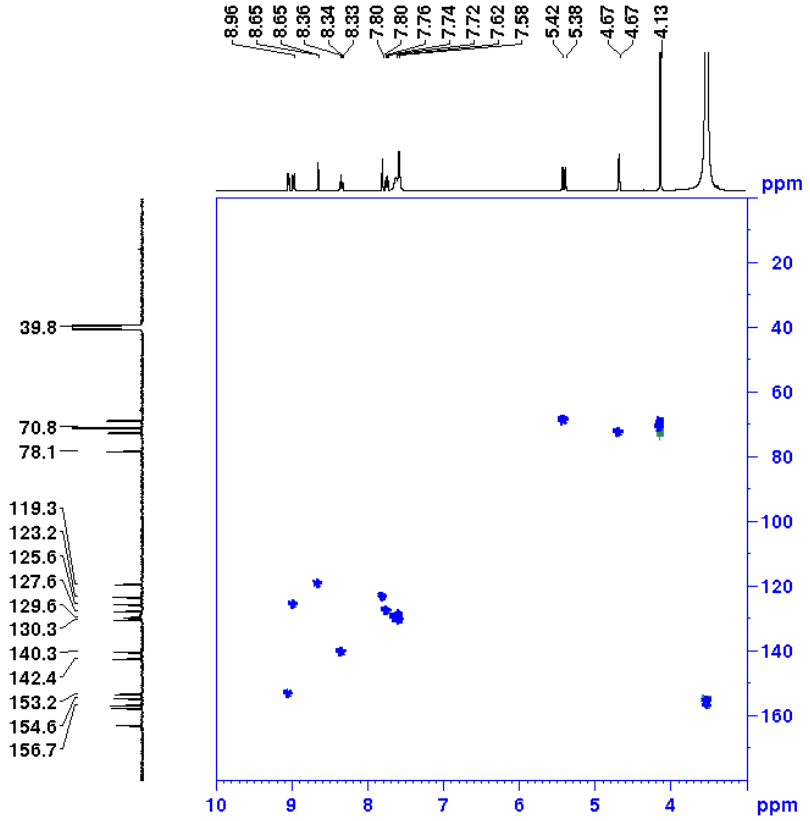

Figure S3ar: HSQC spectrum of **3e** (400 MHz, DMSO-D_6).

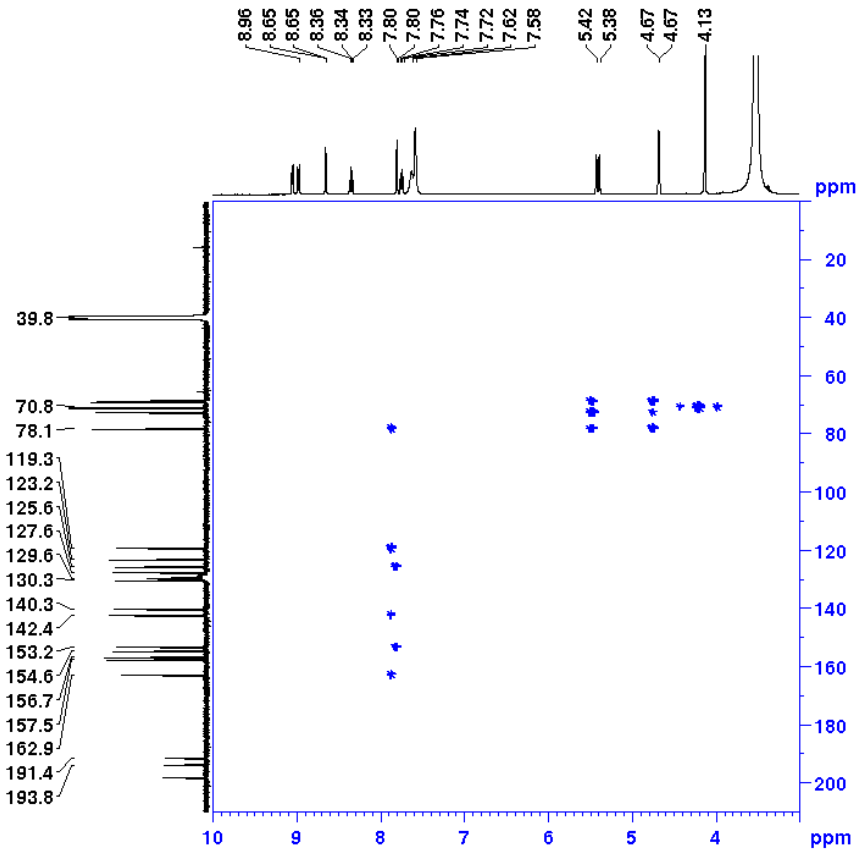

Figure S3as: HMBC spectrum of **3e** (400 MHz, DMSO-D_6).

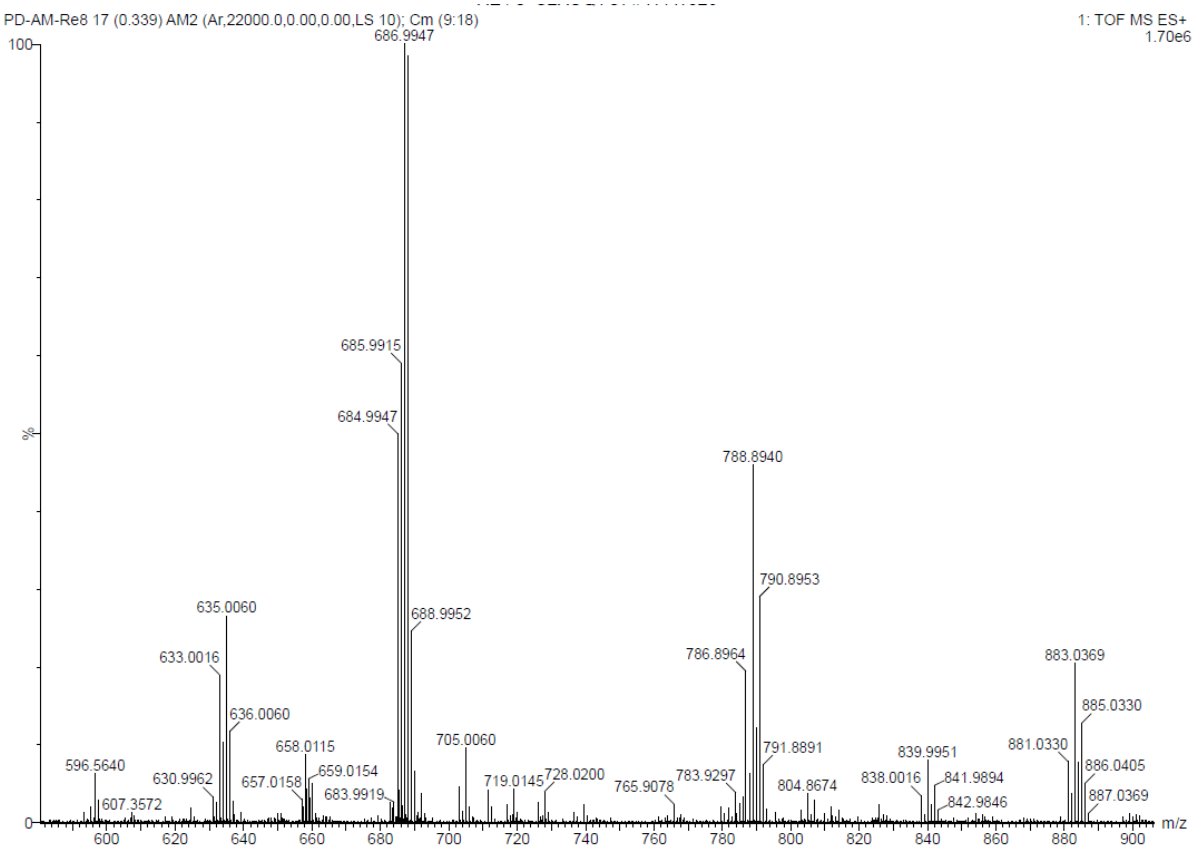

Figure S3at: HRMS spectrum of **3e** (M: $C_{29}H_{20}BrFeN_2O_3Re$) *m/z* calcd for [M+Na$^+$] 788.9480, *m/z* found [M+Na$^+$] 788.8940.

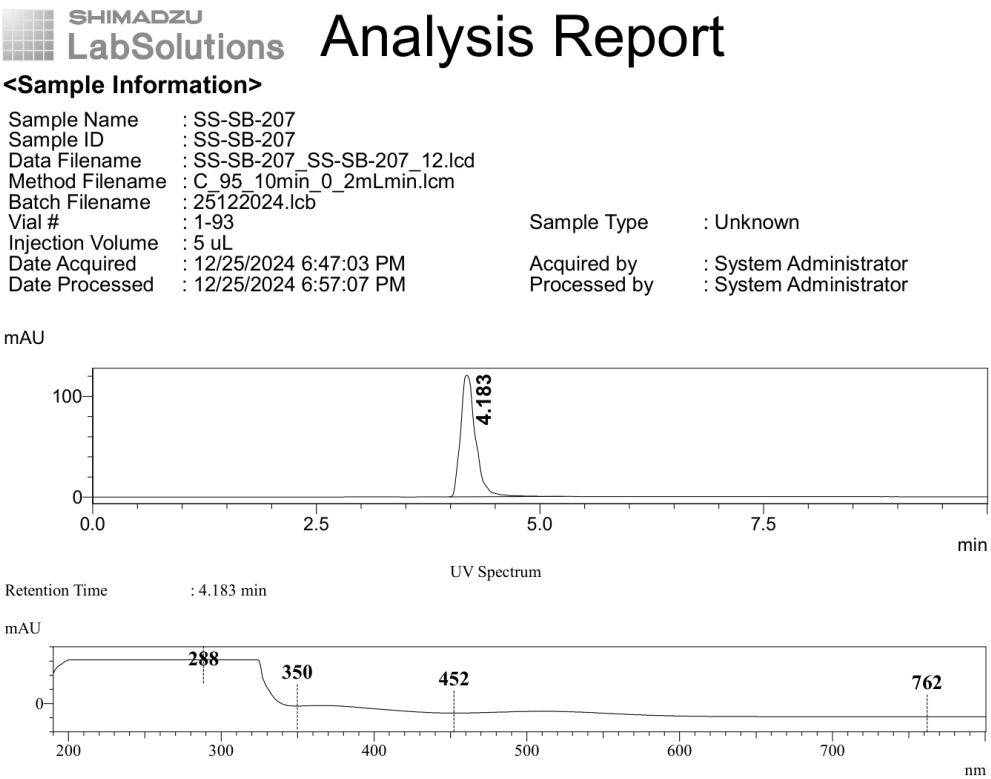

Figure S3au: RP–HPLC–MS of **3e;** HPLC purity 100%; UV–vis spectrum shown at Rt = 4.183 min.

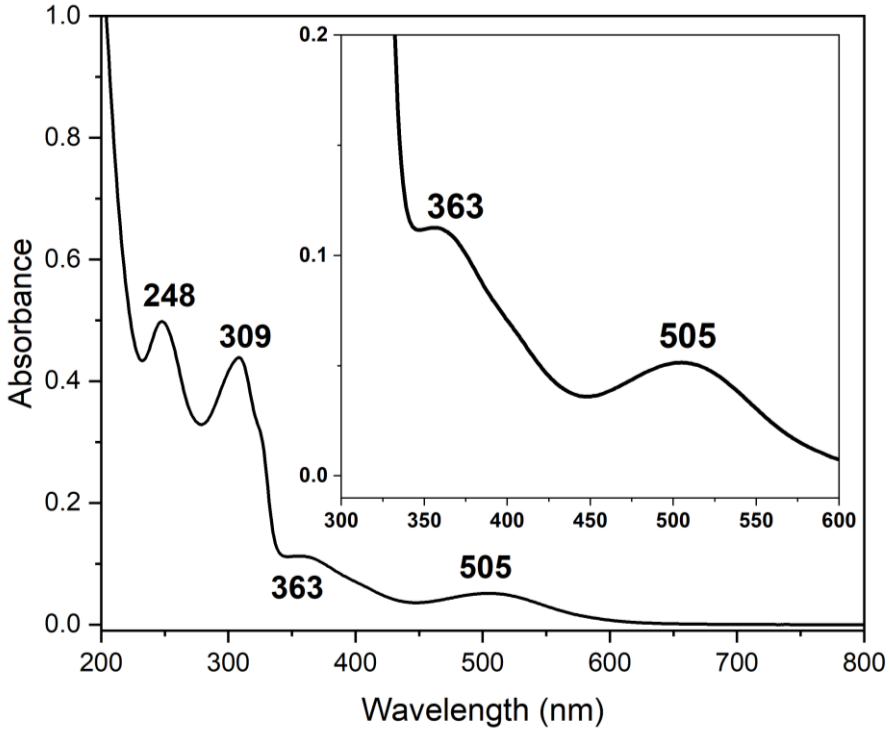

Figure S3av: Absorption spectrum of **3a** (0.1 μM in acetonitrile); inset shows the zoomed region of 300–600 nm.

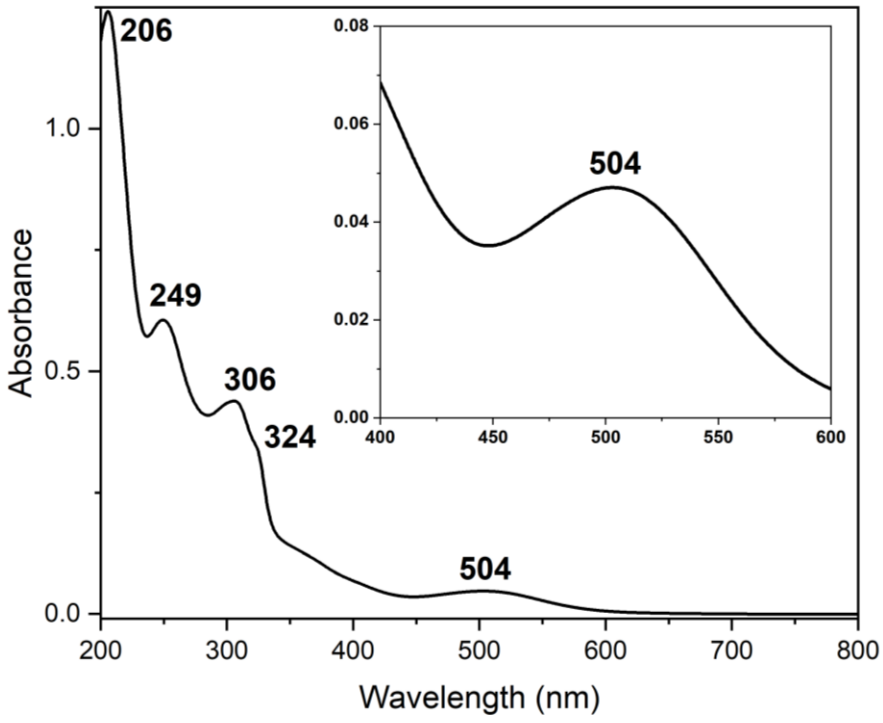

Figure S3aw: Absorption spectrum of **3b** (0.1 μM in acetonitrile); inset shows the zoomed region of 400–600 nm.

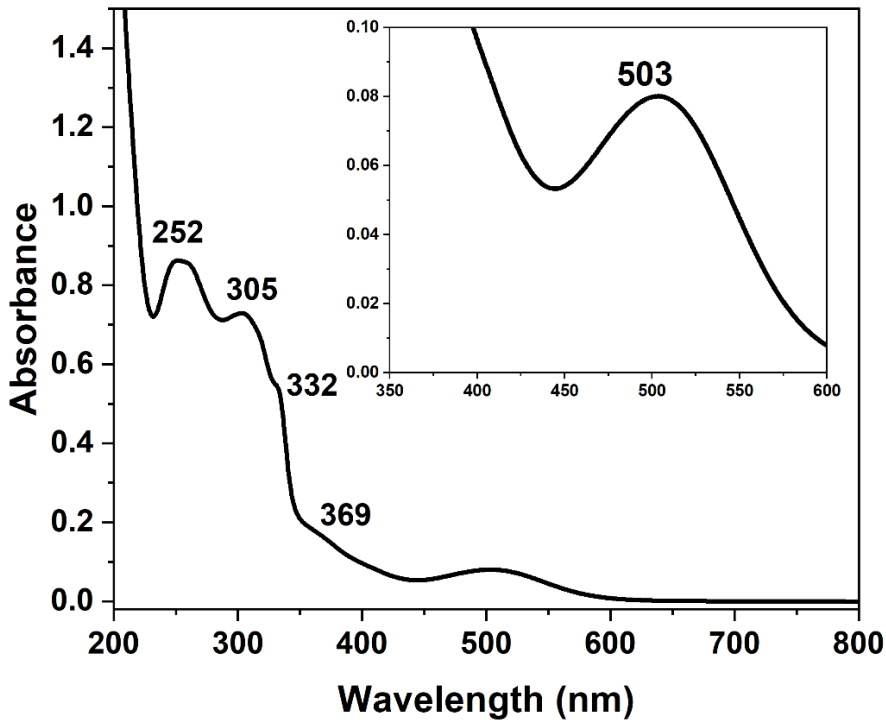

Figure S3ax: Absorption spectrum of **3c** (0.1 μM in acetonitrile); inset shows the zoomed region of 350–600 nm.

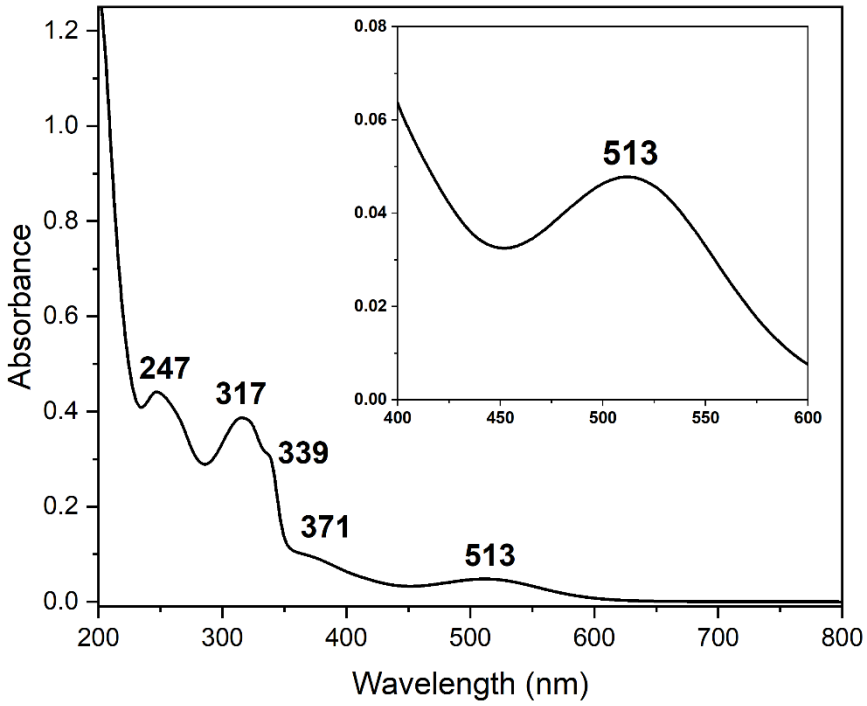

Figure S3ay: Absorption spectrum of **3d** (0.1 μM in acetonitrile); inset shows the zoomed region of 400–600 nm.

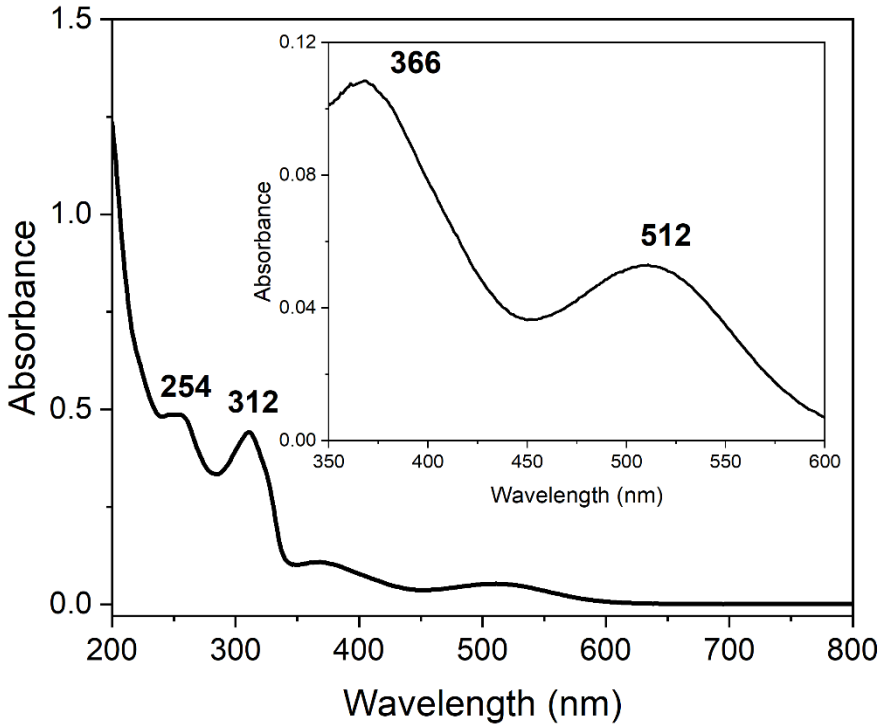

Figure S3az: Absorption spectrum of **3e** (0.1 μM in acetonitrile); inset shows the zoomed region of 350–600 nm.

Table S6: Absorption maxima and molar absorption coefficients of the ligands and metal complexes in 1mM acetonitrile solution; the carbonyl frequencies of the metal complexes, compared with the standard **Rebpy**.

Ligand	**λ_{max}/ nm (ε x 10^3 $Lmol^{-1}cm^{-1}$)**	**Re(I) complex**	**λ_{max}/ nm (ε x 10^3 $Lmol^{-1}cm^{-1}$)**	υ_{str} (C=O) (cm^{-1})
2a	237 (11.2) 285 (9.20) 363 (0.70) 455 (0.28)	**3a**	248 (4.96) 309 (4.38) 363 (1.10) 505 (0.52)	2009, 1896, 1874
2b	207 (12.6) 238 (10.8) 285 (7.96) 348 (1.58) 447 (0.28)	**3b**	206 (12.4) 249 (6.10) 306 (4.40) 324 (3.42) 505 (0.49)	2008, 1884, 1868
2c	239 (14.5) 288 (13.4) 361 (0.10) 453 (0.04)	**3c**	252 (8.62) 305 (7.32) 332 (5.42) 369 (1.67) 503 (0.81)	2007, 1872
2d	240 (6.27) 292 (5.41) 359 (0.35) 456 (0.17)	**3d**	247 (4.41) 317 (3.89) 339 (3.04) 371 (0.97) 513 (0.51)	2006, 1883
2e	248 (5.1) 284 (10.7) 366 (0.97) 454 (0.47)	**3e**	254 (4.89) 312 (4.49) 366 (1.11) 512 (0.57)	2020, 1919, 1892
		Rebpy		2010, 1989, 1867

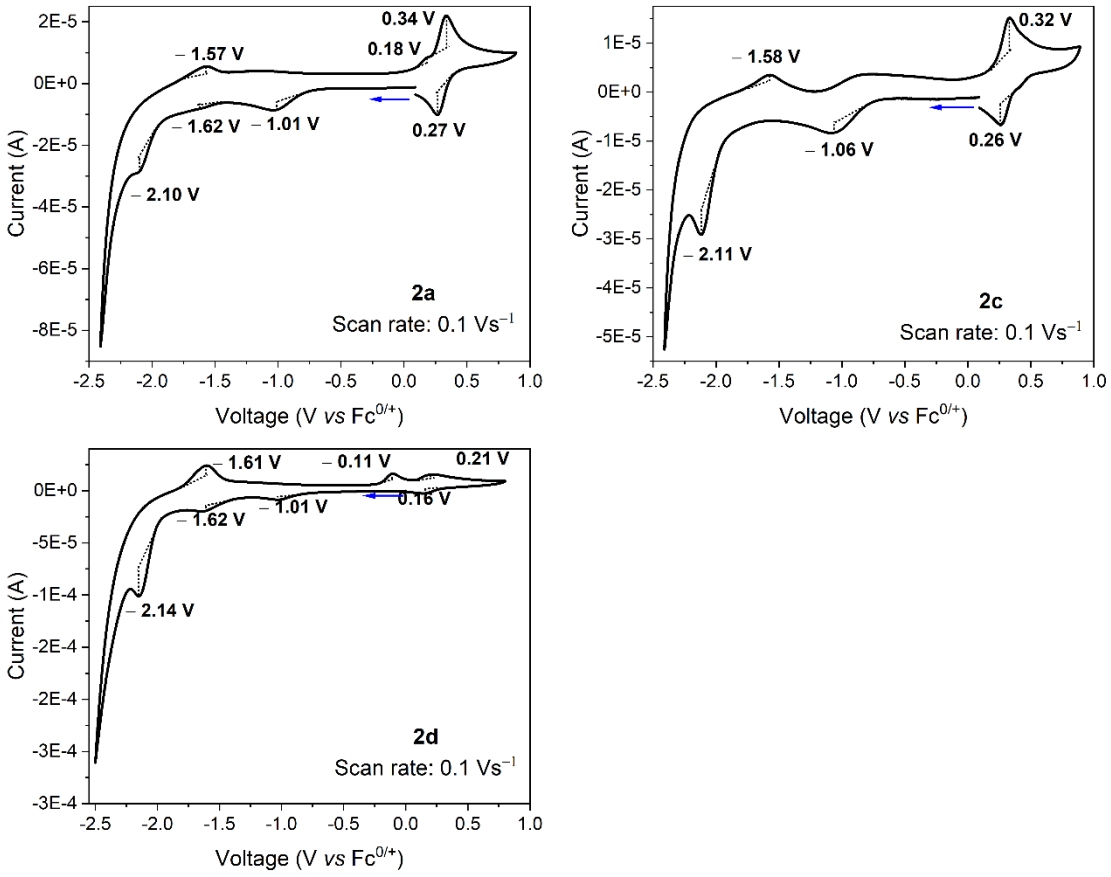

Figure S4: Cyclic voltammograms of **2a**, **2c**, and **2d** in argon (1 mM of ligand in 100 mM of $TBABF_4$ in acetonitrile; WE: glassy carbon, CE: Pt wire, RE: pseudo $Ag|Ag^+$ non-aqueous electrode); potentials are shown with reference to ferrocene as internal standard. The peaks in the region of −1.05 V to 0 V could not be assigned.

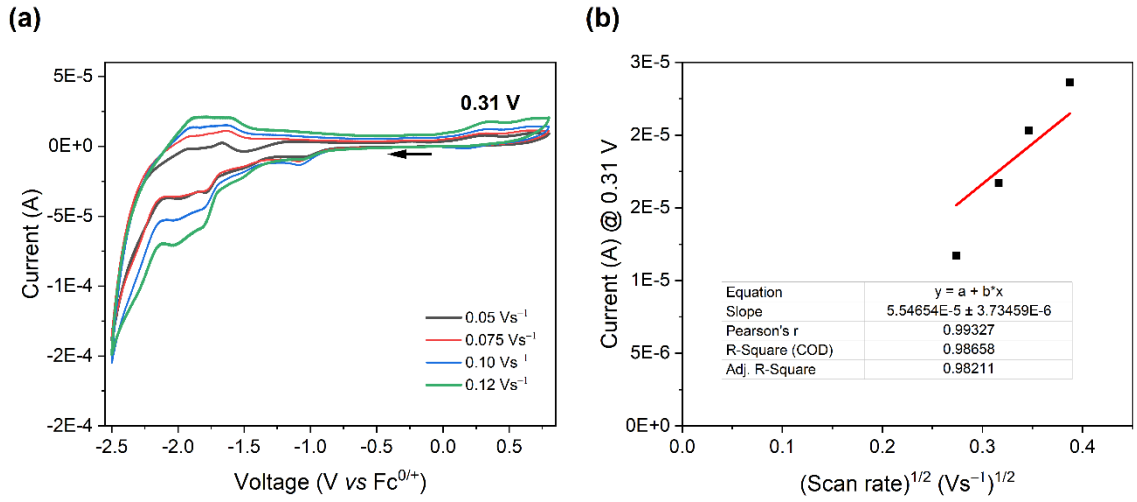

Figure S5: (a) CV of **3a** in scan rates of 0.05 to 0.15 Vs^{-1} in acetonitrile solution under argon; (b) Peak currents for the ferrocene oxidative step (~ 0.40 V) vs the square root of the scan rate.

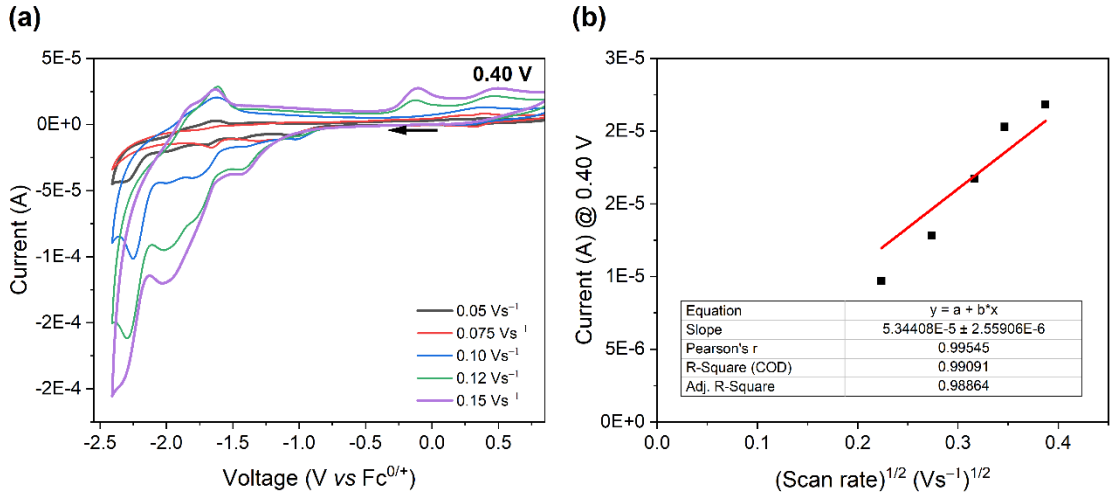

Figure S6: (a) CV of **3b** in scan rates of 0.05 to 0.12 Vs^{-1} in acetonitrile solution under argon; (b) Peak currents for the ferrocene oxidative step (~ 0.31 V) vs the square root of the scan rate.

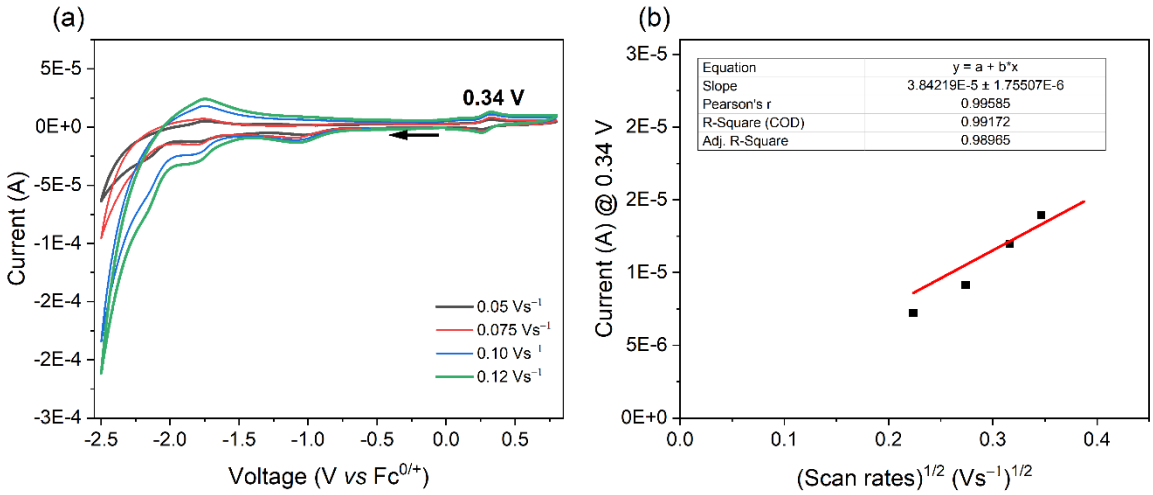

Figure S7: (a) CV of **3c** in scan rates of 0.05 to 0.12 Vs^{-1} in acetonitrile solution under argon; (b) Peak currents for the ferrocene oxidative step (~ 0.32 V) vs the square root of the scan rate.

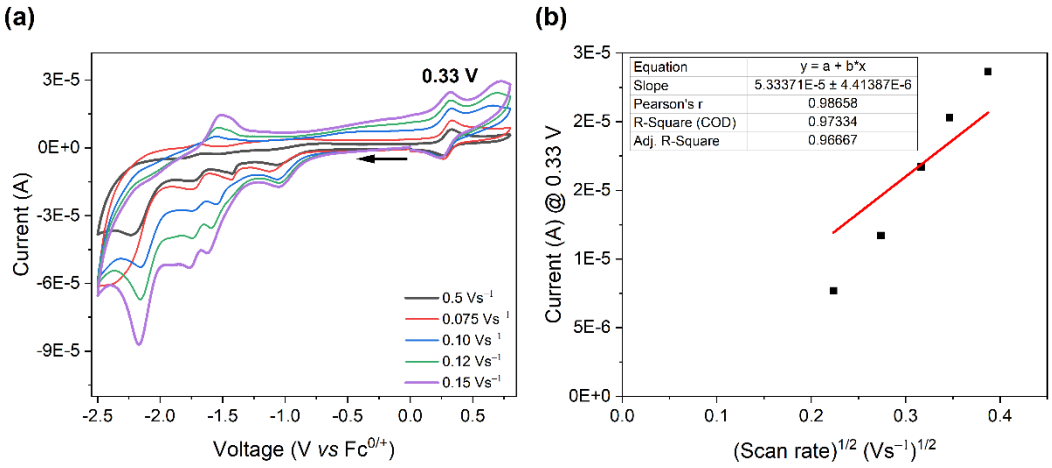

Figure S8: (a) CV of **3d** in scan rates of 0.05 to 0.15 Vs^{-1} in acetonitrile solution under argon; (b) Peak currents for the ferrocene oxidative step (~ –1.78 V) vs the square root of the scan rate.

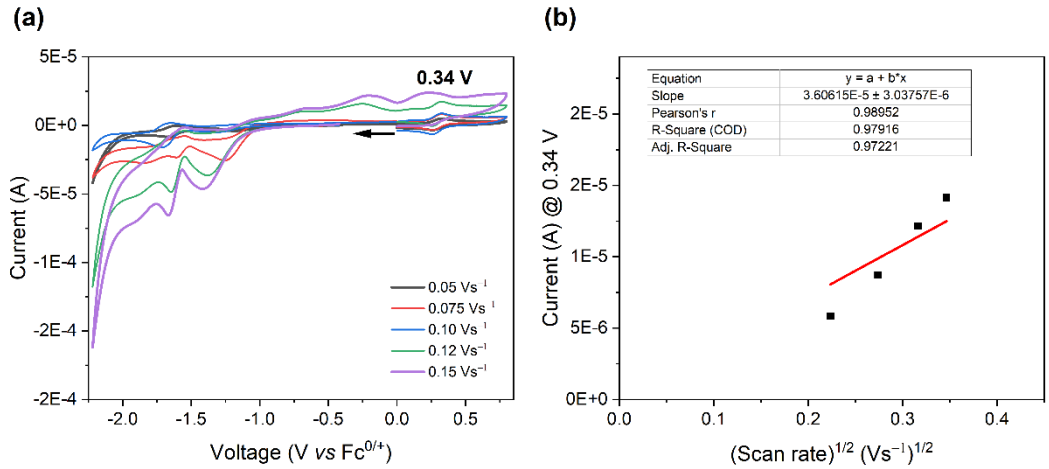

Figure S9: (a) CV of **3e** in scan rates of 0.05 to 0.15 Vs^{-1} in acetonitrile solution under argon; (b) Peak currents for the ferrocene oxidative step (~ 0.34 V) vs the square root of the scan rate.

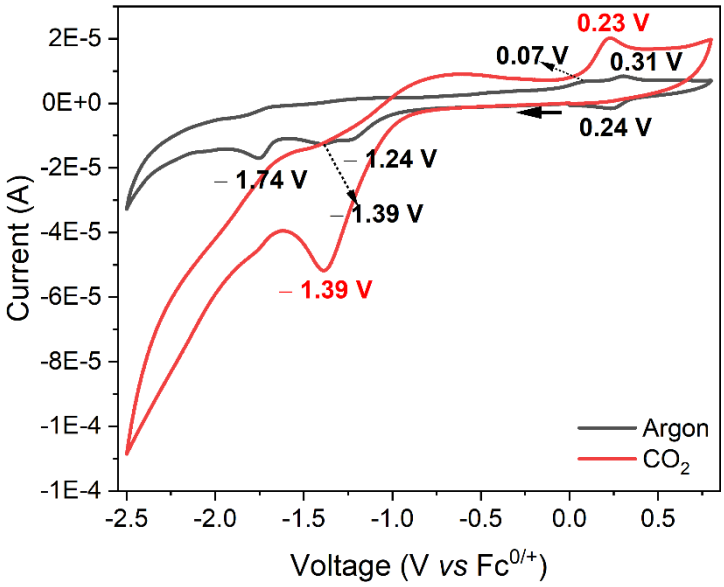

Figure S10: CV of **3a** in argon (1 mM of **3a** in 100 mM of $TBABF_4$ in acetonitrile; WE: glassy carbon, CE: Pt wire, RE: pseudo $Ag|Ag^+$ non-aqueous electrode, scan rate 0.1 Vs^{-1}). The peaks observed in the range of −1.4 V to 0 V are currently not assigned to any electrochemical process.

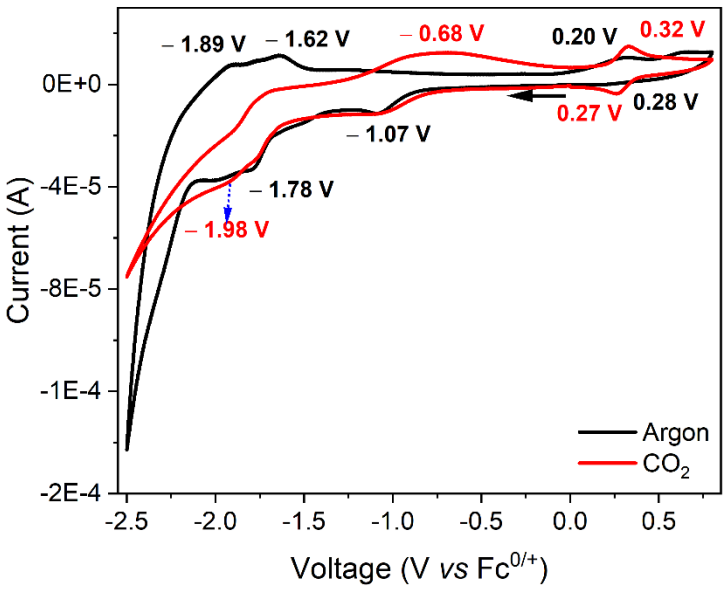

Figure S11: CV of **3b** in argon (1 mM of **3b** in 100 mM of $TBABF_4$ in acetonitrile; WE: glassy carbon, CE: Pt wire, RE: pseudo $Ag|Ag^+$ non-aqueous electrode, scan rate 0.1 Vs^{-1}). The peaks observed in the range of −1.4 V to 0 V are currently not assigned to any electrochemical process.

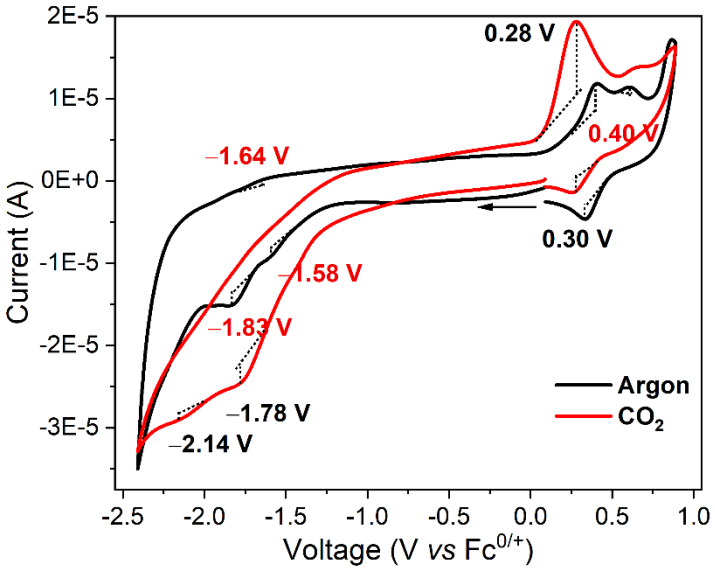

Figure S12: CV of **3c** in argon (1 mM of **3c** in 100 mM of $TBABF_4$ in acetonitrile; WE: glassy carbon, CE: Pt wire, RE: pseudo $Ag|Ag^+$ non-aqueous electrode, scan rate 0.1 Vs^{-1}).

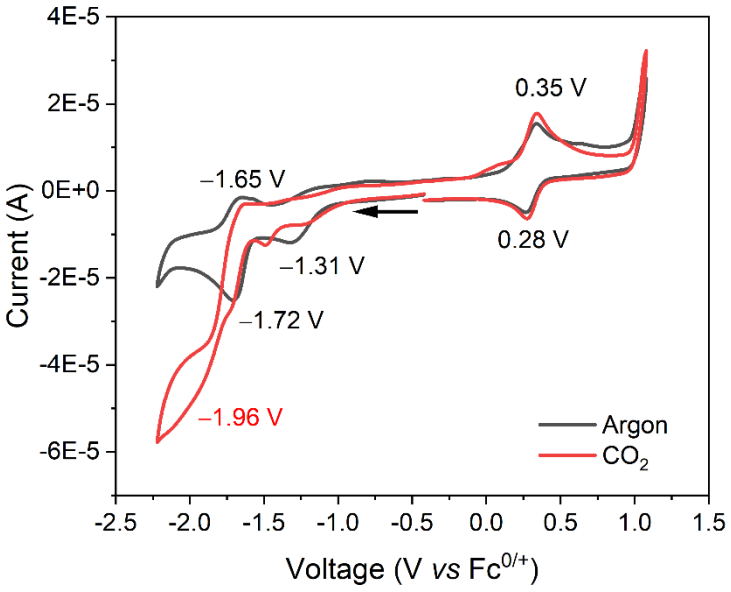

Figure S13: CV of **3e** in argon (1 mM of **3e** in 100 mM of $TBABF_4$ in acetonitrile; WE: glassy carbon, CE: Pt wire, RE: pseudo $Ag|Ag^+$ non-aqueous electrode, scan rate 0.1 Vs^{-1}). The peaks observed in the range of −1.4 V to 0 V are currently not assigned to any electrochemical process.

Table S7: Catalytic parameter (i_{cat}/i_p) calculated for the complexes at the tabulated potentials (scan rate 0.1 Vs^{-1}) (all potentials reported are *vs* $Fc^{0/+}$)

Complex	**Potential (V *vs* $Fc^{0/+}$)**	i_{cat}/i_p
3a	−2.17	4.63
3b	−1.92	1.08
3c	−2.14	1.50
3d	−1.92	4.03
3e	−1.96	2.60

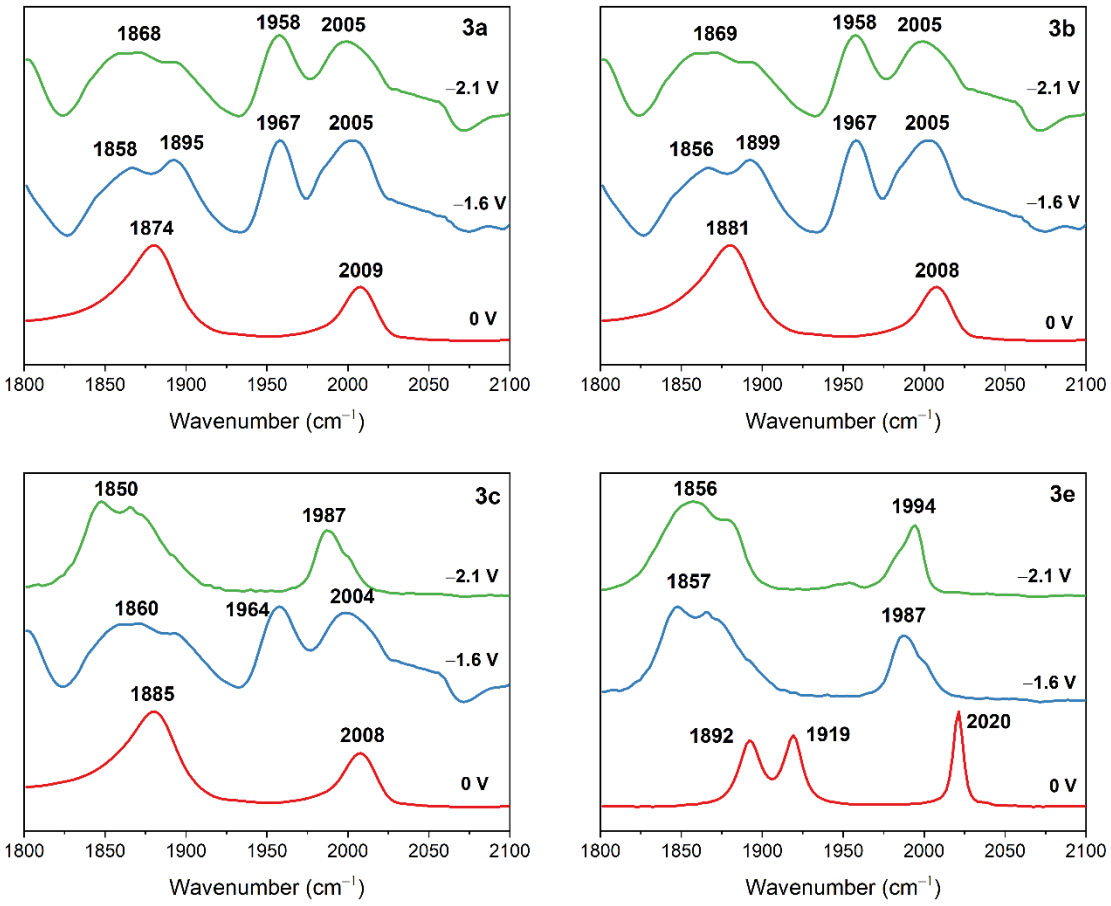

Figure S14: IRSEC spectra of **3a–c**, and **3e** (3 mM in 100 mM $TBABF_4$ in acetonitrile), at different potentials under argon atmosphere.

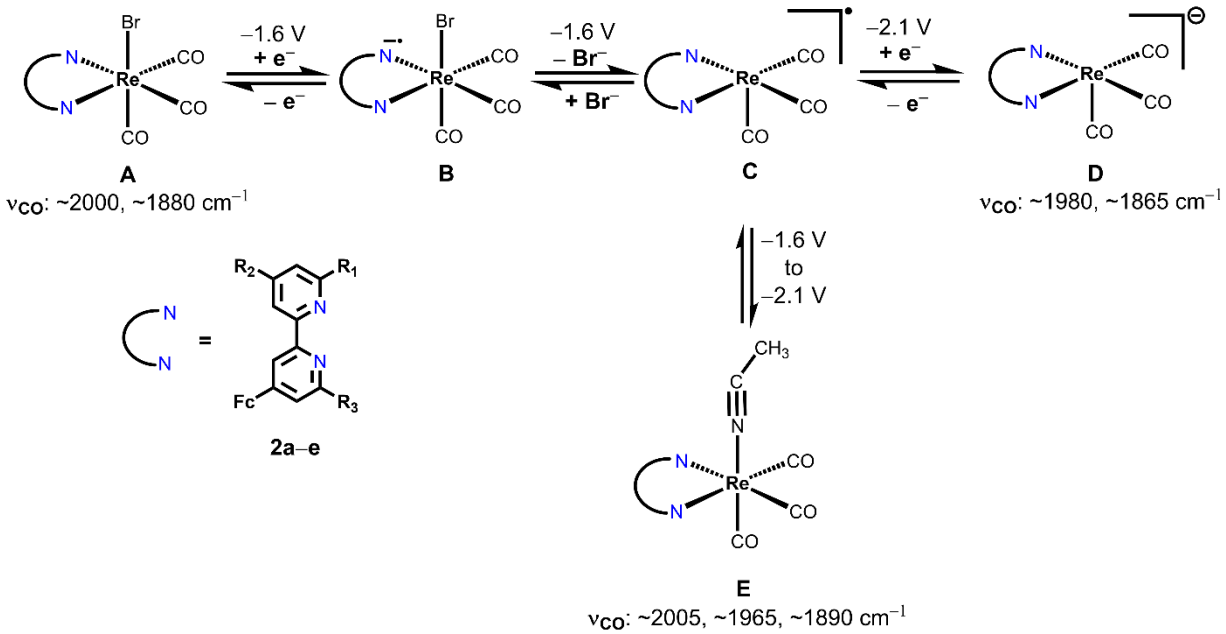

Figure S15: The proposed route of formation for the intermediates for **3a**–**e**, detected by IRSEC experiments. The species **E** is the catalytically active species, and species **D** can be present in equilibrium with it during the catalytic cycle.

Table S8: Photocatalytic CO_2 reduction by the Re complexes after 1 h visible light irradiation in the presence of $[Ru(bpy)_3]Cl_2$[(a)]

Sample	CO (µmol)	H_2 (µmol)	CO selectivity (%)[(b)]
3a	26.47 ± 0.43	2.04 ± 0.03	92.8
3b	20.66 ± 1.39	3.36 ± 0.30	86.0
3c	19.11 ± 0.76	3.43 ± 0.17	84.8
3d	26.55 ± 1.33	2.56 ± 0.07	91.2
3e	24.14 ± 0.67	3.18 ± 0.36	88.4
2e	2.22 ± 0.03	0.202 ± 0.002	91.7
Rebpy	35.04 ± 1.90	0	100

[(a)]Reaction conditions: 0.1 mM Re catalyst, 4 mL of MeCN/TEOA (9:1 v/v), 0.1 mM photosensitizer, 10 mM BIH, visible light (100 mW cm^2, AM 1.5G, λ > 400 nm), and 1 h irradiation.

[(b)]CO selectivity = $\frac{CO_{\mu mol}}{CO_{\mu mol}+H_{2\,\mu mol}} \times 100\%$

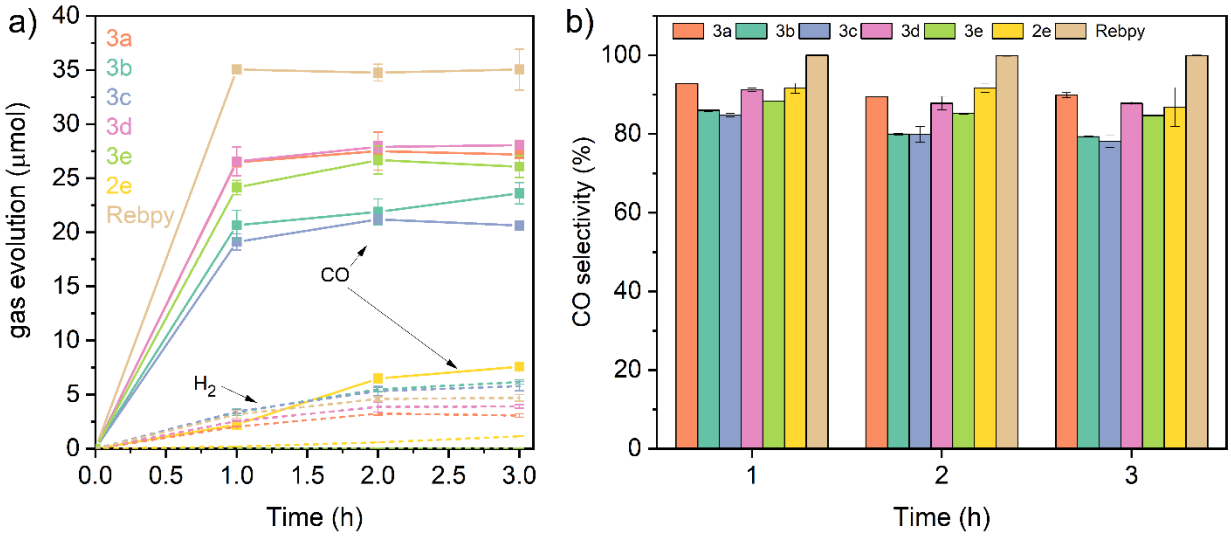

Figure S16: Photocatalytic CO_2 reduction by **3a-e** over longer duration. Figure (a) shows the generation of CO and H_2 over 3 hours visible light irradiation. The solid and dashed lines show CO and H_2 evolution traces, respectively. Figure (b) shows the CO selectivity of the catalysts after 1, 2 and 3 hours of irradiation.

References:

1 A. M. Borys, *Organometallics*, 2023, **42**, 182–196.
2 O. V. Dolomanov, L. J. Bourhis, R. J. Gildea, J. a. K. Howard and H. Puschmann, *J. Appl. Crystallogr.*, 2009, **42**, 339–341.
3 G. M. Sheldrick, *Acta Crystallogr. Sect. Found. Adv.*, 2015, **71**, 3–8.
4 G. M. Sheldrick, *Acta Crystallogr. Sect. C Struct. Chem.*, 2015, **71**, 3–8.
5 A. L. Spek, *Acta Crystallogr. D Biol. Crystallogr.*, 2009, **65**, 148–155.
6 L. J. Farrugia, *J. Appl. Crystallogr.*, 2012, **45**, 849–854.
7 C. F. Macrae, I. Sovago, S. J. Cottrell, P. T. A. Galek, P. McCabe, E. Pidcock, M. Platings, G. P. Shields, J. S. Stevens, M. Towler and P. A. Wood, *J. Appl. Crystallogr.*, 2020, **53**, 226–235.
8 X. Wu, E. R. T. Tiekink, I. Kostetski, N. Kocherginsky, A. L. C. Tan, S. B. Khoo, P. Wilairat and M.-L. Go, *Eur. J. Pharm. Sci.*, 2006, **27**, 175–187.
9 S. M. Delgado-Rivera, G. E. Pérez-Ortiz, A. Molina-Villarino, F. Morales-Fontán, L. M. García-Santos, A. M. González-Albó, A. R. Guadalupe and I. Montes-González, *Inorganica Chim. Acta*, 2017, **468**, 245–251.
10 E. C. Constable, A. J. Edwards, R. Martínez-Máñez and P. R. Raithby, *J. Chem. Soc. Dalton Trans.*, 1995, 3253–3261.
11 S. Saha, T. Doughty, D. Banerjee, S. K. Patel, D. Mallick, E. S. S. Iyer, S. Roy and R. Mitra, *Dalton Trans.*, 2023, **52**, 15394–15411.
12 Z. Meng, C.-L. Ho, H.-F. Wong, Z.-Q. Yu, N. Zhu, G. Li, C.-W. Leung and W.-Y. Wong, *Sci. China Mater.*, 2019, **62**, 566–576.
13 E. E. Benson and C. P. Kubiak, *Chem. Commun.*, 2012, **48**, 7374–7376.
14 G. R. Fulmer, A. J. M. Miller, N. H. Sherden, H. E. Gottlieb, A. Nudelman, B. M. Stoltz, J. E. Bercaw and K. I. Goldberg, *Organometallics*, 2010, **29**, 2176–2179.